ICHNOLOGY OF HOLOCENE GLACIOMARINE SEDIMENTS: MAKTAK, CORONATION AND NORTH PANGNIRTUNG FJORDS, BAFFIN ISLAND, CANADA

A Thesis Submitted to the College of

Graduate Studies and Research

in Partial Fulfillment of the Requirements

for the Degree of Master of Science

in the Department of Geological Sciences

University of Saskatchewan

Saskatoon

By

Elizabeth Rose Schatz

PERMISSION TO USE

In presenting this thesis in partial fulfillment of the requirements for a Postgraduate degree from the University of Saskatchewan, I agree that the Libraries of this University may make it freely available for inspection. I further agree that permission for copying of this thesis in any manner, in whole or in part, for scholarly purposes may be granted by the professor or professors who supervised my thesis work or, in their absence, by the Head of the Department or the Dean of the College in which my thesis work was done. It is understood that any copying or publication or use of this thesis or parts thereof for financial gain shall not be allowed without my written permission. It is also understood that due recognition shall be given to me and to the University of Saskatchewan in any scholarly use which may be made of any material in my thesis.

Requests for permission to copy or to make other use of material in this thesis in whole or part should be addressed to:

Head of the Department of Geological Sciences
University of Saskatchewan
Saskatoon, Saskatchewan S7N 5A5
Canada

OR

Dean
College of Graduate Studies and Research
University of Saskatchewan
107 Administration Place
Saskatoon, Saskatchewan S7N 5A2
Canada

ABSTRACT

North Pangnirtung, Coronation and Maktak fjords are situated on Cumberland Peninsula, Baffin Island, Canada, having a common freshwater source related to the melting of the Penny Ice Cap. Bottom photographs and Holocene core samples analysed for this Thesis were acquired during the 1982 Sedimentology of Arctic Fjords Experiment (S.A.F.E.) cruise of the *CSS Hudson* and were reinterpreted from an ichnological point of view. Bottom photographs were examined to identify epifaunal and infaunal organisms and their associated trails or burrows exposed on the substrate surface. Locomotion and resting traces produced by echinoderms and gastropods, as well as a variety of burrows produced by infaunal organisms, were observed. These biogenic structures were then compared to biogenic structures revealed through x-radiograph images and direct observations from Lehigh cores. Intermediate- and deep-tier structures were observed in the ichnofabric of the glaciomarine sediments. Extensive bioturbation by the shallow-tier epibenthic tracemakers, most notably ophiuroid echinoderms (brittlestars), destroyed much of the primary sedimentary fabric resulting in homogenous silty clay sediments. The dominant deep-tier structure consists of an open burrow three-dimensional boxwork which allows for oxygen penetration into the sediment through the burrow walls at depths below the redox zone. Potential tracemakers for these deep-tier structures are likely polychaetes, particularly capitellids. Sandy event beds, associated with mass wasting of delta front and fjord sidewall sediments, are mostly unaffected by bioturbation. Sedimentation rates during these events were high and re-establishment of the three-dimensional burrow boxwork occurred quickly as normal conditions of suspension fall-out resumed. Deep-tier structures are not observed in sandy intervals indicating that the tracemaker preferred finer-grained sediments. The three-dimensional burrow boxwork occurs pervasively in the cores, though the intensity of bioturbation is greater in cores distal to the fjord head.

AKNOWLEDGEMENTS

I would like to thank my supervisors Dr. Gabriela Mángano and Dr. Alec Aitken for providing me with the opportunity to study this exciting topic and also their patience in slow but steady progress. I would also like to thank them for their financial support; funding was provided by Natural Sciences and Engineering Research Council (NSERC) Discovery Grants 311727-05/08 and University of Saskatchewan Start-up funds (Mangano), and the Office of the Provost, University of Saskatchewan (Aitken). Also, a personal thank you to Gabriela for her friendship and guidance throughout my undergraduate and graduate degrees.

Thank you to Kate Jarrett and Owen Brown from the Bedford Institute of Oceanography for help in locating core samples, providing additional x-radiograph images and for instruction in sediment grain size analysis!

Thank you to my friends and family for their interest in my topic and for always being willing to listen to my explanations. I would also like to thank them for my sanity; without them, I would have none. In particular, thank you to my partner Lonnie for his undying support, continued optimism and for always believing in me.

Finally, thank you to the Department of Geological Sciences at the University of Saskatchewan for providing me with a welcoming environment and funding to cover my living costs.

TABLE OF CONTENTS

PERMISSION TO USE…… i

ABSTRACT…….. ii

AKNOWLEDGEMENTS……. iii

TABLE OF CONTENTS…….. iv

LIST OF TABLES…… vi

LIST OF FIGURES…….. vii

1 Introduction……... 1

1.1 Research Objectives…….. 2

2 Literature Review…….. 3

2.1 Fjords…… 3

2.1.1 Fjord Models……. 3

2.1.2 Baffin Island Fjords…….. 7

2.1.2.1 Maktak, Coronation and North Pangnirtung Fjords…….…… 8

2.1.2.2 Biota……..…… 11

2.1.3 Canadian and European Fjords……. 14

2.2 Ichnology…….. 16

2.2.1 Neoichnology vs. Paleoichnology…… 18

2.2.2 Classification of Trace Fossils……..... 18

2.2.2.1 Stratinomic Classification……. 18

2.2.2.2 Ethologic Classification…… 19

2.2.2.3 Ichnotaxonomic Classification…….. 20

2.2.3 Substrate Consolidation and Trace Fossil Morphology….... 24

2.2.4 Ichnofabrics and Tiering……... 25

2.2.4.1 Tiering in Response to Sedimentation…….. 29

2.2.5 Fjord Models in Ichnology…… 30

3 Ichnology of Holocene Glaciomarine Sediments……. 33

3.1 Introduction……... 33

3.1.1 Study Location…….. 33

3.1.2 Geological Setting……. 35

3.2 Methods……. 36
3.3 Ichnology……... 39
3.3.1 Core Systematic Ichnology……... 39
3.3.2 Photographic Ichnologic Survey……... 44
3.4 Faunal Communities of Maktak, Coronation and North Pangnirtung Fjords……. 57
3.5 Discussion……. 58
3.5.1 Taphonomy……... 58
3.5.2 Potential Tracemakers…….. 64
3.5.3 Environmental Controls…… 68
4 Conclusions……... 74
5 References……. 77
APPENDIX I: Grain Size Analysis of Cores……..... 87

LIST OF TABLES

Table 2.1.	List of organisms recovered from Pangnirtung Fjord, Baffin Island….	12
Table 3.1.	Summary of data for sample locations…….	35
Table 3.2.	Compilation of data from visual bottom photographic survey of identifiable biota……...	57

LIST OF FIGURES

Figure 2.1.	Five end-member fjord models based on sedimentary processes……..	5
Figure 2.2.	Broughton Trough……..	8
Figure 2.3.	Stratinomic classification of trace fossils……...	20
Figure 2.4.	Ethology of trace fossils…….	22
Figure 2.5.	Examples of the ichnogenus *Protovirgularia*…….	26
Figure 2.6.	General diagram for tiering of biogenic sedimentary structures……	28
Figure 2.7.	Tiering in response to variations in sedimentation rate and style……..	29
Figure 2.8.	Current ichnofacies model for fjord and fjord lake environments…….	31
Figure 3.1.	View of the three studied fjords…….....	34
Figure 3.2.	Sedimentology of Maktak, Coronation and North Pangnirtung Lehigh core samples…….....	37
Figure 3.3.	Photographs of core samples from station NP3…….....	41
Figure 3.4.	Photograph and x-ray of core sample from station CO4…….....	43
Figure 3.5.	Incipient Archaeonassa……...	48
Figure 3.6.	Traces from the modern sea bottom……...	51
Figure 3.7.	Ophiroid trackways with producers…….....	53
Figure 3.8.	Traces from the modern sea floor……...	56
Figure 3.9.	Lehigh core logs depicting ichnofabric and sedimentological data for Maktak Fjord……...	60
Figure 3.10.	Two Lehigh cores depicting ichnofabric and sedimentology of Coronation Fjord…….....	61
Figure 3.11.	Two Lehigh cores depicting ichnofabric and sedimentological data from North Pangnirtung Fjord…….....	62
Figure 3.12.	Diagram illustrating the three-dimensional boxwork burrow system....	67

1 Introduction

Fjords are complex and constantly changing environments. Many studies of Arctic fjord sedimentology have been conducted to explain the numerous processes and factors inherent in these environments (e.g. Gilbert, 1982a; Gilbert, 1983; Syvitski *et al.*, 1987; Syvitski, 1989; Syvitski and Shaw, 1995). While the sedimentology of Canadian Arctic fjords is fairly well explored, very few studies have been conducted on the biological communities present within them (e.g. Dale *et al.*, 1989; Syvitski *et al.*, 1989; Dale, 1992; Aitken and Fournier, 1993). Even fewer studies have been conducted to study animal-substrate interactions within Canadian Arctic fjord environments (e.g. Aitken *et al.*, 1988).

Fjords represent a new frontier for the study of ichnology. Upper Paleozoic fjord environments make up the bulk of the research conducted at present (e.g. Buatois and Mángano, 2003; Balistieri *et al.*, 2002; Gandini *et al.*, 2007; Buatois *et al.*, 2006, 2010; Schatz *et al.*, 2011) with a few examples from the Cenozoic (e.g. Eyles *et al.*, 1992). Together, these studies have been combined to produce an ichnofacies model of fjord environments (Buatois and Mángano, 2011a). However, as many Paleozoic fjords were characterized by high sediment and freshwater discharge this model does not accurately reflect modern fjord analogs (Eyles *et al.*, 1992; Buatois *et al.*, 2006). Most Arctic fjords have a limited melt season and exceptionally low sedimentation rates everywhere within the fjord basins except at the head (Gilbert, 1982a; Syvitski, 1989; Syvitski and Shaw, 1995; Gilbert, 2000). Therefore, it is of the greatest importance that more studies of modern fjords (Arctic and elsewhere) be conducted from an ichnological perspective to further refine and expand on fjord models in ichnology and increase our knowledge of the complex and diverse environments that are fjords.

The purpose of this research is to study animal-substrate interactions within fjord environments to further expand our understanding of the biologic and physical processes that characterize Canadian Arctic fjords. The project attempts an integrative approach of two data sets: recent biogenic structures on the seafloor (based on seafloor photographs) and ichnofabrics of Holocene glaciomarine sediment core samples from Maktak, Coronation and North Pangnirtung Fjords in eastern Baffin Island, Canada. The results of this study will contribute to expanding and refining ideas on ichnofacies models of fjords, establishing an agenda for future research in the ichnology of high-latitude depositional systems.

1.1 Research Objectives

There are three main objectives for this project. The first is to compare the ichnology of the recent seafloor with the biogenic sedimentary structures present in the Holocene core samples and determine if the diversity of biogenic sedimentary structures present on the recent seafloor is accurately represented in the core samples. If a disparity exists between the two data sets, this project will attempt to provide working hypotheses to explain these differences (e.g. explore possible taphonomic controls in the diversity and abundance of biogenic sedimentary structures). Secondly, we will attempt to identify proximal-distal trends between the fjord heads and more open marine localities of the three studied fjords. Finally, the results of this study will be framed within the current ichnofacies model of fjord environments (Buatois and Mángano, 2011a).

2 Literature Review

2.1 Fjords

Fjords are defined as glacially carved, steep U-shaped valleys with marine influence at the mouth and fresh water input resulting from glacial melting at the head (Syvitski *et al.*, 1987; Syvitski and Shaw, 1995). These are drowned glacial troughs, originating as river valleys formed during the Tertiary Era (Gilbert, 1983). The modern fjords of eastern Baffin Island were excavated during the Pleistocene ice age and subsequently flooded by rising sea-level during deglaciation (Gilbert, 1982b; Syvitski *et al.*, 1987).

Fjords are considered to be a subcategory of estuaries due to their drowned-valley morphology. However, fjords are longer and narrower than typical estuaries and are commonly surrounded by mountains or steep-sided hills (Syvitski *et al.*, 1987). They also have water depths ranging from several meters at the head to several hundred meters at the mouth and may contain (but are not required to by definition) one or more sills. These sills act as a buffer against wave or tidal activity in the adjacent ocean basin, typically restricting circulation of water and sediments within the fjord (Gilbert, 1983; Syvitski, 1989; Syvitski and Shaw, 1995).

2.1.1 Fjord Models

To further investigate the complex sediment-water interactions of fjord environments, we must first examine some proposed fjord models. There are five main types of fjords based on sediment input and dominant physical processes (Syvitski, 1989; Syvitski and Shaw, 1995). Each fjord type is displayed in Figure 2.1, which shows both the longitudinal and cross-sectional views of the sediment accumulation in a fjord.

Fluvially-dominated fjords (Fig. 2.1a) receive a large sediment and freshwater input from seasonal melting of snow and glacial ice (Syvitski and Shaw, 1995). It is common for a delta to form at the fjord head and prograde seaward over time, gradually filling the fjord valley (Syvitski and Shaw, 1995). If a sill is present, it will buffer the wave energy at the mouth of the fjord and create a more sheltered inner-fjord environment commonly causing limited circulation to occur at depth. Thermal stratification contributes to stratification of oxygenated waters, resulting in the development of anoxic bottom waters and the accumulation of organic-rich muds (Syvitski *et al.*,

1989; Syvitski and Shaw, 1995). The sources for this organic matter are commonly terrestrial (delivered through fluvial input) but it also includes marine plankton derived from circulating of marine water within the fjord basin (Macko *et al.*, 1987; Syvitski and Shaw, 1995).

Wave- and tide-dominated fjords receive sediment from both fluvial and marine inputs and the deposits are constantly reworked by wave and tidal current activity (Syvitski and Shaw, 1995). These types of fjords commonly show sediment accumulation only in depressions on the fjord floor (Fig. 2.1b). Sills composed of glacial till are commonly eroded over time, though not completely removed. The constant mixing of the fjord waters due to wave and tidal current activity limits the development of thermohaline stratification in bottom sediments as well as stagnation of the bottom waters themselves (Syvitski and Shaw, 1995). The substrates tend to be quite coarse and pebbly, specifically along fjord sidewalls and the crests of sills, while finer particles remain in suspension providing excellent living conditions for suspension feeding organisms (Dale *et al.*, 1989; Syvitski, 1989).

Glacially-dominated fjords represent the third of the main fjord types (Fig. 2.1e). Typically, the glacier supplies the majority of the freshwater and sediment at the fjord head, occupying a portion of the fjord trough (tidewater glaciers). Floating glaciers may extend well into the fjord trough or out onto the continental shelf and are suspended above the seafloor by buoyant forces (Gilbert, 1983; Syvitski, 1989; Syvitski and Shaw, 1995). Glaciers can also reside much further inland (hinterland glaciers) in which case sandar are common at the fjord head as sub-aerially exposed outwash plains, commonly composed of medium grained sand (Church, 1970; McKenna-Neuman and Gilbert, 1986; Syvitski, 1989).

In the case of tidewater glaciers, supraglacial melting provides a low energy freshwater supply while englacial and basal melting produce high energy jets which rise as plumes due to differences in water densities with the adjacent marine environment. Greater particle density overcomes the buoyant force of the freshwater carrying it, thus basal deposits accumulate only a short distance from the glacier (Syvitski, 1989; Syvitski and Shaw, 1995). Jets rise very rapidly until their density is matched by the surrounding basin waters; equalization of the water densities between the jet and the main fjord waters usually occurs close to or at the surface (Syvitski and Shaw, 1995). This creates a layer of freshwater, laden with sediment, which travels down the fjord as an overflowing plume slowly releasing the sediment load via suspension

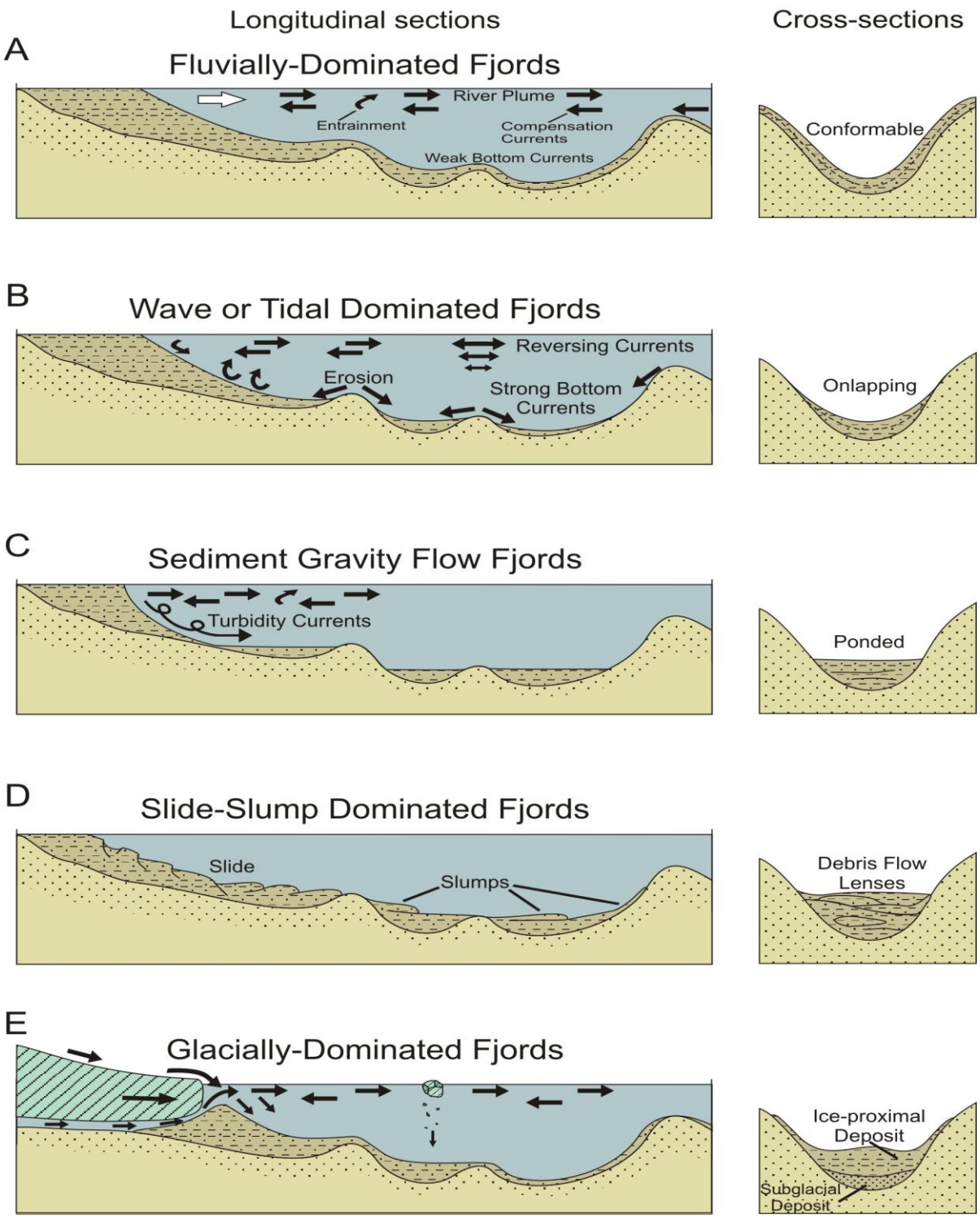

Figure 2.1. Five end-member fjord models based on sedimentary processes. Diagrams show typical depositional architecture within a fjord which contains a prominent sill proximal to the ocean. Active sediment input and water currents are indicated (arrows). Longitudinal and cross-sectional views are shown. Modified from Syvitski and Shaw (1995).

settling (Syvitski, 1989; Syvitski and Shaw, 1995). This results in the accumulation of coarser material proximal to the glacier with increasingly finer sediments being deposited seaward (see Fig. 2.1e). As all fjords are initially glacially-dominated, glacial till typically forms the basal unit found resting unconformably on top of the eroded country rock (e.g. Schatz *et al*., 2011; see Fig 2.1e, cross-section).

The final two fjord models represent a combination of fjord types. Sediment gravity flow fjords are formed when there is little marine influence (possibly due to a sill barrier) and seasonally controlled fluvial input (Syvitski, 1989; Syvitski and Shaw, 1995). Surges in water input related to increased precipitation and/or seasonal melting of ice caps can cause instability in the delta slope at the fjord head (Syvitski and Shaw, 1995). This will result in slope collapse and turbidity flows along the fjord floor (Fig. 2.1c). A ponded sediment accumulation is typical in these fjord environments (Fig. 2.1c, cross-section; Syvitski, 1989; Syvitski and Shaw, 1995).

In the case of slide-slump fjords, instability of the fjord walls is the dominant force (see Fig. 2.1d) even though other sediment sources and depositional processes may be common. Wall slope failure can occur for a number of reasons; 1) the melting of snow on the fjord margins causes sediment flows down the fjord walls; 2) lateral moraine deposits, eroded over time by wind and water, become over steepened and fail; and 3) fractures and joints on fjord walls cause structural instability due to freeze and thaw cycles (Church *et al.*, 1979; Syvitski, 1989; Syvitski and Shaw, 1995).

Sea ice formation is an important environmental factor in high latitude fjords and is likely an active process in each of the five fjord models discussed previously. Sea ice may shelter surface waters from mixing by wind and promote stratification due to both the lack of mixing and the release of freshwater at the surface by melting icebergs (Gilbert, 1983; Syvitski, 1989; Syvitski and Shaw, 1995). The production of sea ice also encourages vigorous mixing of basin waters at great depths during the winter through the processes of brine rejection, mainly due to changes in water density associated with increasing salinity through freshwater removal (Lewis and Perkin, 1982; Gilbert, 1983).

During winter months, sediment can be transported by wind from glacial margins or sandar and subsequently trapped on floating sea ice (McKenna-Neuman, 1989; Syvitski and Shaw, 1995).

Aeolian sediments frozen within sea ice may contribute to suspension fall-out sedimentation in summer months when sea ice melts (Gilbert, 1982a, 1983). These sediments can be transported great distances within the fjord valley allowing deposition in areas of the fjord too distal to receive sediment input from fluvial processes or glacial melting at the head (Gilbert, 1983; Syvitski, 1989; Syvitski and Shaw, 1995).

Most fjords will be influenced by a combination of the main processes listed above. Fjords that are glacially-dominated in the beginning may progress to more fluvially-dominated over time as deglaciation continues. Side-slump processes and ice-rafted sedimentation from floating ice sheets and sea ice may be combined with fluvially-dominated sedimentation resulting in a very complex sedimentary environment.

2.1.2 Baffin Island Fjords

Baffin Island is situated on the eastern coast of Baffin Bay and is one of the many islands which make up the Canadian Arctic Archipelago. Baffin Island's basement rock, in the vicinity of Maktak, Coronation, and North Pangnirtung fjords specifically, is composed predominantly of Paleoproterozoic metamorphosed intrusive igneous rock (Jackson and Taylor, 1972; Keim *et al*., 2011). Along the eastern coastline of Cumberland Peninsula is an elongate depression known as the Broughton Trough (see Fig. 2.2; Gilbert, 1982b). The trough likely originated during hot spot upwelling in Davis Strait beginning in the Paleocene (Hyndman, 1975; Gilbert, 1982b). A graben-horst complex is thought to have resulted from structural failures related to the uplift, creating three main basin depressions in Broughton Trough (see Fig. 2.2; Gilbert, 1982b). The trough was then partially filled by deltaic progradation which continued until just prior to Pleistocene glaciation (Hyndman, 1975; Gilbert, 1982b). Several of the main drainage river valleys from Baffin Island into Broughton Trough were carved out more deeply by the advance of the Pleistocene ice sheet and are now active fjord valleys (Gilbert, 1982b).

Three main basins are present within Broughton Trough (Fig. 2.2). The most proximal (A) and middle (B) basins were excavated by glacial advance during the Pleistocene and it is likely that the glacier extended further seaward without contacting the seafloor (Fig. 2.2; Gilbert, 1982b). Glacial till was deposited throughout Broughton Trough, the majority of which filled the middle

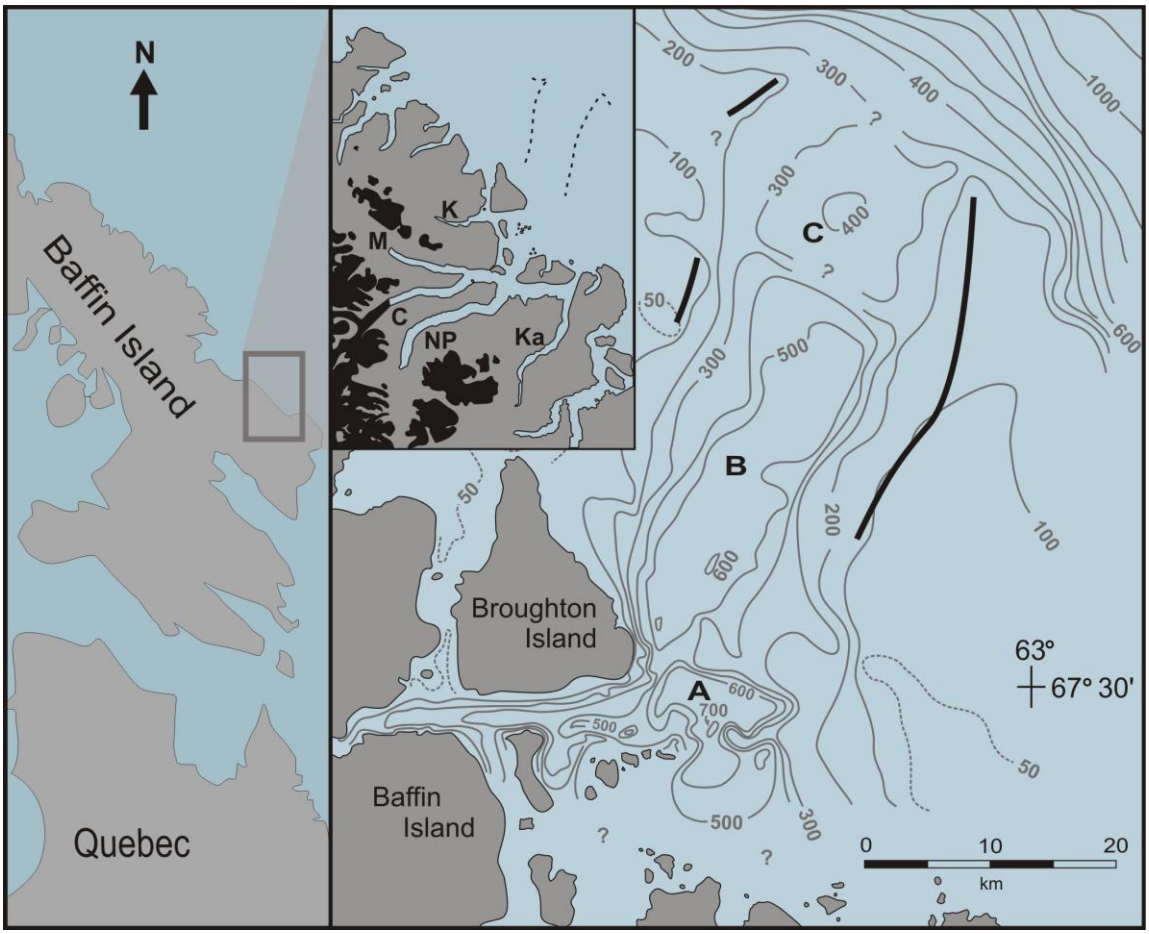

Figure 2.2. Broughton Trough extending seaward from Cumberland Peninsula, Baffin Island. Heavy lines indicate lateral moraine deposits on the troughs margin. Letters A, B, and C indicate the location of the three main basins within Broughton Trough with bathymetric contour lines indicating their respective depths. There are 3 main fjords shown to drain into the trough area, and 2 minor fjords: M-Maktak Fjord, C-Coronation Fjord, NP-North Pangnirtung Fjord, K-Kingnelling Fjord, Ka-Kangert Fjord. Black area in insert indicates glacier cover. Modified from Gilbert (1982b).

and proximal basins (Gilbert, 1982b). Glacial ice retreat is thought to have begun between 10,000 and 8000 B.P. (Brigham, 1983).

2.1.2.1 Maktak, Coronation and North Pangnirtung Fjords

Maktak, Coronation and North Pangnirtung are all confluent fjords receiving freshwater from glaciers originating from Penny Ice Cap (Gilbert, 1982a). These fjords are well oxygenated (>3 $ml \cdot L^{-1}$) as they do not contain sills that would otherwise limit water circulation at depth within

the fjords (Syvitski *et al.*, 1989). This also relates to the fact that Arctic fjords are typically well mixed due to the thin freshwater cap and extensive wind induced wave activity (Gilbert, 1983, 2000). The bottom waters maintain normal marine salinities (32-35‰) almost everywhere within the fjords with the exception of fjord heads (Gilbert, 1982a). Sedimentation rates are low (only several millimetres per year) throughout the fjords with the highest sediment input occurring during a very short spring thaw and summer period (Gilbert, 1982a; Syvitski and Shaw, 1995).

Coronation Fjord receives much of its freshwater input from Coronation Glacier at its head. The glacier is recorded to be retreating approximately 15m yr^{-1} at present, releasing the majority of its sediment load within the first kilometre of the fjord (Gilbert, 1982a). The sedimentation rate is high proximal to the glacier, though no seasonal measurements have been undertaken (Gilbert, 1982a). Both Maktak and North Pangnirtung fjords have active sandar at their heads and are fluvially-dominated environments (see section 2.1.1 Fjord Models). Sedimentation rates are markedly lower than in Coronation Fjord, though the sandar contribute an undocumented amount of sediment through aeolian transport (Gilbert, 1982a; Gilbert, 1983; McKenna-Neuman and Gilbert, 1986). Gilbert (1982a) noted that fine-grained suspended sediments within Maktak Fjord were highly prone to flocculation. This process causes sediments to be deposited more rapidly from suspension and closer to the fjord head.

Four main depositional processes occur within the three fjords: 1) ice rafted debris and subaerial rock slide from fjord walls; 2) suspended load fall out; 3) turbidity gravity flows; and 4) aeolian transport originating from sandar deposits (Gilbert, 1982a). Ice rafted material is fairly uncommon in the depositional record of these fjords and is likely only a concern with regards to Coronation Fjord. Slumping of lateral moraine deposits of the fjord side walls does occur as documented by Gilbert (1982a) during a reconnaissance survey. These events deposit poorly sorted cobble sized sediments to large boulders throughout the fjord bottom and can cover several hundred square meters in area (Gilbert, 1982a; Dale *et al*., 1989).

Much of the fine-grained sedimentation is the result of suspension fall out processes. Though only contributing several millimetres per year to the seafloor accretion, this is likely the main sedimentary process away from the fjord head (Gilbert, 1982a). Delivery of suspended particles down fjord is dependent on high freshwater input in an already stratified fjord basin. When peak

discharge occurs, it is possible for sediment suspended in fresh surface water to be transported as far as the fjord mouth and shelf (Syvitski, 1989).

During seasonal melting in Coronation Fjord, periods of high discharge may induce gravity flows of sediment accumulated on the slope adjacent to Coronation Glacier (Gilbert, 1982a; Syvitski, 1989). A similar process may also occur in over steepened sandar slopes of Maktak and North Pangnirtung Fjords. If turbidity flows are sufficiently vigorous, sediment may become re-suspended, increasing sedimentation rates down fjord briefly. However, the main body of the turbidity deposit is not likely to extend more than five kilometres from the source (Gilbert, 1982a; Syvitski, 1989).

The extent of aeolian transport has not been measured though it has been witnessed to occur in these fjords (Gilbert, 1982a). Deposition of windblown particles may be one of the main sources of sedimentation during the winter months though the majority of the particles will get stranded on sea ice until late into the summer when melting finally releases the sediment (Gilbert, 1983). Accumulation of aeolian deposits on sea ice can decrease albedo and speed up the process of melting (Gilbert, 1982a; Gilbert, 1983; Syvitski, 1989; Syvitski and Shaw, 1995). The sediment is then deposited relatively close to where the ice raft was located (Gilbert, 1983).

Other aspects influencing sedimentation in these fjords are side entry drainage, tidal currents, wave activity, and the Coriolis force. While these fjords have fairly dominant freshwater and sediment input sources at their heads, the surrounding mountains contain numerous tributary glacial troughs as observed in satellite images. These channels supply freshwater directly to the fjord basin from the melting of small glaciers and snow. Freeze-thaw cycles combined with seasonal melting will initiate mass wasting of debris from the fjord side walls into the basin (Church *et al.*, 1979).

Gilbert (1982a) documented a microtidal range for Maktak, Coronation and North Pangnirtung Fjords. The semidiurnal tide produces an approximate one meter change in sea level (Gilbert, 1982a). Tidal activity only allows penetration of seawater into the fjord for little more than 100 meters during these events (Gilbert, 1982a). The Coriolis force is also well documented in these fjords and is very influential in controlling the deposition of suspended particles (Gilbert, 1982a; Gilbert, 1983; Syvitski, 1989; Syvitski and Shaw, 1995). The force causes a noticeably higher

accumulation of sediment along the southern side of the fjords as compared to the north (Gilbert, 1982a; Syvitski, 1989).

2.1.2.2 Biota

Several studies have been carried out within Baffin Island fjords to catalogue the diversity of the marine benthos present in these environments. During the 1982 cruise of the *CSS Hudson*, both grab samples and bottom photographs were collected and later analysed by George E. Farrow at the University of Glasgow (Schafer, 1983). Farrow was able to compile an inventory of the organisms inhabiting the ten studied fjords. Syvitski *et al.* (1989) re-evaluated that inventory in an attempt to relate faunal communities to stages in glacial retreat. A more recent study conducted by Aitken and Fournier (1993) was able to add thirty-eight new organisms to the list of biota recorded in three eastern Baffin Island fjords; Cambridge Fjord, Itirbilung Fjord and McBeth Fjord. However, the observations of Syvitski *et al.* (1989) and Aitken and Fournier (1993) were based on reconnaissance surveys of the fjords in Baffin Island and therefore only work by Dale (1992) on the biota of Pangnirtung Fjord can be considered comprehensive.

Dale (1992) compiled an extensive list of organisms from Pangnirtung Fjord. Eighteen classes of marine invertebrates were identified within eight phyla and an additional 3 phyla (with no class distinction) were also discovered, making a total of 270 invertebrate species. The following table lists some of the organisms identified within Pangnirtung Fjord, Baffin Island.

Distinct animal communities have a tendency to inhabit locations within the fjord associated with specific sedimentological conditions (e.g. Aitken *et al*., 1988; Dale *et al*., 1989; Syvitski *et al*., 1989; Dale, 1992; Aitken and Fournier, 1993; Holte and Gulliksen, 1998). Based on available data, some general characteristics about the communities inhabiting different subenvironments can be extracted. Fjord head environments are characterized by opportunistic mobile organisms, typically small in size. These organisms may decrease their body mass to surface area ratio as an attempt to stay above the sediment water interface in areas prone to high sedimentation rates and low sediment shear strengths (Thayer, 1979). Softground communities, typically located 5 km away from the fjord head, are dominated by ophiuroids of various sizes and burrowing anemones (Dale *et al.*, 1989). Shallow, sandy tidal flats along fjord margins are commonly inhabited by large populations of bivalve species such as *Macoma balthica* and *Mya*

Table 2.1. List of organisms recovered from Pangnirtung Fjord, Baffin Island (Dale, 1992).

Class	Family	Genus and species
Polychaeta (Errantia)	Dorvilleidae	
	Lumbrineridae	*Lumbrineris minuta*
		Lumbrineris acuta
	Nephtyidae	*Nephtys neotena*
		Nephtys ciliata
	Nereididae	
	Onuphidae	*Nothria conchylega*
	Pholoidae	*Pholoe pallida*
	Phyllodocidae	
	Polynoidea	*Enipo torelli*
	Spaeodoridae	
	Syllidae	*Sphaerosyllia erinaceus*
Polychaeta (Sedentaria)	Paraonidae	*Aricidae nolani*
	Cirratulidae	*Chaetozone setosa*
		Chaetozone sp.
		Tharyx acutus
	Flabellgeridae	*Diplocirrus longisetosus*
	Serpulidae	*Filograns implexa*
	Oweniidae	*Galathowenia oculata*
	Capitellidae	*Mediomastus ambiseta*
		Myriochele danielsseni
		Myriochele fragilis
	Opheliidae	*Ophelina abranchiata*
	Pectinariidae	*Pectinaria granulata*
	Sabellidae	*Potamilla torelli*
	Spionidae	*Prionospio steenstrupi*
		Spio setosa
	Terebellidae	*Terebellides atlantis*
	Trochochaetidae	*Trochochaeta multisetosa*
	Orbiniidae	
	Cossunidae	
	Scalibregmatidae	
	Maldenidae	
	Arenicolidae	
	Ampharetidae	
	Spirorbidae	

Class	Family	Genus and Species
Bivalvia		*Axinopsida orbiculata* *Clinocardium ciliatum* *Macoma balthica* *Macoma calcaea* *Mya truncata* *Hiatella arctica* *Nucula belloti* *Nuculana minuta* *Portlandia arctica siliqua* *Thyasira gouldi* *Yoldia hyperborea*
Gastropoda		*Acmaea* cf. *rubeila* *Buccinum sericatum* *Capulacmaea radiata* *Cylichna alba* *Cylichna occulta* *Lepeta caeca* *Littorina saxatilis* *Margarites olivaceus* *Margarites* sp. *Margarites umbilicalis* *Oenopota incisula* *Oenpota arctica* *Retusa obtusa*
Echinodermata	Ophiuroidea Echinoidea Crinoidea Asteroidea	cf. *Amphiophiura* sp. *Gorgonocephalus arcticus* *Ophiocten sericeum* *Ophiura rebusta* *Ophiura sarsi* *Ophiuroid* sp. *Stegophiura nodosa* *Strongylocentrotus droebachiensis* *Meliometra glacialis* *Stephanasterias albula*
Coelenterata		*Actinauge rugosa* *Actinauge* sp. *Gersemia* sp. *Metridia* sp. *Paraedwardsia* sp.

Class	Family	Genus and species
Isopoda		*Arcturus baffini* *Mesidotea sabini*
Sipunculids		*Golfingia* sp. *Phascolia* sp.
Ascidiacea (Tunicata)		*Ascidia prunus* *Boltenia ovifera* *Dendrodoa aggregata* *Kukenthalia borealis* *Styela rustica*
Brachiopoda		*Hemithiris psittacea*
Pycnogonidae		

truncata (Aitken and Gilbert, 1986; Aitken *et al*., 1988). Towards the fjord mouth, firmground and hardground communities include crinoids, anemones, and sponges in addition to the already prolific errant polychaete and epifaunal bivalve populations (Dale, 1992). Crinoids and bryozoans attach to large boulders and cobbles creating "faunal islands" which are not likely to be preserved in the geological record (Dale *et al.*, 1989; Aitken, 1990).

It is obvious from the data collected in Pangnirtung Fjord that more comprehensive studies are needed to identify the variety of biota present in Canadian Arctic fjords and to determine what conditions influence their distribution within those fjords. Dale (1992) was able to extend the range of several species, adding them to the list of known Arctic biota. For example, the polychaete, *Mediomastus ambiseta*, had a previous known northern limit within the Bay of Fundy before its discovery within Pangnirtung Fjord. These data expand our knowledge of the diversity of Arctic biota and will help to improve paleoenvironmental reconstructions of Arctic fjords as well as contribute to a greater understanding of modern fjord tracemakers.

2.1.3 Canadian and European Fjords

Variations between fjord environments and their biological communities have been observed. The most notable difference exists between Arctic fjords and temperate ones, such as those located on the Canadian west coast and European fjords. In this section we will attempt to illuminate some of the main differences in water circulation, sedimentary environments and biological communities between Arctic and temperate fjords.

Many temperate fjords are considered to be mature fjords as their glacial source has long since receded and disappeared. It is common for these fjords to receive much of their freshwater input from winter snow melt and rain storms (Syvitski and Shaw, 1995). Though sedimentation rates are on average slightly higher than in Arctic fjords, the content of those deposits are slightly different (Syvitski and Shaw, 1995; Schafer *et al*., 1989). Input from rivers and mountain runoff in temperate fjords are higher in terrestrial carbon than Arctic fjords which are dominated by marine-derived particulate matter (Valdenhaug and Gray, 1984; Syvitski and Shaw, 1995; Larsen, 1997). Arctic fjord sediments are dominated by organic matter derived from marine planktonic sources in the main basin with varying amounts of terrestrial carbon deposited near the head during spring melt (Macko *et al*., 1987). The composition of the temperate fjord waters is also highly polluted due to the increase in human activity relative to their locations (Mirza and Gray, 1981; Larsen, 1997).

Due to the higher summer temperatures, temperate fjords are prone to thermal stratification of basin waters (Voldenhaug and Gray, 1984; Syvitski and Shaw, 1995). Warm ocean water suppresses temperature-induced circulation at the fjord mouths. This commonly leads to anoxia in the deepest part of the fjord basins. This process is typically aided by the presence of shallow sills. Wind mixing of surface waters is also of lesser importance in temperate fjords than it is in Arctic fjords; strong Arctic winds cause turbulence and wave-induced mixing of freshwater at the surface (Gilbert, 1983; Syvitski, 1989; Syvitski and Shaw, 1995). The limited extent or absence of sea ice in temperate fjords may also be a restrictive factor in the promotion of vertical circulation as a result of brine rejection during sea ice formation (see section 2.1.1 Fjord Models; Gilbert, 1983).

The biological community present in temperate fjords does not vary greatly from that of Arctic fjords when examined at the family level. On a species basis, temperate fjords tend to be more diverse likely in response to the more favourable seasonal temperature range. However, oxygen stratification of bottom waters in temperate fjords causes a significant difference in the diversity of the endobenthic community as compared to that of Arctic fjords.

In Norwegian fjords, the capitellid *Heteromastus filiformis*, which is well known for creating deep, branching conveyer-belt type burrows, has been recorded extensively. (Schäfer, 1952; Cadée, 1979; Gingras *et al*., 2008). While *Heteromastus* is absent in Arctic fjords, the capitellid

Mediomastus sp. was documented in Pangintung Fjord, Baffin Island, Canada (Dale, 1992). While both genera are similar in body morphology, there has yet to be documented proof of *Mediomastus* producing burrows in recent marine sediments similar to those of *H. filiformis* (Schäfer, 1952; Cadée, 1979; Gingras *et al*., 2008).

Bivalves occupying intertidal sand flats are typically dominated by active burrowing tellinids (e.g. *Macoma* sp.) in both Arctic and temperate fjords while muddy substrates are inhabited by nuculids (e.g. *Yoldiella* sp., and *Nuculana* sp.) in Arctic fjords (Dale *et al*., 1989; Holte and Gulliksen, 1998; Oug, 2001). A member of the temperate community, which was only recently observed in Arctic fjords (see Dale, 1992), is the genus *Thyasira* which produce deep, dendritic, intricate structures in muddy substrates (Dando and Southward, 1986; Seilacher, 1990; Holte and Gulliksen, 1998). In addition to these taxa, studies of temperate fjord biota have documented a more diverse association of arthropods (including ostracods, isopods, amphipods, and decapods; Oug, 2001).

The work by Dale *et al*. (1989), Syvitski *et al*. (1989), Dale (1992) and Aitken and Fournier (1993) have broadened our knowledge base of Baffin Island fjord benthos. It is clear, however, that more comprehensive studies must be performed within Canadian Arctic fjords before an accurate comparison between benthic communities within temperate and Arctic fjords can be considered.

2.2 Ichnology

This section will highlight aspects of the study of ichnology that are key in deciphering animal-sediment interactions at different scales of analysis. It will provide a basic introduction to the principles of ichnology and the guidelines followed for describing biogenic structures in recent sediments and in the fossil record.

Ichnology is the study of trackways, trails, burrows or any behavioural structure produced by organisms as they interact with the substrate and surrounding environment. *Trackways* are composed of a succession of footprints (e.g. tracks) left most commonly by vertebrates and insects in continental settings, but also produced by the walking motion of many marine arthropods on the ocean floor. A trackway is defined as a repetitive series of disconnected impressions made by the coordinated action of walking appendages of one organism while a

track refers to an individual impression of an appendage (Bromley, 1996; Seilacher, 2007; Buatois and Mángano, 2011a).

Burrows are permanently maintained structures that fulfill the basic needs of the organism for shelter and protection (Bromley, 1996). As a result, burrows provide the producer with a sheltered area to feed and respire. Burrows can be very simple, containing only one tunnel with no branching (e.g. *Skolithos*), or they can be quite complex forming vast networks such as the trace fossil *Thalassinoides*. Burrows may be constructed in a wide variety of ways (e.g. using peristaltic movements, push-and-pulling, circular shovelling).

A continuous trace produced on the surface of the sediment or very shallowly is referred to as a *trail*. An example of a grazing trail is *Archaeonassa* which consists of a flattened or bilobate central area with raised ridges on the margins (Buatois and Mángano, 2002; Jensen *et al.*, 2006). This trail has been attributed to gastropods based on the analogy with modern structures, but it can be produced by other organisms using essentially the same locomotion mechanism (e.g. glide-crawling *sensu* Buatois and Mángano, 2011a). The general term *"trace"* includes trackways, burrows, intrusions, and trails produced in soft substrates and also includes borings produced in hard substrates.

Ichnology is fundamentally the study of animal behaviour as understood in its interactions with the substrate. Epibenthic and particularly endobenthic communities represent the main focus of ichnology though nektonic organisms, such as fish, may also leave a significant ichnologic record (e.g. de Gibert *et al*., 1999). Bromley (1996) stated that animals create traces for several reasons; to feed, to find shelter and protection, but also during the processes of locomotion, resting, and predation. Learning how to identify key features in the morphology of biogenic structures (e.g. ichnotaxobases) is crucial to deciphering the ethological meaning of biogenic structures. How we name a distinctive biogenic structure (e.g. the ichnotaxonomic classification) is based on a careful analysis of the morphology of the structure considering its mode of construction and filtering out any taphonomic constraints. Accordingly, the ichnotaxonomic classification is morpho-ethologic (*sensu* Bromley, 1996, see section 2.2.2). The morphology of a trace reveals the ethology of the producer and is the foundation of the name. It is also important to outline another fundamental principle of ichnology: the same biogenic structure can be

produced by multiple tracemakers (e.g. behavioral convergency) (Bromley, 1996; Buatois and Mángano, 2011a).

2.2.1 Neoichnology vs. Paleoichnology

There are two branches of ichnology. Neoichnology is the study of modern biogenic structures, and represents a branch of ichnology concerned with an organism's relationship to the substrate in which it lives, from a biologist's perspective (Bromley, 1996). Paleoichnology studies the preserved biogenic sedimentary structures found in rock, and investigates animal-substrate relationships through time in a variety of environments. Paleoichnology also looks at trace-fossil assemblages and how they change over time within stratigraphic successions (Bromley, 1996; Buatois and Mángano, 2004). The study of paleoichnology includes also careful evaluation of taphonomic processes that are involved in the final product: a particular ichnofabric or a trace fossil assemblage hosted in a rock.

2.2.2 Classification of Trace Fossils

Three types of classification schemes have been proposed to describe trace fossils. These classification schemes emphasize different aspects of trace fossil formation: its relation to the substrate as a casting medium (e.g. stratinomic classification), its behavioral interpretation (e.g. ethologic classification), and the binomial classification (e.g. based on morphology as a reflection of the function and independent from the binomial biologic classification). In the present study, Holocene structures are named at the ichnogenus level using the term "incipient" before the ichnogenus, if its morphology is identical to previously defined trace fossils. Stratinomic, ethologic and ichnotaxonomic (binomial) classifications are briefly introduced below.

2.2.2.1 Stratinomic Classifications

There have been many proposals for stratinomic classifications. Seilacher (1964) and Martinsson (1965) are the most widely used and accepted. The classification proposed by Seilacher (1964) is used in the description of the biogenic structures observed in the cores from Baffin Island, Canada.

Certain lithologies are prone to breakage along cleavage surfaces. This typically occurs in shales, whose platy, clay-sized particles have undergone compaction during lithification processes. Differences in grain size between sedimentary layers can also produce cleavage breaks or denote bedding planes, as is the case between sandstone and mudstone. Traces that occur on these surfaces are referred to as semireliefs within Seilacher's (1964) classification. These can be either positive (protruding outside of the bedding surface) or negative (extending into the host rock). A further clarification is to refer to semirelief traces on the top of the bed as **epireliefs**, and likewise, those on the sole of the bed as **hyporelief**s. It is also common within homogeneous sedimentary successions that no cleavage breaks occur or that the trace fossil is contained predominantly within one of the sedimentary layers as a 3-D structure; the trace fossil is then preserved in **full relief**. Figure 2.3 illustrates the stratinomic classification of Seilacher (1964).

Within the Martinsson (1965) classification, differentiation is made between the casting layer and the surrounding beds: for explanation purposes, we will use a sandstone layer surrounded by mudstone intervals as an example. Any trace that is preserved in full relief within the sandstone layer is an **endichnia** while any full relief trace within the mudstone (and possibly infilled with sand) is an **exichnia**. Traces on the bedding plane of the sandstone layer are **epichnia** and can be either concave or convex upon that layer. Likewise, traces on the sole of the sandstone bed are **hypichnia**, and can also be either concave or convex (Martinsson, 1965).

These classifications provide a common framework on which to build trace fossil descriptions. It is important to be familiar with all classification terminologies to better understand and interpret trace fossil studies in all cases.

2.2.2.2 Ethologic Classification

Trace fossils are grouped into behavioural categories known as ethological categories. Criteria to define these categories are based on morphologic features of the trace fossils. Figure 2.4 illustrates some of the main groups.

Resting traces are known as **Cubichnia**, and typically show anatomical detail of their producer. Ophiuroids are very common producers of the star-shaped resting trace *Asteriacites* (see Photographic Ichnologic Survey). **Repichnia** represent locomotion traces, while **Pascichnia** represent feeding as well as locomotion (e.g. tightly meandering structures such as *Nereites* or

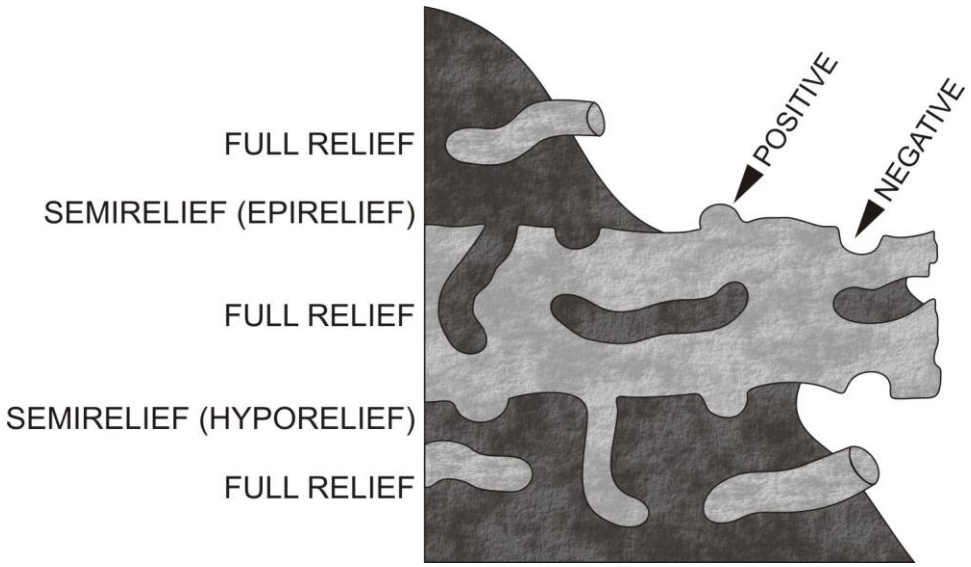

Figure 2.3. Stratinomic classification of trace fossil as proposed by Seilacher (1964) shown with two casting mediums of differing lithology. Adapted from Bromley (1996).

the bilobated *Cruziana*). Feeding traces, **Fodinichnia**, commonly contain spreite (though are not required to by definition). *Diplocraterion* is interpreted as a dwelling trace or **Domichnia** and can also be interpreted as an **Equilibrichnia** (gradual adjustment of burrow position due to accumulation or erosion of the surrounding sediment). Spreite may be preserved in the trace fossil *Diplocraterion* due to the organism's vertical upward or downward migration to maintain contact with the sediment-water interface during either periods of high sedimentation or erosion, respectively. Additional ethological categories are **Fugichnia** (escape traces), **Impedichnia** (an endosymbiotic structure within skeletal material), **Fixichnia** (anchoring traces), **Pupichnia** (pupation chambers), **Calichnia** (nesting traces), **Praedichnia** (predation traces), **Mortichnia** (death traces), and **Agrichnia** (traps and farming traces) (Buatois and Mángano, 2011a). The ethologic classification and relationships between different categories are illustrated in Figure 2.4.

2.2.2.3 Ichnotaxonomic Classification

The descriptive tools used for interpreting traces in both rock and unlithified sediments are called *ichnotaxobases*. This refers to the characteristics of the trace fossil that lead ultimately to naming it (Bromley, 1996). There are four main criteria to be observed; general form, wall and lining,

branching, and fill (Bromley, 1996). These are divided into subcategories that aid in the understanding of the organism behaviour and can help to identify the producing organism at a higher taxonomic level. The ichnotaxobases discussed here do not, however, apply to vertebrate and invertebrate trackways which have their own descriptive scheme (Trewin, 1994).

General form involves the architectural plan and spatial orientation of a trace fossil (Bromley, 1996). Networks, horizontal meandering trails, and vertical tubes are all variable forms. This criterion segregates traces on the basis of their most basic morphology, and allows them to be divided among the major groups of ichnotaxa. A common example of an ichnotaxon that is typically characterized as an open, horizontal network is *Thalassinoides*.

Wall details and the lining (or the absence of it) of burrows may provide information on an organism's movement mechanism and behaviour. There are many types that have been documented in trace fossils and modern biogenic structures. The first and most simple of these burrows, exhibits a sharp contact boundary with the host rock and an absence of a lining. Slight compaction of the burrow wall may be evident. The second is a dust film lining. Some organisms produce a mucus coating on the interior of their burrow either as a stabilizing or protective agent. The mucus is sticky and inevitably collects fine particulate matter that enters the burrow from the substrate surface, forming a dust film. This lining is typically very subtle as only the fine-grained coating is preserved but aids in the recognition of some trace fossils particularly when the burrow fill is similar to the host rock (Bromley, 1996).

Constructed walls or linings are typically the easiest to recognize and are produced as an additional burrow stabilizer. The trace fossil *Ophiomorpha* is one of the best known examples of this, having a thick constructional wall composed of pellets. This type of reinforcement is utilized in high-energy environments where substrate instability is common (see section 2.2.3 Animal-Substrate Interactions; e.g. loosegrounds). A comparable trace fossil, *Spongeliomorpha*, shows an ornamented interior wall surface, rather than a constructed wall. This burrow network is produced in a firm substrate where additional reinforcement of the burrow wall is not needed. Scratch marks produced by the organism's digging appendages are clearly visible on the interior wall.

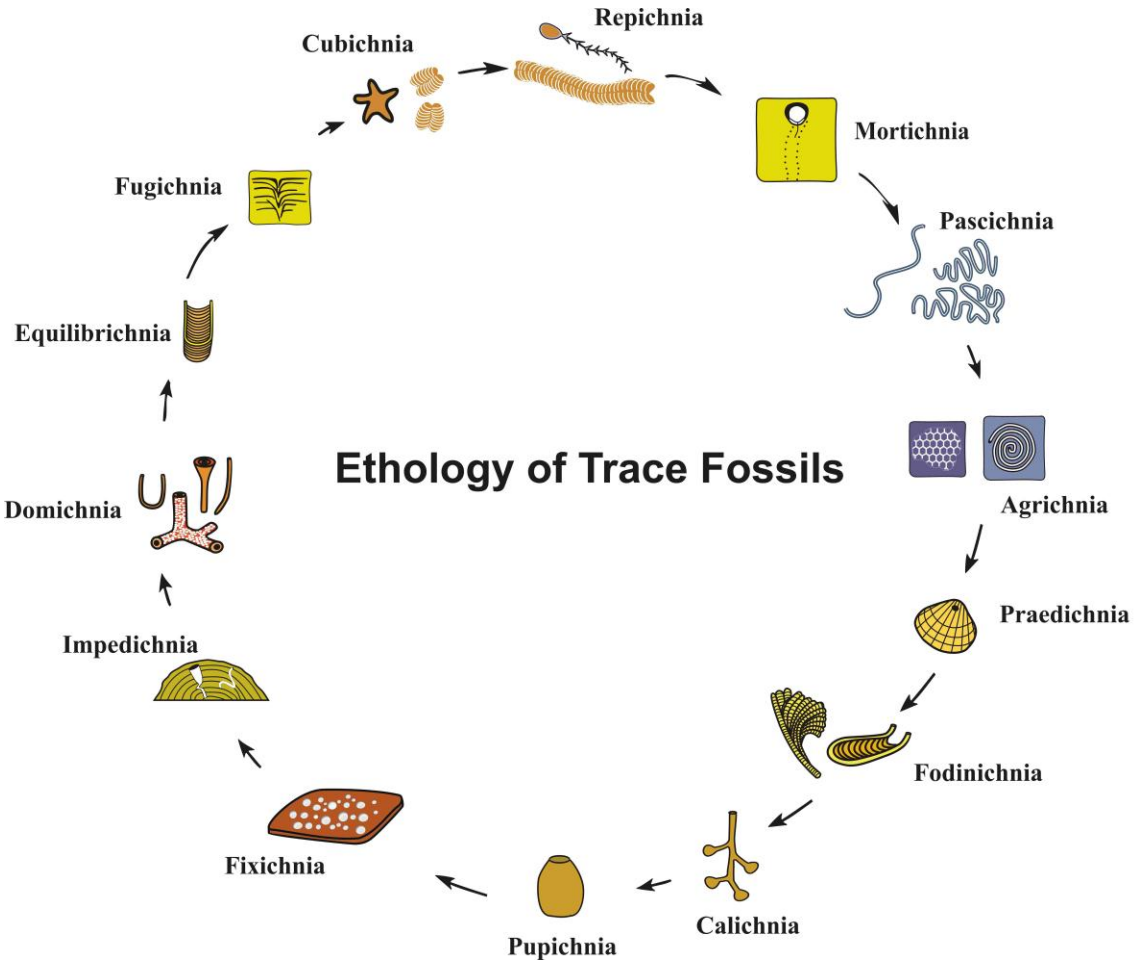

Figure 2.4. Ethology of trace fossils (Buatois and Mangáno, 2011).

The final two examples are zoned fill and diagenetic halos. In endogenic traces where the structure is immediately filled as the organism moves through the substrate, what appears to be a lining is formed as a consequence of the animals muscle contractions. Essentially, the animal uses peristaltic muscular contractions for locomotion which moves material backwards producing a lining-type fill adjacent to the main backfill called a zoned fill (see Bromley, 1996; figure 8.4). A diagenetic halo is produced during burial or lithification of the trace. It is a chemical or mineralogical change commonly resulting in a change of colour within the host rock or sediment surrounding the burrow or trace. A rusty halo can also be produced in a burrow that has circulated oxygen at depths where the sediment is anoxic. Oxidation of the burrow wall can penetrate into the host rock or sediment causing a similar appearance to a diagenetically formed

halo (Bromley, 1996). Diagenetic halos, as well as diagenetic replacements, are not considered valid ichnotaxobases.

Branching can be divided into two types: true branching and false branching. True branching is further subdivided into primary successive, secondary successive and simultaneous branching. A primary successive branching structure is produced through successive burrows originating from an original central burrow (see Bromley, 1996; figure 8.8c). Each successive burrow overlaps the previous structure as the organism retreats backwards through the original burrow. This is a common method of feeding observed in the trace fossil *Chondrites*, a typical deep-tier structure.

Secondary successive branching occurs when the original, unbranched burrow is re-used at a later time. The organism may enter from the side and proceed to re-work the fill of the original path. In simultaneous branching, the order of burrow formation is not important as the burrows are open and utilized at the same instance. This is common in many network burrow structures such as *Thalassinoides* and *Ophiomorpha*. In false branching one trace will intersect another unintentionally producing the appearance of a branch if the cross-cut burrow is not completely preserved (Bromley, 1996; figure 8.8b).

Burrow fill can either be actively produced by the organisms or can result from the passive accumulation of sediment within an open burrow. As an organism consumes organic particles (or entire grains covered in bacterial coating) within the substrate, it re-deposits them as faecal matter in the posterior end. This causes the material to have a different colour than the host sediment in most cases. The backfill will also exhibit a sort of layering of successive deposits that indicate the direction of the organism's movement. Meniscus backfill displays a layering structure where the fill contiguous to the host rock is subparallel to the boundary and overlapping with previous fill layers. This is may be confused with a type of wall lining (Bromley, 1996).

The characteristics described above are used to infer the feeding strategy and locomotion behaviour of the tracemaker. They can also provide information about substrate consolidation at the time of production. Ultimately these tools are used to provide an ichnotaxonomical description of the trace or trace fossil. If the structure is fossilized, the data collected from the ichnotaxobases can aid in placement of the trace into an ichnogenus and possibly help identify

the ichnospecies. The binomial classification of trace fossils is based predominantly on evaluating these morphological characteristics.

Bromley and Fürsich (1980) followed the recommendations of the Code of Zoological Nomenclature in the sense that trace fossils are to be named only from fossilized material. However, these authors proposed that modern structures may be described using the same criteria as for trace fossils (same ichnotaxobases) and must be named as 'incipient' ichnotaxa. This is the approach followed in the present study.

2.2.3 Substrate Consolidation and Trace Fossil Morphology

There are three main categories of substrate consolidation and three slightly more specialized cases. The main categories are soupground, softground, and firmground and apply to fine-grained substrates (Ekdale, 1985). An additional three categories include hardgrounds, woodgrounds, and loosegrounds, a term first introduced by Goldring (1995) to describe shifting sandy sediments.

Following Ekdale (1985), soupy substrates have high water contents and are incompetent allowing for little to no preservation of traces except in exceptional circumstances. Swimming strategies are the most effective means of locomotion for many animals within this type of substrate, though ploughing and other forms of locomotion are also used (Ekdale, 1985; Bromley, 1996). Softgrounds have slightly lower water content than soupgrounds and are commonly situated below the soupy sediments (Ekdale, 1985; Savrda, 1992). Softgrounds are ideal for trace production and later preservation of trace fossils, though these sediments are still prone to slight compaction with burial.

Firmgrounds are substrates that have undergone considerable dewatering and are well compacted. The sediment grains are not yet cemented together allowing organisms to burrow freely through them (Ekdale, 1985). Firm substrates typically occur at depths below normal bioturbation activity and are commonly associated with chemosymbiotic traces and some deposit feeding structures common to low oxygen environments (Bromley, 1996). Trace fossils produced in firm substrates display little to no compaction and are characterized by a sharp contact boundary with the host rock. These structures have the highest preservation potential of all previously mentioned substrate consistencies (Bromley, 1996). Exhumation and erosion of

softer surface sediments may result in a firmground substrate at the seafloor surface (Bromley, 1996).

Firmgrounds can also result from stabilization by microbial activity. This process may have been involved in distal fjord locations characterized by slow sedimentation rates under very low energy conditions. Microbial stabilization commonly increases the quality of preservation of biogenic structures (Seilacher, 2008; Noffke, 2010; Buatois and Mángano, 2011b).

Looseground applies to well-sorted sandy substrates which are prone to shifting and instability (Goldring, 1995). The trace fossil *Ophiomorpha* is commonly produced in this type of substrate as the thick wall construction enables it to withstand shifting sands. This type of substrate is typical in foreshore to upper-shoreface settings.

Burrows in hardgrounds are referred to as borings as the substrate is already or currently undergoing lithification. In either case, hardgrounds are distinguished from firmgrounds in that the sediment grains have been cemented together (Ekdale, 1985). Classical examples of borings in hardgrounds are *Trypanites* and *Gastrochaenolites*. These borings were likely produced by annelid worms and bivalves, respectively (Ekdale, 1985; Goldring, 1995).

Woodgrounds are xylic substrates or coals. Borings in these substrates are exemplified by the ichnogenus *Teredolites* (Ekdale, 1985). This ichnogenus is produced by bivalves adapted to penetrate wood, such as the genera *Teredo* and *Martesia*.

An interesting aspect of substrate consolidation is its effect on the appearance of trace fossils. The trace fossil *Protovirgularia* is produced by the locomotion-feeding activities of protobranch bivalves in tidal flat facies from the Upper Carboniferous of eastern Kansas and displays multiple preservational variants (Mángano *et al*., 1998). Several specimens were discovered having different morphologies, but essentially recording the same behaviour. These different morphologies were speculated to have come about due to differences in substrate consolidation (Fig. 2.5).

2.2.4 Ichnofabrics and Tiering

The way in which the primary sedimentary fabric has been modified by biogenic activity is known as ichnofabric. This has been assessed by the degree of bioturbation within the sediment

(see Bottjer and Droser, 1991; Droser and Bottjer, 1993; Taylor *et al*., 2003). However, several authors have noted that there are other more important aspects to be aware of when studying ichnofabrics, such as tiering relationships and ichnoguilds (e.g. Bromley 1990; Ekdale and Bromley, 1991; Buatois and Mángano, 2011a).

Infaunal tiering refers to the vertical arrangement of a community within the substrate. This can be caused by differences in feeding behaviours of the organisms, as well as the physical characteristics of the substrate (e.g. oxygen gradient). The shallow-tier is described as including the upper few centimetres of sediment below the sediment water interface, and may include the

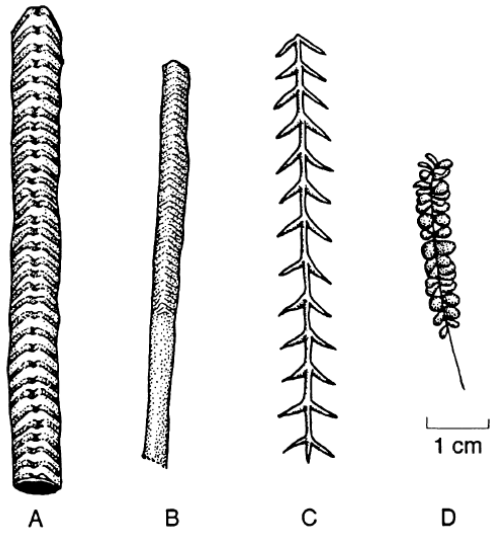

Figure 2.5. Examples of the ichnogenus *Protovirgularia*. A-B, short distance of chevron placement may indicate and increased shell friction on a firm substrate. C, longer distance of chevrons is likely related to a faster pace of locomotion due to lowered shell friction on a substrate still able to support the pull of the foot. D, irregular structure and unclear preservation of chevrons is likely due to a soupy substrate. Close proximity of each pair of chevrons may indicate difficulty in moving do to a lack of grip by the foot. After Mángano *et al*. (1998).

epibenthic region. Shallow-tier traces are typically produced in soupy substrates and are prone to severe deformation and smearing if preserved (Ekdale, 1985). Mid-tier structures are produced in soft substrates below the shallow tier. Deep-tier structures are produced in firm substrates; compaction as well as dewatering of the substrate has occurred with burial as well as dewatering (Ekdale, 1985).

An ichnoguild is a group of trace fossils that depicts a specific feeding strategy at a specific tier depth (Bromley, 1996). An ichnoguild is defined on the basis of three elements: 1) the bauplan of the structure refers to whether the organism is stationary or moving in transition to another area; 2) the source of food as it relates to the trophic level of the trace-producing organisms; and 3) the spatial location of the organism within the substrate (tiering). For example, the *Chondrites*-*Zoophycus* ichnoguild represents a stationary fodinichnia/domichnia type bauplan of deep-tier deposit feeders or chemosymbionts. Ichnoguilds are commonly applied to paleoichnological studies, though the information and the understanding of biological communities they provide are helpful for neoichnology as well.

Communities of organisms are most active at the sediment-water interface as this area typically contains the highest amount of organic matter (Bromley, 1990; Mángano and Buatois, 1999). In modern well-oxygenated environments, the uppermost part of the sediment (typically 5-8 cm) is thoroughly bioturbated, and is known as the mixed layer (see Fig. 2.6; Savrda, 1992). This also represents the shallowest-tier community, whose traces are rarely preserved due to overprinting by deeper tiers (as vertical migration occurs over time) or erased by erosion (e.g. due to episodic storm or turbidite events) (Savrda, 1992).

Below the mixed layer is the so-called transition layer where both the intermediate- and deep-tier structures can be observed (Fig. 2.6). The mid-tier mainly consists of deposit feeders, while the deep-tier is assumed to be mostly chemosymbionts or farmers (agrichnia) due to the organic matter being refractory at great depths and unable to support a deposit-feeding strategy (Walker and Bambach, 1974; Bromley, 1990; Savrda, 1992). Under normal conditions of permanent accretion of the seafloor the deep-tier traces will overprint both the mid- and shallow-tier structures. As sediment accumulation continues, the deep tier will gradually cross-cut and obliterate much of the shallower tiers. The abandoned traces at depth then become part of the historical layer and will be undisturbed by further biogenic activity (Savrda, 1992; Bromley, 1996).

Having a constant supply of oxygenated water at the sediment-water interface is crucial to the survival of benthic communities. All burrowers maintain a connection to the sediment-water interface for oxygen circulation at depth (Bromley, 1996). If conditions occur that limit the

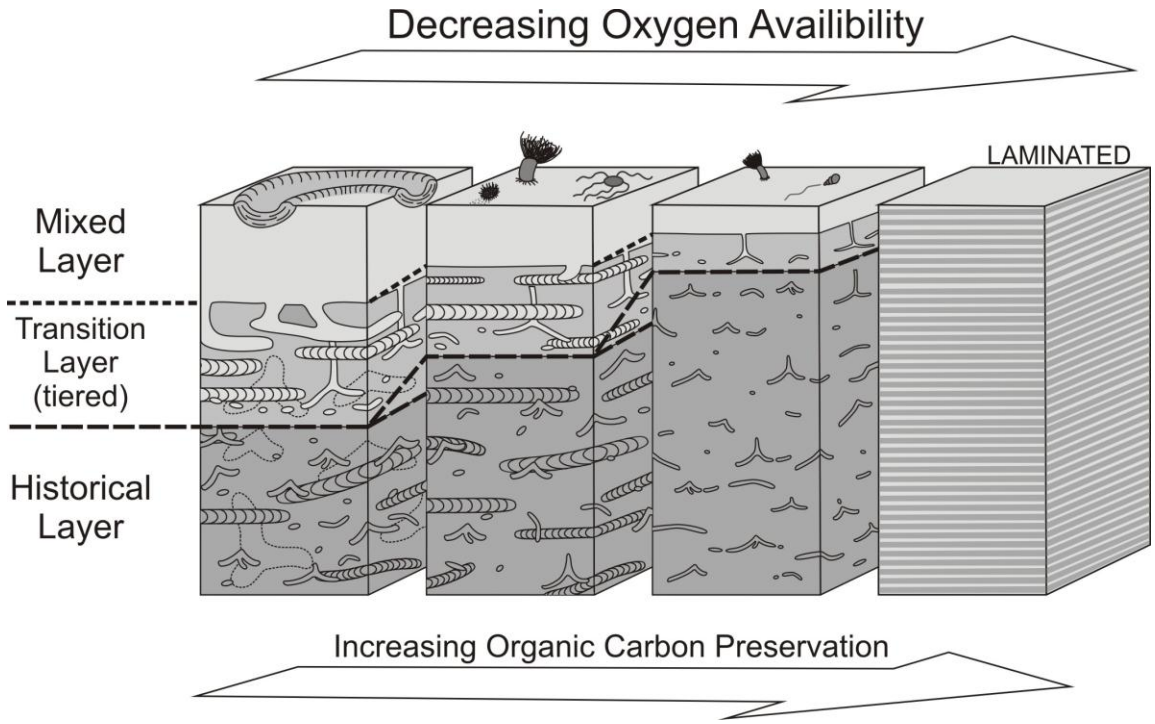

Figure 2.6. General diagram illustrating how the tiering stratigraphy and biogenic sedimentary structures may change with decreasing oxygenation. Shown in the Transition layer are *Thalissinoides* (large burrows originating from the Mixed layer of the first block), *Zoophycus* (long, horizontal backfilled structure), and *Chondrites* (small inverted Y-shaped structures). The fourth block appears finely laminated all though it may include micro- and meiofauna. Notice the diminished ichnodiversity and small size of the *Chondrites* in the third block that develops in response to the decreasing oxygen conditions. Adapted from Savrda (1992).

supply of oxygen to the sediment, the effects will be seen most clearly in the diminishing development of the mixed layer (Fig. 2.6). Shallow deposit feeding organisms of the shallow tier commonly rely on oxygen within the pore space of the sediment grains for respiration. If the oxygen levels deteriorate to the point where there is minimal oxygen penetration into the sediment, it is likely that both the shallow- and intermediate-tiers will be absent with only a very undersized deep-tier traces remaining (see Bromley, 1996; figure 12.1).

2.2.4.1 Tiering in Response to Sedimentation

There are three models that depict how a tiering structure may develop in response to specific sedimentation conditions. For the purpose of our example, let us consider an endobenthic community composed of three basic tiers: shallow, intermediate and deep. First, sedimentation can be gradual (background sedimentation), causing the gradual upward migration of all three tiers as they maintain a connection with the sediment-water interface (Fig. 2.7, center block). The ichnofabric preserved from this is commonly very highly bioturbated with a clear dominance of

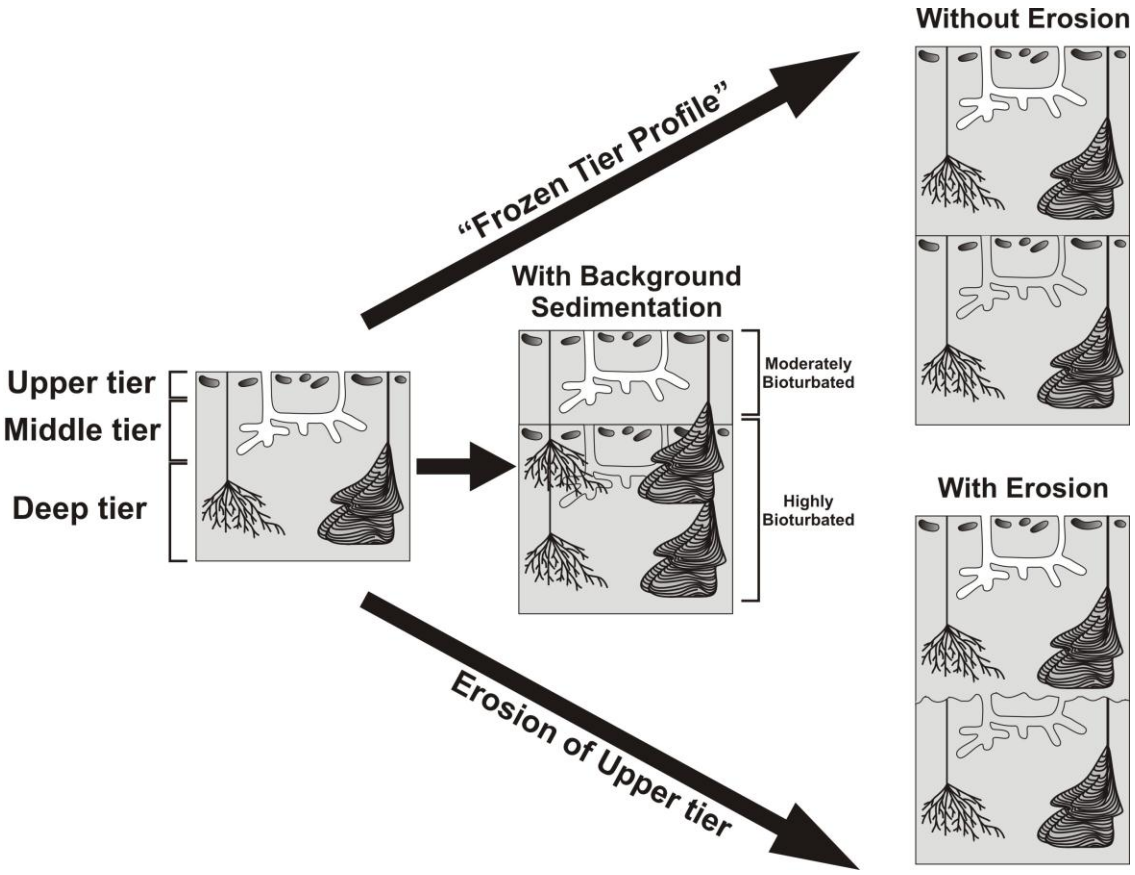

Figure 2.7. Tiering in response to variations in sedimentation rate and style (e.g. background vs. episodic). Modified from Orr (1994) and Buatois and Mángano (2011).

deep-tier structures overprinting all shallower structures (Orr, 1994). Second, if episodic sedimentation takes place there are two possibilities: sedimentation with or without erosion (Fig. 2.7, right blocks). If sedimentation occurs without erosion, all three tiers will be preserved in the layer immediately below the episodic bed (e.g. frozen-tier profile; cf. Orr, 1994), and a new community will begin to inhabit the new layer above according to the new environmental conditions. However, the most common situation will involve some degree of erosion occurring with episodic sedimentation, in which case the shallow tier will not be preserved in the recorded ichnofabric (Orr, 1994).

2.2.5 Fjord Models in Ichnology

Research conducted on modern fjord ichnology is limited (e.g. Aitken *et al*., 1988) though considerable research has focused on Paleozoic Gondwana glacial fjords (e.g. Buatois and Mángano, 2003; Balistieri *et al*., 2002; Gandini *et al*. 2007; Buatois *et al*., 2006, 2010; Schatz *et al*., 2011). Current ichnofacies models are primarily based on upper Paleozoic fjords (and some Cenozoic fjords; e.g. Eyles *et al*., 1992) and differentiate between four environments: fjord lakes, fjord head, brackish-water embayments and autogenic firmgrounds (Buatois and Mángano, 2011a). Each environment contains an association of trace fossils found to occur typically in Paleozoic and Cenozoic fjords. Fjord lakes show an abundance of epigenic traces while the other environments are almost completely dominated by endogenic burrows and feeding structures (Fig. 2.8).

Paleozoic fjords are typically accepted to be brackish water environments with salinities varying from low at the fjord head to high at the fjord mouth. However, Arctic fjords have been found to exhibit fully marine salinities at depth related to limited seasonal melting of freshwater sources (see Dale *et al.*, 1989; Syvitski *et al.*, 1989). Trace fossil assemblages are commonly impoverished in brackish water settings, resulting in smaller trace sizes and a lower abundance of structures (as compared to marine examples; see Schatz *et al*., 2011). There is also a problem

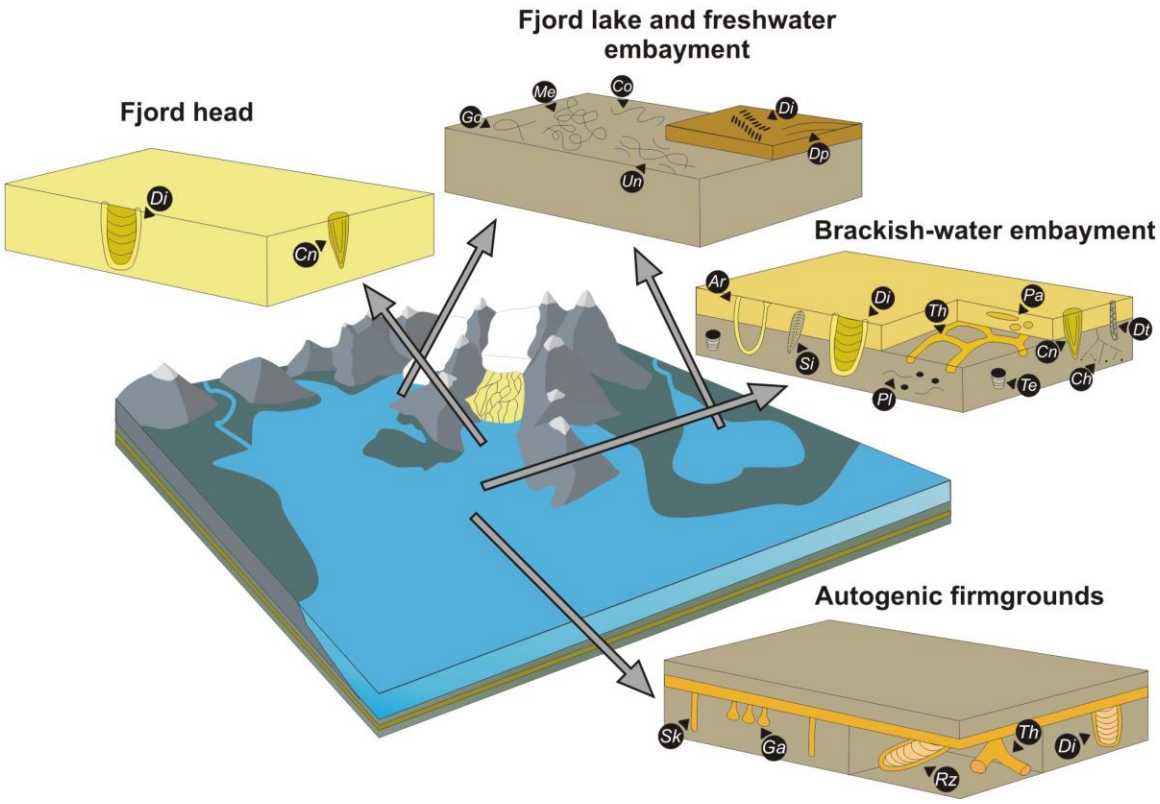

Figure 2.8. Current ichnofacies model for fjord and fjord lake environments (Buatois and Mángano, 2011a). Fjord head deposits contain *Diplocraterion* (*Di*) and *Conichnus* (*Cn*). Fjord lake and freshwater embayments are characterized by surficial trails including *Gordia* (*Go*), *Mermia* (*Me*), *Cochlichnus* (*Co*), *Undichna* (*Un*), *Diplichnites* (*Di*), and *Diploplodichnus* (*Dp*). Brackish-water embayments display a very diverse association of traces such as *Arenicoloites* (*Ar*), *Siphonichnus* (*Si*), *Diplocraterion* (*Di*), *Planolites* (*Pl*), *Thalassinoides* (*Th*), *Teichichnus* (*Te*), *Palaeophycus* (*Pa*), *Conichnus* (*Cn*), *Chondrites* (*Ch*), and *Diopatrichnus* (*Dt*). Autogenic firmgrounds typically contain *Skolithos* (*Sk*), *Gastrochaenolites* (*Ga*), *Rhizocorallium* (*Rz*), *Thalassinoides* (*Th*), and *Diplocraterion* (*Di*).

with preservation; many traces require a casting medium which differs in texture from the sediment of the fjord floor for them to be preserved. As we have discovered in many modern analogs of fjord environments, seasonal sedimentation is common and deep, narrow basins provide protection from storm activity (see section 2.1.2.1 Maktak, Coronation and North Pangnirtung Fjords). Both circumstances ensure that little sediment reaches the fjord basin in the quantities needed to preferentially preserve most traces; during the nival period, most deposition

occurs within a few kilometres of the head while storm activity rarely produces the erosion and redeposition observed in marine settings (Gilbert, 1983; Syvitski, 1989). This provides little opportunity for the preservation of epibenthic and shallow endobenthic traces, unless exceptional circumstances ensue.

3 Ichnology of Holocene Glaciomarine Sediments

3.1 Introduction

The 1982 cruise of the *CSS Hudson* collected core samples (Lehigh and piston), grab samples and bottom photographs from ten fjords in Baffin Island, Canada. Sedimentological data, geochemical analyses, studies of foraminifera communities and identification of macrofauna were undertaken and compiled for the Sedimentology of Arctic Fjords Experiment (S.A.F.E.). The purpose of this project was to collect a wide variety of data to develop a more comprehensive understanding of fjord sedimentary environments and animal-substrate interactions in the three studied fjords.

By combining ichnology with sedimentological studies of fjord environments, we gain a broader view of the conditions present within fjords. Biogenic sedimentary structures can provide information related to salinity, oxygenation, sedimentation rate and sediment shear strength. This is beneficial when dealing with environments where changes in these conditions are not evident in the sedimentology of seafloor sediments. This study has the added advantage of being able to study biogenic sedimentary structures in cores as well as on the recent seafloor using the bottom photographs collected during the original S.A.F.E. cruises. The combination of both recent and preserved ichnological records provides the unique opportunity to view a multi-tiered community and observe its response to specific environmental conditions.

3.1.1 Study Location

The three fjords, Maktak, Coronation and North Pangnirtung, examined in this study are situated on the eastern coast of Cumberland Peninsula, Baffin Island. All three fjords were carved into Precambrian bedrock during the Pleistocene glaciation by the advance of the Penny Ice Cap (Gilbert, 1982a; Syvitski and Shaw, 1995). In-fill due to glacial retreat is suggested to have begun during a warming climatic period beginning approximately 10,000 years ago (Brigham, 1983).

These fjords are confluent trenches flowing into Baffin Bay. Both Maktak and North Pangnirtung have active sandar at their heads, while Coronation Fjord receives sediment

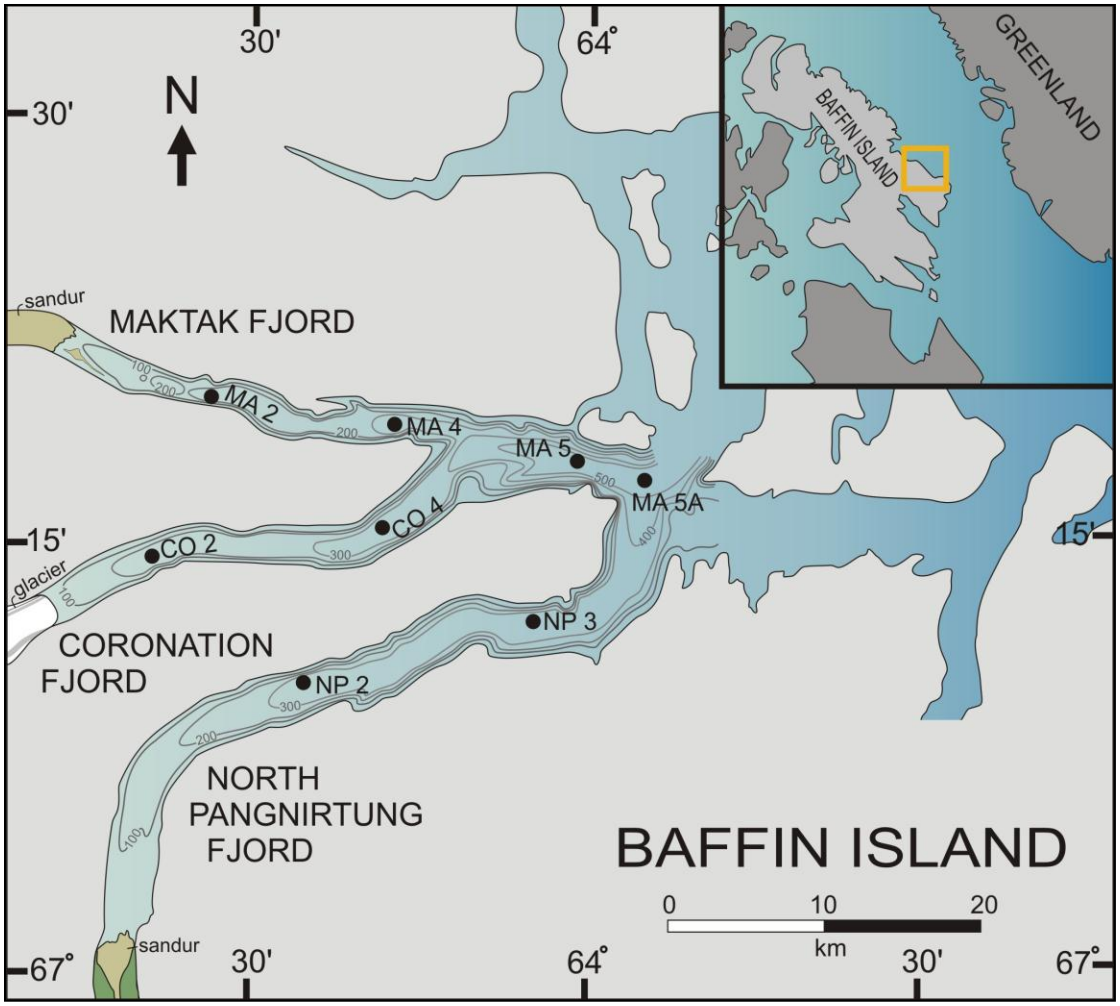

Figure 3.1. View of the three studied fjords showing depth profiles and locations of all sampled stations. Modified from Syvitski and Blakeney (1983) and Syvitski *et al.* (1987).

and freshwater input from Coronation Glacier (see Fig. 3.1; Gilbert, 1982a). All three fjords have well oxygenated bottom waters with fully marine salinities (32-35‰; Gilbert, 1982a; Syvitski *et al.*, 1989). There are no sills present in any of the fjords allowing free exchange with the waters of Baffin Bay (Gilbert, 1982a; Syvitski, 1989). Though tides are semidiurnal, the low tidal range only allows mixing to occur approximately 100 meters into the fjord at their mouths (Gilbert, 1982a).

Data were collected from eight stations within the three fjords during the cruise of the *CSS Hudson* for the Sedimentology of Arctic Fjords Experiment (S.A.F.E.; Syvitski and Blakeney,

1983). Four stations were located within Maktak Fjord, two were from Coronation Fjord and two were from North Pangnirtung Fjord. Additional information on these locations is summarized in Table 3.1. The location of each station within the fjords and their relation to each other can be seen in Figure 3.1.

Table 3.1. Summary of data for sample locations of Maktak (MA), Coronation (CO) and North Pangnirtung (NP) fjords in Baffin Island, Canada.

Station ID	Latitude (N)	Longitude (W)	Water Depth (m)
MA2	67˚19.7’	64˚33.6’	257
MA4	67˚18.9’	64˚17.0’	333
MA5	67˚17.5’	64˚01.0’	585
MA5A	67˚16.8’	63˚55.0’	575
CO2	67˚14.1’	64˚38.0’	248
CO4	67˚15.2’	64˚18.2’	356
NP2	67˚09.5’	64˚25.0’	347
NP3	67˚11.6’	64˚05.0’	333

3.1.2 Geological Setting

Gilbert (1982a, 1983) and Syvitski (1989) studied the main sedimentation processes active in the fjords of Cumberland Peninsula, Baffin Island. Four processes were described, representing the main sources of sedimentation in Maktak, Coronation and North Pangnirtung Fjords: 1) suspension fallout from brackish water overflow resulting in deposition of fine-grained sand to flocculated muds; 2) gravity flows and turbidity currents producing graded beds of medium-grained sand to fine silt; 3) deposition of coarse-grained sediment from ice rafting and coarse, often poorly sorted material from subaerial rock fall and 4) medium-grained sand deposited by aeolian transport from adjacent sandar surfaces.

Suspension fall-out appears to be the main processes occurring within the fjords, though the rate of seafloor accumulation is incredibly slow. Only a few millimetres of deposition occurs each year most everywhere within the fjords except for locations proximal to the fjord heads (within 5

km distance; Gilbert, 1982a). Proximal to the fjord heads, large quantities of sediment are deposited in response to the sharp density contrast between the sediment laden freshwater and the more saline fjord waters. Slope failure at the fjord head contributes to the generation of turbitity flows that affect sedimentation as far as 5 km down fjord (Fig. 3.2b; Gilbert, 1982a; Syvitski, 1989).

Ice-bergs are a common occurrence in Coronation Fjord. However, only one cobble-sized dropstone was observed in Lehigh core samples from station CO4 (Fig. 3.2d), leading to the conclusion that ice rafting of large particles is not as important a depositional process as ice rafting fall-out of fine-grained material. All three fjords may be subject to fine-grained sedimentation due to melting sea ice, although the extent to which this process contributes to sedimentation is difficult to assess.

3.2 Methods

A total of eight Lehigh cores were recovered from Maktak, Coronation and North Pangnirtung Fjords during the S.A.F.E. cruise; four cores from Maktak, two from Coronation and two from North Pangnirtung. The cores were split, examined and stored in a refrigerated room at the Bedford Institute of Oceanography in Dartmouth, Nova Scotia, Canada. Sometime in the past 10 years, the cores were moved into ambient storage which resulted in the cores drying out. This is where they were being kept during their examination for this research project.

X-radiograph images of the 8 Lehigh cores were obtained from the Bedford Institute of Oceanography. The original, hard copy images show sedimentary structures and extensive bioturbation that is less apparent in the more recent digital x-radiograph images. This may be due to the deteriorating condition of the cores associated with transfer to ambient storage; the cores showed considerable shrinkage, secondary mineral growth and were strongly fractured. However, during direct observation of the cores it was clear that the burrows observed in the original x-rays were in fact biogenic structures still displaying considerably good preservation. The original S.A.F.E. report used x-radiograph images for describing and sketching the core samples; many of the burrows, mottling and sedimentary structures described in the report could not be verified during direct observation of the cores during this study.

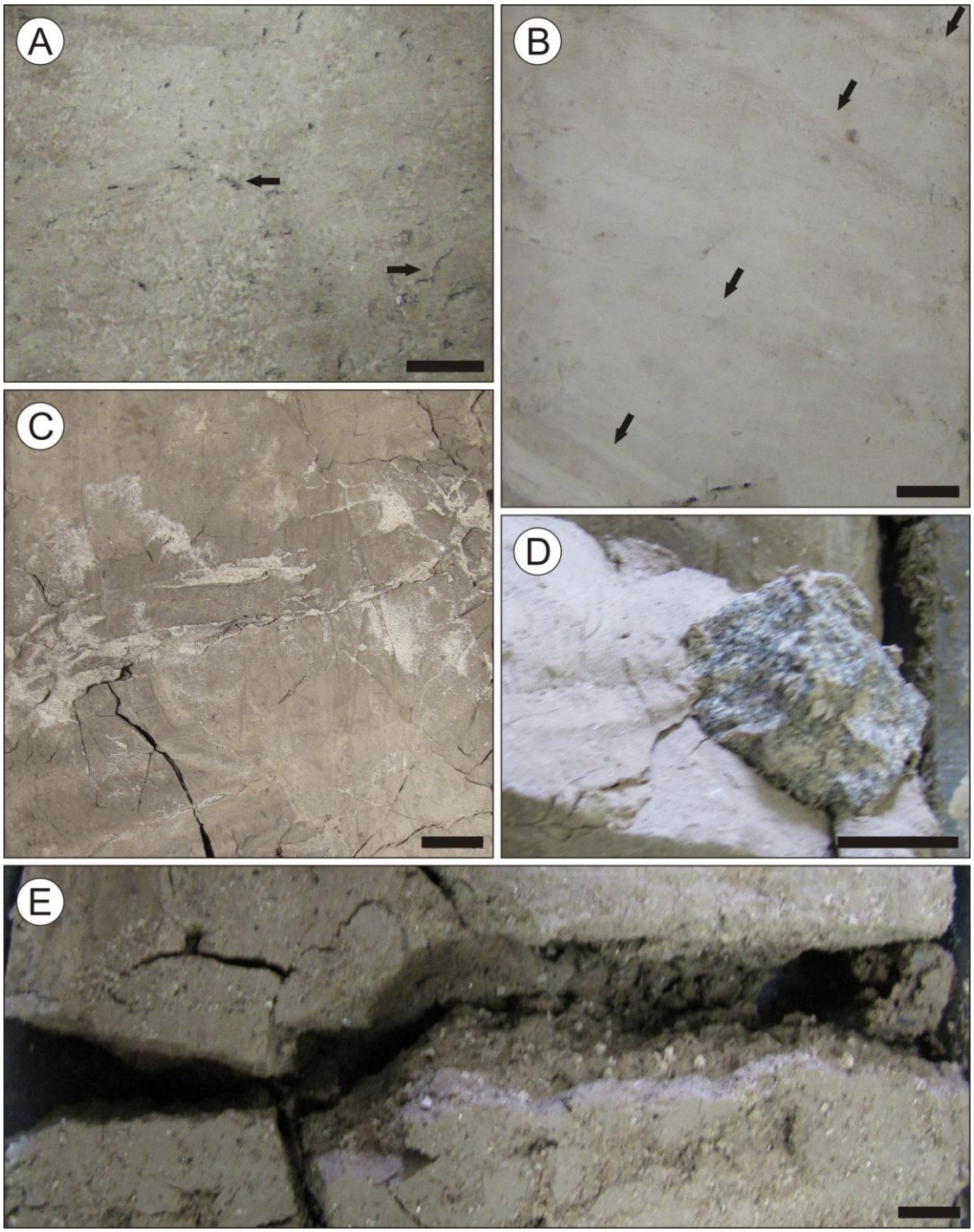

Figure 3.2. Sedimentology of Maktak, Coronation and North Pangnirtung Lehigh core samples. A, MA5 core, homogeneous fine silty clay with black, organic filled burrows throughout. B, MA5A core turbidity sequence at top of Lehigh. Arrow marks the medium to fine-grained sand bottoms of each layer. C, CO4 core with 'blobs' of coarse to medium silt interspersed within the fine silty clay matrix. D, cobble sized dropstone from CO4 core. E, coarse silt with large mica flakes forming a poorly sorted, irregular layer, likely produced through side-wall failure. Scale bars are 1 cm.

Core logs were created from examination of both sets of x-radiograph images along with the sediment grain size data compiled in the S.A.F.E. report (Hein and Longstaffe, 1983). These core logs were then compared to the actual core samples with respect to burrow location, bioturbation and grain size. Core samples were moistened, cleaned (only the working half was scraped) and photographed.

Recorded positions of geophysical and sediment grain size samples within the working half of the cores were used to determine original core depths prior to disturbance by shrinkage. However, issues still arose with core measurements and some of the core logs created for this study are slightly shorter than the S.A.F.E. report has documented (see Hein and Longstaffe, 1983).

Burrow intensity of the boxwork system, as seen in x-ray images, was confirmed in core samples (see 3.3.1 Core Systematic Ichnology below). Measurements of burrow diameters and burrow lengths were made as well as detailed descriptions of all observed burrows with respect to burrow orientation, lining and fill. The intensity of bioturbation by the boxwork burrow system was variable throughout the core logs. As traditional methods of measuring bioturbation intensity were ineffective on these millimetric-scale structures, an alternative method was employed.

When observation of a 40 cm^2 area of core showed one to five horizontal boxwork tunnels penetrating the surface of the core face, this area was described as having a low intensity (typically a 4 cm length by 10 cm width was used for split core faces). X-ray images of low intensity areas typically displayed more internal connective tunnels than could be seen in the core samples. However, sections of low intensity (as defined above) observed in the x-ray images were consistent with respect to the total number of burrows present throughout all core samples. Areas of the core with five to ten horizontal burrows appearing on a 40 cm^2 core face were designated as medium to low intensity. More than ten burrows but less than twenty are considered high to medium intensity, while more than twenty burrows are regarded as high bioturbation intensity.

Additional grain size samples were taken to verify changes in substrate consolidation observed directly in the cores (see Appendix I). These samples were extracted from the working half of the cores and analyzed using a Beckman Coulter LS230 Laser diffraction analyser located at the

Bedford Institute of Oceanography. The raw data from the Beckman Coulter LS230 were input into GRADISTAT®, run through Microsoft Excel, for a rapid calculation of grain size statistics (see Blott and Pye, 2001). These data were then used to confirm the sedimentology originally recorded by the S.A.F.E. report and any visually observed changes in sediment grain size within the core samples and to modify, if necessary, these aspects within the newly created core logs.

Through observation and documentation of the bottom photographs from the Maktak, Coronation and North Pangnirtung Fjords and comparison with the S.A.F.E data report, a table of epifaunal macrofauna relative abundance was created (Table 3.2; see Farrow, 1983). Organisms received a count of "1" for their appearance in one of the photographs of a particular station, regardless of abundance or number of individuals observed. A percentage was calculated for each type of organism based on their total count compared to the total number of photographs for each station. For example, large ophiuroids were present in eight of the thirteen photographs taken from the station CO-2, thus receiving a percent ranking of 62%. The groups of organisms were then categorized as follows: rare (r) 0-35%, common (c) 36-65%, and abundant (a) 66-100% (see Table 3.2).

3.3 Ichnology

3.3.1 Core Systematic Ichnology

A formal taxonomic classification (e.g. Linnean binomial classification) has not been encouraged for recent biogenic structures (section 8.2.1, Bromley, 1996). Traces are informally named based on general morphology (e.g. bauplan, *sensu* Bromley, 1996) and orientation. The stratinomic classification presented here is based on Seilacher (1964). The ethological classification is discussed based on a detailed morpho-functional analysis of the structures.

Boxwork burrow

Figure 3.3

Specimens: Hundreds of specimens in a total of seven cores (CO4, MA2, MA4, MA5, MA5a, NP2, NP3).

Description: three-dimensional branching burrow system. Tunnels are open with a sharp boundary, circular in cross-section. Very rarely a black, fine-grained sediment locally infills the tunnels. Tunnels are straight to curving to locally sinuous with diameters 0.89-1.36 mm, but commonly 1.04-1.11 mm. Tunnel lengths between junctions are 2.90-12.67 mm. Minor expansion at junctions may be present, 1.10-1.66 mm in diameter but commonly 1.30-1.45 mm. Junctions are typically Y- and X-shaped, but may have up to five tunnels intersecting at one point (see Fig. 3.3b). Boxwork burrows are preserved as open full reliefs within the muddy substrate of the core samples investigated.

Remarks: These networks are the most pervasive structure in the cores investigated for this study. Most of the burrows are open and empty. However, some burrows contain a black, powdery substance, either as a thin lining or as partial infill, apparently at the deepest part of the tunnel. Oxidation has also been detected covering the internal surface of or as an oxidized partial infill within the burrows. Partial infills observed in some structures are interpreted as passive, resulting from collapse. Locally, a thicker oxidation halo, about 1-2 mm thick, has been observed. Interestingly, core NP2 is characterized by an abundance of burrows with oxidized infills. This is interpreted as a secondary alteration most likely related to sealing the cores in plastic wrap before the sediments were completely dry. Wet cores taken from anoxic environments are more susceptible to oxidation when stored in plastic bags as this prolongs the time for the reaction to take place (see Hilton and Lishman, 1985).

The very sharp boundary and subcircular cross-section of the burrow, clearly indicates a firm substrate. These structures represent “elite” traces (section 6.4, Bromley, 1996). They record a relatively deep tier and are, by far, the most noticeable biogenic structures in the analyzed cores.

Distribution: The core samples are composed of homogenous silty clay with local intercalations of medium silt to fine-grained sand. The boxwork burrows have been found consistently throughout the muddy intervals of most cores. Interestingly, the boxwork burrows are strikingly absent in CO2, the most proximal station to the Coronation Glacier. Burrows penetrate thin sand layers less than 2 cm thick with one or two vertical tunnels, but are otherwise absent in thicker sand layers.

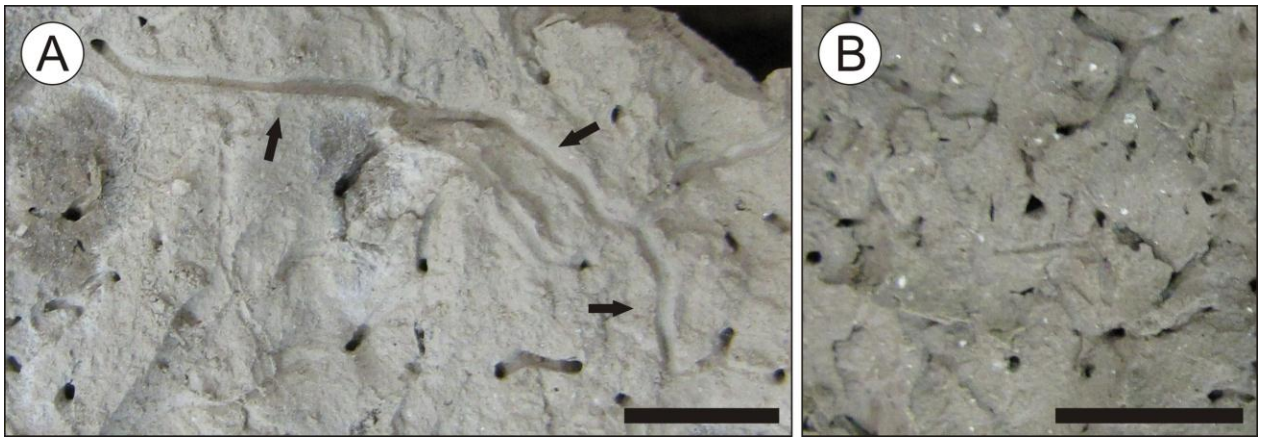

Figure 3.3. Photographs of core samples from station NP3. A, Y-shaped branching of the three dimensional boxwork burrows. Note the sinuous pattern of the tunnels (arrows). B, Boxwork burrows shown in high density where multiple tunnels intersect and branch off one another. Scale bars are 1 cm.

Simple horizontal burrows

Figure 3.4

Specimens: Sixteen specimens; four in CO4, three in NP2, one in NP3, two in MA2, and six in MA5.

Description: Horizontal, open burrows with sharp, slightly compacted burrow boundaries. Structures are straight with an ovoid cross-section. Burrow opening has a horizontal diameter of 2.33-5.01 mm with a corresponding vertical diameter of 1.55-3.63 mm. Some specimens are partially filled with sediment similar to the host sediment. Under magnification of some core specimens, the interior surface of the burrow contains corrugations (Fig. 3.4c). Overall burrow length is variable and not easily measured in core samples. However, in x-rays, burrows are typically 34-56 mm in length. The burrows are preserved as full reliefs.

Remarks: Simple horizontal burrows are relatively rare in the cores analyzed. Although no clear evidence of crosscutting with the boxwork burrows has been observed, most likely these structures record shallow-tier structures that only rarely survived the fossilization barrier. The partial infill of some horizontal burrows by sediment similar to the host sediment may be the result of downward advection and suggests that these structures were most likely connected to

the sediment-water interface and kept open by their producer(s). Additional evidence to support this interpretation is the rare presence of oxidation halos which are typically the result of active oxygen circulation within burrows (see Zorn *et al.*, 2006).

Distribution: Simple horizontal burrows occur locally in the homogenous muddy silt in most cores. These structures are common in Lehigh core tops but are also present at locations within the core sample where the boxwork burrows have relatively low density. However, they are absent in the CO2 core (see section3.5.3. Environmental Controls). Interestingly, the structures are also absent in the most distal core MA5A as well as MA4.

Incipient *Skolithos*

Figure 3.4 a and b

Specimens: Eleven specimens; two in CO4, three in MA2, five in MA5, and one in NP3.

Description: Simple, vertical, cylindrical burrows with sharp contacts showing slight compaction of the surrounding sediment. Burrows are typically straight and open, though locally show passive infill of sediment similar to the host sediment. A few open burrows were observed in the core examination showing corrugations on the interior burrow wall. Commonly, specimens display an oxidation halo. Burrow openings are commonly ovoid in cross-section providing a maximum burrow diameter of 3.10-6.23 mm with a corresponding minimum diameter of 1.68-3.54 mm. Oxidation halos, if present, typically measure 0.50-1.23 mm away from inner burrow wall. Overall burrow length varies from 28-84 mm based on observation of core x-rays. The traces are preserved as full reliefs.

Remarks: Similar to the simple horizontal burrows, incipient *Skolithos* are rare elements in the analyzed cores. The scarcity of these structures may reflect a taphonomic overprint. The presence of an oxidation halo suggests contact with the sediment-water interface and that active circulation of oxygenated water may have occurred within the burrow. They show no evidence of crosscutting with the boxwork burrow system, neither do they with the simple horizontal burrows. The ovoid cross-section of the burrows is likely a secondary effect due to deformation by hydraulic pressure during core sampling. Ethologically these structures can be interpreted as dwelling structures (domichnia) of shallow to intermediate tier organisms.

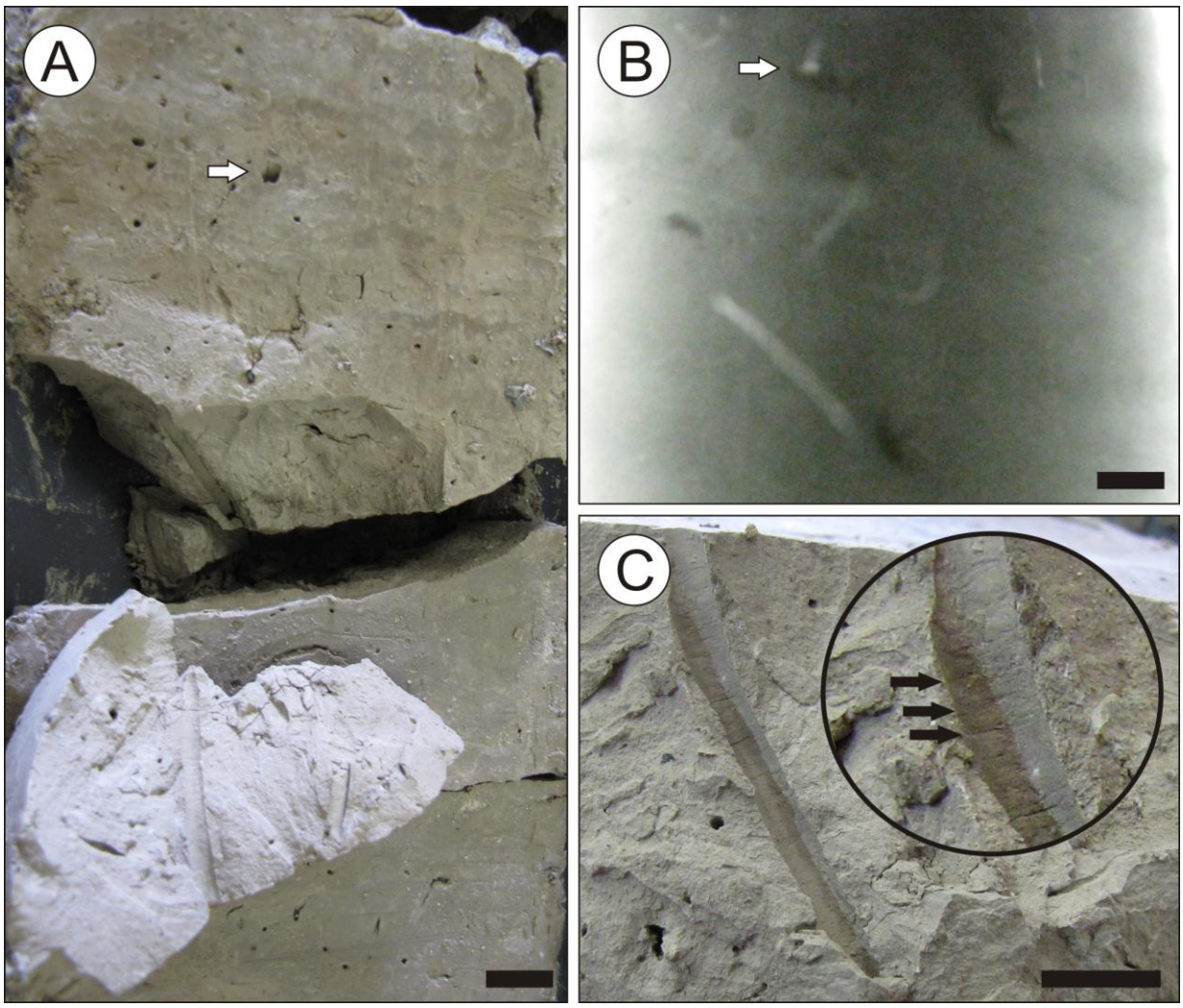

Figure 3.4. Photograph and x-ray of core sample from station CO4. A, Core sample showing both horizontal (arrow) and vertical simple burrows. B, X-ray image of horizontal (arrow) and vertical simple burrows from previous photograph. C, View of a horizontal simple burrow showing corrugations on the interior burrow surface (arrows). Scale bars are 1 cm.

Distribution: Simple vertical burrows are associated with the uppermost part of the Lehigh cores, composed of mostly homogenous silty clay, in three of the four cores. In Lehigh core NP3, one vertical burrow appears at 1.2 m depth within the core associated with a section displaying a lower intensity of boxwork burrows in homogenous silty clay (see Fig. 3.11). Two vertical burrows occur at 0.65 m in MA5, just below a normally graded layer of very fine-grained sand to medium-grained silt. There may be clear implications in the tiering position of these burrows as they occur only in sections where the boxwork burrow fabric is poorly developed.

3.3.2 Photographic Ichnologic Survey

Bottom photographs were taken during the original S.A.F.E. cruise in all three studied fjords. The photographs were obtained by releasing a compass bearing weight that triggered a Benthos stereo camera at depth resulting in a 1.68 m by 1.22 m photographed area (Syvitski, *et al.*, 1989). Bottom photographs were magnified 16 times which allowed for more accurate cataloguing of the organisms and their associated trails or burrows. Organisms were counted for abundance in each photograph.

It is clear from examining the bottom photographs that ophiuroids are a common inhabitant of all three fjords. These organisms are quite active mobile benthos and they have been caugh*t in fraganti* in movement in many photographs. Their associated traces (many resembling the trace fossils *Asteriacites* – *Arcichnus*) and trackways are clearly dominant, commonly overprinting many of the other epifaunal trails (Fig. 3.6a, b). Gastropods are locally present and in some cases produce wide, flat trails on the fjord floor (Fig. 3.5a). Other members of the community include onuphid and other tubiculous polychaetes, burrowing anemones, asteroid echinoderms (starfish) and holothurians (Fig. 3.5b, c). Unfortunately, reliable identification of infaunal invertebrates below the family level is impossible as no living benthos were recovered from these three fjords during the S.A.F.E. cruise; single and paired burrow openings are commonly seen in the bottom photographs though their orientation and producer/inhabitant can only be speculated in most cases.

The naming of these modern traces observed in the fjord bottom photographs follows the suggestion of Bromley and Fürsich as stated in the Bulletin of Zoological Nomenclature (1980). The word “incipient” is adopted when naming recent structures according to their fossil equivalent.

Incipient *Archaeonassa* (Large)

Figure 3.5a

Description: Smooth, horizontal trails with raised marginal levées. Trails are straight to gently curving. The central depression is flat to slightly convex with an internal width of 16-18 mm. Raised levées are irregular in shape. Levées have a width of 2-8 mm giving a total trace width of

18-36 mm. Recorded as grooves with adjacent rims (e.g. negative epireliefs with positive relief marginal levées). The gastropod producer is commonly observed at one end of the structure.

Remarks: The trace fossil *Archaeonassa* is described by Jensen *et al*. (2006) as either a bilobate trail or a trail consisting of a central area with raised marginal ridges on either side. This is typically seen as a positive epirelief, similar to the example shown in the modern seafloor (Fig. 3.5a).

The levées of the modern trail show considerable variation within individual specimens. The nature of its formation may lead to this inconsistency; the producer is pushing sediment aside as it travels. However, these are buccinid gastropods which are known predators/scavengers of some bivalve species and barnacles (Himmelman and Hamel, 1993). The substrate surface appears very mottled in the photographs making identification of the true levée difficult to determine in some cases.

Location Site: Four specimens of large incipient *Archaeonassa* have been observed in three of the bottom photographs: CO4-3-4, MA2-3-1, and MA5-3-4. The trails were observed in association with small and medium incipient *Archaeonassa* specimens and surficial burrow openings. Large ophiuroids are also commonly observed in the photographs.

Incipient *Archaeonassa* (Medium)

Figures 3.5b

Description: Horizontal trails with raised marginal levées. Trails are straight to sinuous, locally producing a circular arrangement. Cross-cutting of more than one specimen is common. The central area of the trail is concave and has an irregular surface, intermittently showing striations parallel to the direction of movement. The trail is 5-11 mm in diameter. The raised levées are 1-3 mm thick. The central furrow gradually curves upwards into the levée with no sharp contact or separation between the two. Splays in the outer boundary of the trail can be seen on sharply curving specimens. The trails appear as furrows (e.g. negative epireliefs) with positive relief levées forming at the margins. Onuphid polychaetes have been observed directly associated with these structures (Fig. 3.5b, top center).

Remarks: This smaller form of incipient *Archaeonassa* also fits with Jensen *et al*. (2006) description of the Ediacaran *Archaeonassa*. Though morphologically quite similar, this trail is lacking the sharp contact between the flattened central area and raised levees seen in the larger version. The splay observed in tight turns reveals a long-body tracemaker, and is a significant morphologic difference with large *Archaeonassa*.

The density of this modern structure is high in photograph locations where onuphid polychaetes are abundant. Rarely, a sharp turn in the trail direction can be observed which contains straight, narrow impressions radiating outwards from the outer edge of the curve (see Fig. 3.7b, lower center). This addition to the typical trail structure is likely a by-product of the long body size and limited flexibility of the producer's constructed tube.

Location Site: Numerous specimens are found throughout the photographs from CO4 and MA4 stations. Other photographs containing rare specimens are CO2-3-5, MA2-3-1, NP3-4-1, and NP3-4-4. These sites correspond exactly to the observed distribution of the onuphid polychaete population within all three studied fjords (see Table 3.2).

Incipient *Archaeonassa* (Small)

Figures 3.5c

Description: Horizontal trail with raised marginal levées. The trails are straight to sinuous, locally producing a semi-circular arrangement. The levées are prominent, rounded, extending up and outwards from the central furrow. Cross-cutting is rare among specimens. The central depression is narrow not exceeding 3 mm in width. Marginal levées are typically 3 mm in fresh specimens, ranging to a maximum of 6mm in some examples. The trail length is 15-72 mm. Marginal levees appear as positive relief ridges on either side of the narrow depression.

Remarks: The small incipient *Archaeonassa* best resembles the bilobate structure of the Ediacaran trace fossil *Archaeonassa* as it contains such a narrow central area whose base cannot be easily observed (cf. Jensen *et al*., 2006). In fresh specimens, this is readily apparent; however, with time specimens are prone to collapse and widening of the central area. This is likely a preservational outcome of being produced in softgrounds.

Though the producer is absent from the modern seafloor photographs, it is common to observe a holothurian at what appears to be the terminus of the trace. This occurs in several photographs (see Fig. 3.5c), though it is unclear whether the holothurian is actually producing the trail or its presence is simply coincidental. Throughout all three fjords, holothurians are common, commonly occurring in numbers as high as 40 per photograph. Only twice are individual holothurians observed 'producing' these structures; otherwise these organisms do not appear to be visibly altering the sediment surface at all as they typically hold their bodies above the substrate surface walking on their tube feet.

Location Site: These modern structures appear predominantly in photographs taken from MA2 station: MA2-1-5, MA2-2-4, MA2-3-1, MA2-3-3, and MA2-3-5. There is one occurrence in the photograph MA4-2-1, which is the second of two photographs exhibiting holothurians 'producers' (the other being MA2-3-5; see Fig 3.5c).

Incipient *Asteriacites*

Figures 3.6a and b

Description: Star-shaped horizontal impressions with a central pentagonal disk and five arm indents. The central disk impression may appear slightly convex in some specimens, but it typically concave. Two size cohorts can be distinguished: large specimens with a disk diameter of 30-55 mm, and smaller specimens with a disk diameter 7-18 mm, but commonly 10-15 mm. Arm depressions are typically straight to slightly curving. Arm length is 44-160 mm, but typically 100-132 mm in large specimens. Small specimens show arm lengths of 10-40 mm. Arm morphologies are diverse and commonly poorly preserved in small specimens, which clearly display a smaller arm length/central disk diameter ratio. Arm width is larger proximal to the central disk depression, tapering off toward the tip of the arm. More than one arm depression may be present in close proximity creating a branching appearance. A second, rarer morphotype lacks the central pentagonal disk impression and all five arm impressions simple merge to a point (Fig. 3.6b). Incipient *Asteriacites* are recorded as negative impressions on the sediment surface. The ophiuroid producer can be closely associated with the trace, though in some cases the producer is absent from the picture.

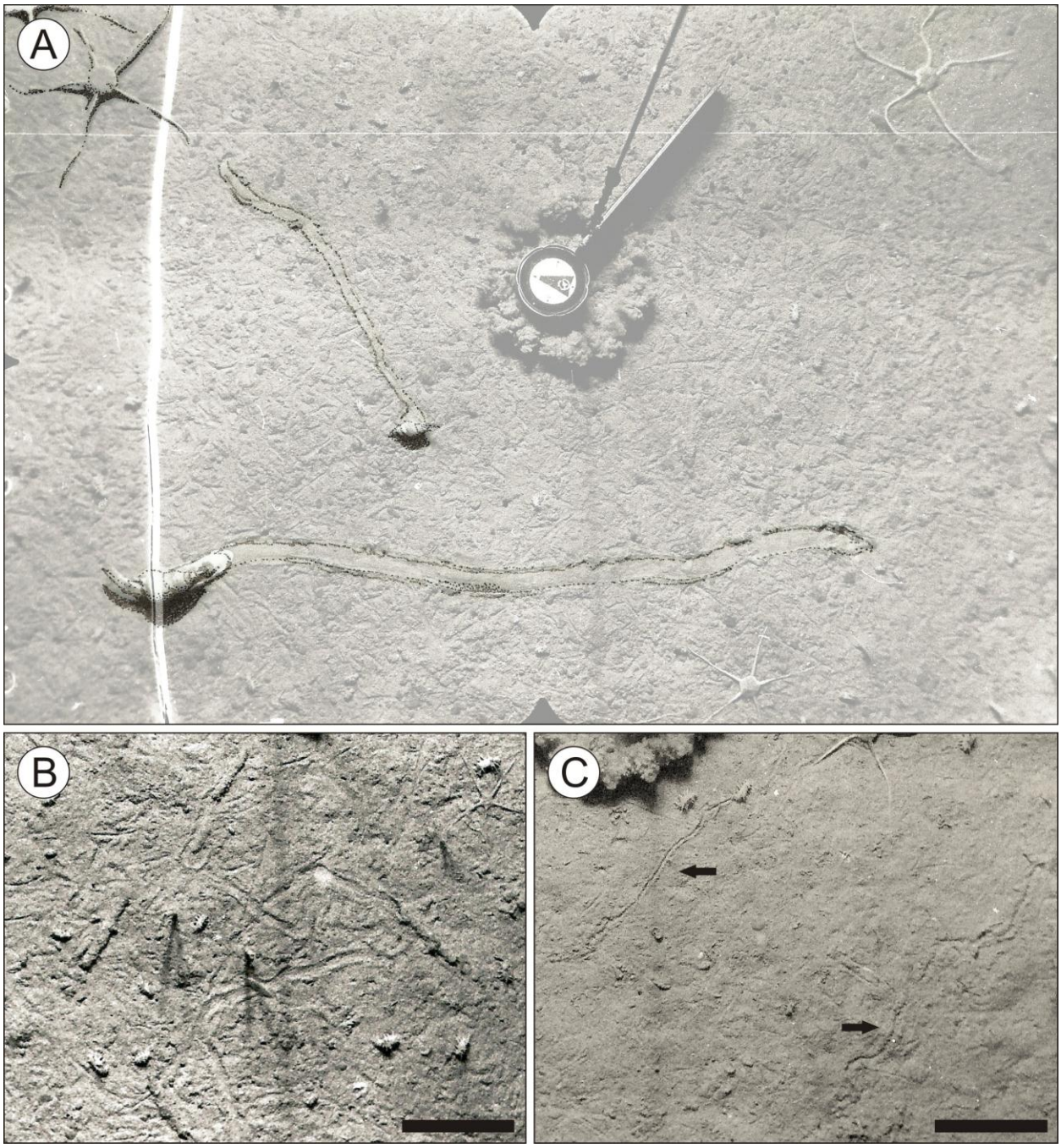

Figure 3.5. Incipient *Archaeonassa*. A, Photograph MA5-1-2, large and small gastropods (Family Buccinidae) producing a trail similar in morphology to the trace fossil *Archaeonassa*. Sketch overlay has outlined the trails and their producers on the sea bottom. B, Photograph MA4-1-4, onuphid polychaetes producing medium *Archaeonassa*-like trails. C, Photograph MA2-3-5, very small *Archaeonassa* l with unknown producer. One fresh trail with holothurian suspiciously stationed at the assumed trail terminus (left arrow) and one old trail (right arrow) are featured. Scale bars are 10 cm. Diameter of the compass weight is 7.5 cm.

Remarks: Incipient *Asteriacites* very closely resemble the trace fossil *Asteriacites lumbricalis* (Seilacher, 1953; Mángano *et al*., 1999). If present, the diameter of the central impression is typically smaller in *A. lumbricalis* than in the observed modern examples. This may be due to a difference in size of the producing organisms, though the general morphology of fossil and recent traces is quite similar. However, arm lengths of the modern resting trace are considerably greater than the trace fossil. This may be due to different preservation and behaviour recorded by modern and fossil examples. The most common preservation of *Asteriacites* is as positive hyporeliefs, typically at the sole of sandstones. Ophiuroid burrowing activity results in a central disk deeply immersed within the sandstone, the arms extending upwards with the tips attached to the sediment-water interface. On the contrary, incipient *Asteriates* illustrated herein record the activity of epibethic ophiuroids that simply rest on the muddy substrate; these impressions (negative epireliefs) tend to reflect more accurately the length of the arm of the producer. Interestingly enough, incipient *Asteriacites* has no preservational potential other than exceptional cases in which they may be casted (and not eroded) by a sandy turbidity current.

The second morphotype, though incredibly rare, more closely resembles the trace fossil *A. quinquefolius* rather than *A. lumbricalis* (Seilacher, 1953). Seilacher (1953) discussed that the production of *A. quinquefolius* is related to the activity of the tube feet of asteroids (starfish) which possess less flexible arms than ophiuroids. The absence of a disk impression is related to the sweeping action of the proximal tube feet, the arms remaining relatively stationary and extended on the sediment surface. In the specimens analysed herein the difference in appearance is most likely not related to a different tracemaker. It may simply record a change in behaviour of the ophiuroid, using a "sweeping mechanism" more akin to asteroids, or may be the product of collapse of the central part of the structure exposed at the sediment-water interface.

Location Site: The resting structure is common in both MA2 and NP3 station photographs with appearances in photographs CO2-3-3, CO4-2-2, and MA5-2-5.

Incipient *Helminthopsis*?

Figure 3.6c

Description: Meandering trail containing an irregular compressional boundary. Diameter of the trail with rim is 1-2 mm. Length is typically 40-88 mm. There is no cross-cutting of specimens. These traces are preserved as impressions on the sediment surface.

Remarks: The trace fossil *Helminthopsis* is considered to be a grazing trace which could be produced by a wide range of animals, including annelid worms in brackish to fully marine settings (Buatois *et al*., 1998). Though the trace fossil can be preserved as either a positive hyporelief or a negative epirelief, it is thought that preservation of the modern structure would require non-erosional burial by fine-grained material which would result in it being cast and preserved at the base of that layer. This may be difficult in the current setting as the trail only occurs in the most soupy of substrates observed in the modern bottom photographs from Coronation Fjord station CO2. Soupgrounds are commonly poor mediums for trace fossil preservation.

Location Site: 2 specimens appear in two photographs from station CO2: CO2-1-2 and CO2-3-3.

Incipient *Ophioichnus*

Figure 3.6d

Description: Hook-shaped horizontal impressions. Locally appearing as pairs of two hook-shaped traces mirroring one another across a third, straight arm impression. The third, straight impression measures 6 cm in length. The two curved impressions form regular semi-circles with a radius of 1.6-1.7 cm. The curved impressions are separated by 1.5 cm at the top of the image and 6.7 cm at the bottom (Fig. 3.6d). Structures observed as thin, furrows on the sediment surface.

Remarks: Though this trace was only observed once in the bottom photographs of the three studied fjords, it is a very distinctive structure that resembles the holotype of *Ophioichnus aysenensis* from the Cretaceous Apeleg Formation of southern Chile (figure 8 of Bell, 2004). This ichnotaxon was interpreted as being produced by the walking motion of ophiuroids. Unquestionable locomotion trackways directly associated with ophiuroid producers are documented within these fjords, but they differ from *Ophiurichnus* (see Ophiuroid trackway, Fig.

3.7). Although they are not directly associated with ophiuroid producers, the most parsimonious explanation is that incipient *Ophiurichnus* records a less common gait of an ophiuroid trackway. The hook-like shape of incipient *Ophiurichnus* also displays similarities to the horseshoe shaped track of *Arcichnus saltatus*, though it is interpreted as a leaping trace due to the greater repeat distance between individual tracks (Sutcliffe, 1997).

Location Site: Occurs only in photograph CO2-2-4 in association with numerous small ophiuroids and surficial burrow openings.

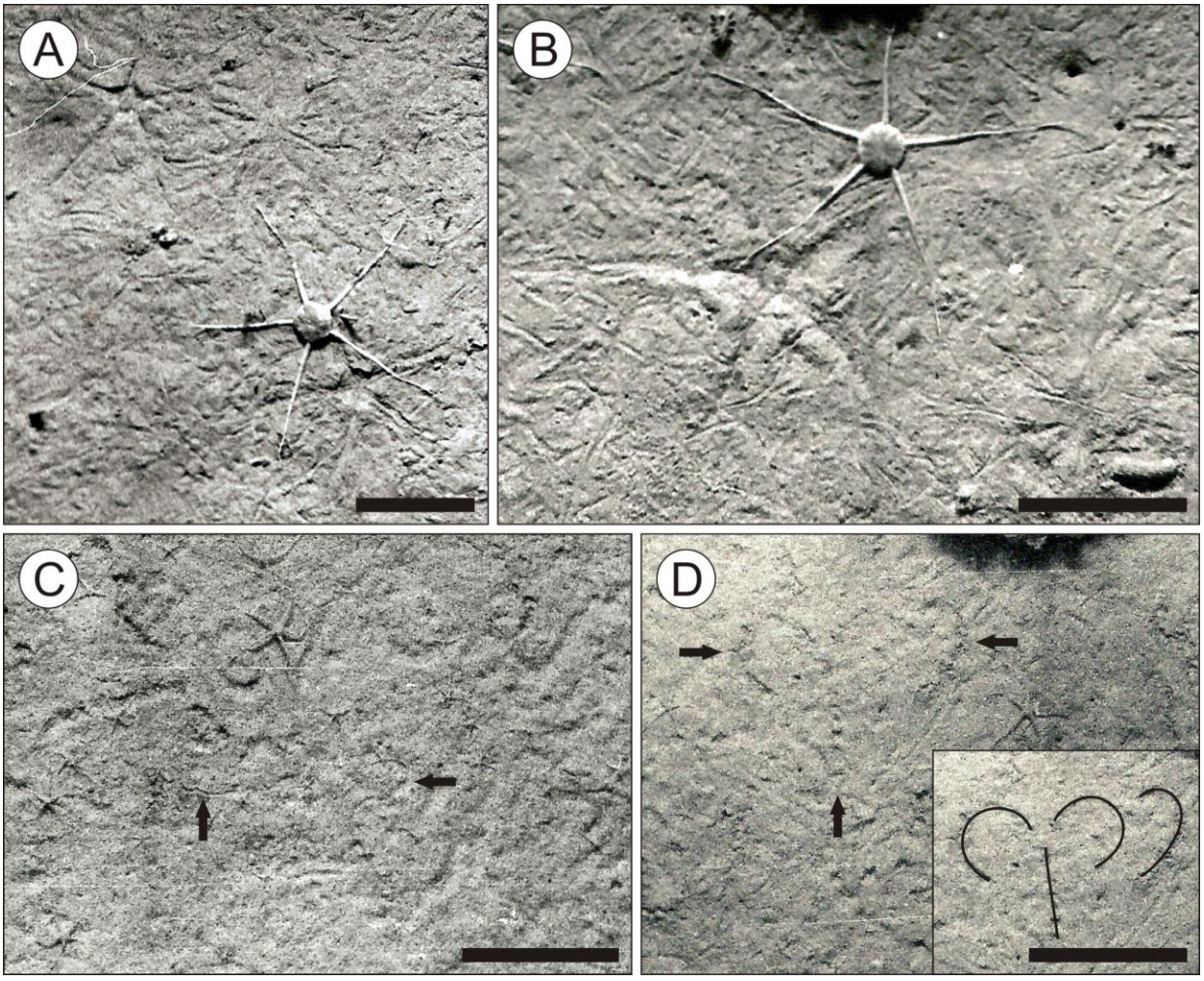

Figure 3.6. Traces from the modern sea bottom. A, Photograph NP3-4-3, two incipient *Asteriacites*, one with producer. B, Photograph CO4-2-2, morphotype of incipient *Asteriacites* in which no central disk impression is present. C, Photograph CO2-3-3, incipient *Helminthopsis* (arrows). D, Photograph CO2-2-4, incipient *Ophioichnus* (arrows) with insert indicating the location of three hook-like impressions and one straight impression. Scale bars are 10 cm.

Ophiuroid trackways

Figure 3.7

Description: Straight trackway composed of two opposing subparallel to oblique elongate impressions and one central elongate impression parallel to the midline. Individual impressions are straight to curving with a length of 2-4 cm. The widths of individual impressions are millimetric. External width between paired indents is 7.2-8.6 cm while the internal width is 3.1-5.9 cm. The distance between the same track impressions in two consecutive series (stride) is typically 6 cm but can be as low as 4 cm. Two paired impressions form a disconnected "V" pointing in the direction of movement with a third impression in front of the pair, though it is only occasionally visible. The third impression is straight, 1.7-3.5 cm in length, and typically occurs 4-5 cm in front of the "V" point of the paired impressions. A circular depression of disturbed sediment may occur at the center of the three impressions. Total trackway length is 44-96 cm. The traces are observed as negative impressions on the substrate surface.

Remarks: Most examples of this type of locomotion trackway are observed with the ophiuroid producer at the terminus. In photographs, arm impressions are difficult to track as they typically occur on an already fully bioturbated sediment consolidation. However, in a few cases a distinct track was detected (Fig. 3.7 b and c). Trackway morphology and stride length suggest that the producer is moving quite quickly across the substrate using mainly three of the five arms in a galloping style (cf. Schäfer, 1972). The disk occasionally impacted on the substrate producing a disturbed area of sediment between the arm impressions. Based on Schäfer (1972), two arms are producing a rowing motion while the other two arms act as stabilizers (the fifth arm is passive). It seems that only the impressions created by the two stabilizing arms and occasionally an impression of the passive arm are preserved in this case.

In the trace fossil record, traces associated with ophiuroids include the resting structure *Asteriacites* and the hook-shaped negative epirelief of *Ophioichnus* (Seilacher, 1953; Mángano *et* al., 1999; Bell, 2004). There is also the trace fossil *Arcichnus saltatus*, described by Sutcliffe (1997), interpreted to be the result of ophiuroid locomotion when a current is involved, allowing the producer to float between strides. However, as a whole, the modern structure appears very different from any known ophiuroid locomotion trace fossils, continuing on a straight pathway

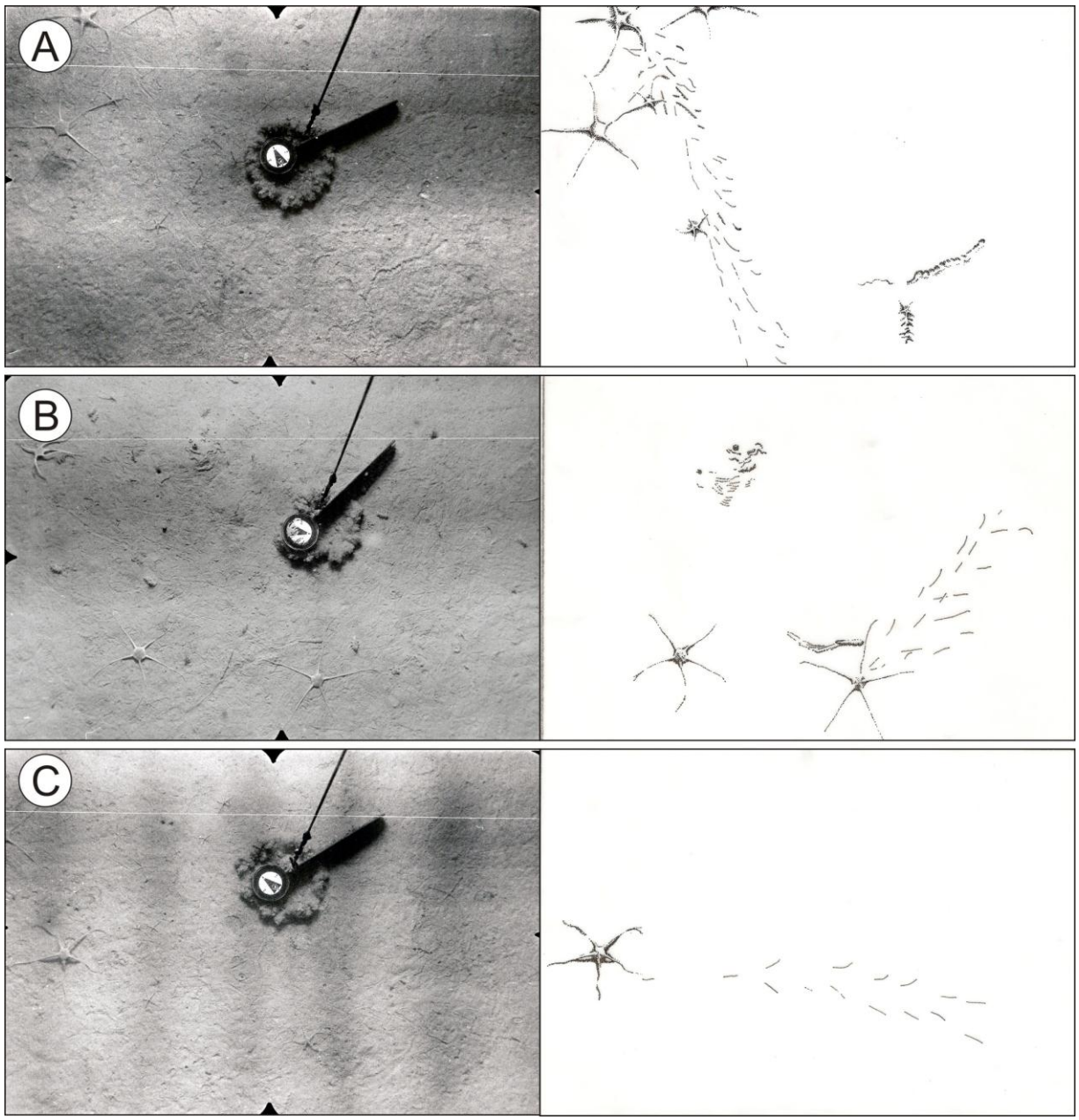

Figure 3.7. Ophiuroid trackways with producers. Original photograph of seafloor (left) with accompanying sketch highlighting the individual impressions of the trackway (right). Diameter of the compass weight is 7.5 cm.

for long distances (approx. 1 m or less is captured in photograph). This structure is moderately common throughout all photograph stations. It is likely that it is produced epigenically and does not penetrate deeply into the surficial sediment making it a poor candidate for preservation.

Location Site: Full trackways (as opposed to individual arm impressions) were observed in the following photographs: MA2-3-2, MA2-2-2, CO2-3-1, CO2-3-2, MA4-2-4, CO4-2-2, CO4-1-3, CO4-3-3, NP3-4-3, and MA5-2-3.

Series of Indentations

Figure 3.8a and b

Description: Horizontal, uniserial row of interconnected, subspherical indentations. Straight to curving, occasionally forming a circular arrangement (Fig. 3.6b, top left). Indentations have a diameter of 8-14 mm. The boundary between indentations is typically lower than the surrounding sediment though appears as a small levée adjacent to the deeper indentations. Separation between the margins of adjacent indents is typically less than 3 mm. The traces appear as negative impressions on the substrate.

Remarks: The producer of the trace is unknown as well as the mode of production. However, it does resemble other modern structures observed from the deep sea. Several authors describe similar round impressions as being produced by 'sea stars' or ophiuroids (Hollister *et al*., 1975; Gaillard, 1991). This possibility cannot be completely discarded as the structures in Coronation Fjord are observed in association with a high abundance of small ophiuroids whose disk diameters overlap the size of these indentations.

Location Site: This structure only occurs in photographs from station CO2.

Surficial burrow opening with scratch marks

Figure 3.8c

Description: Subcircular opening with grooves radiating out from it. The cross-sectional view of the main burrow opening is subcircular with a diameter of 10 mm. Grooves are overlapping with a maximum distance of 104 mm from the surficial opening. Grooves appear as negative impressions around a full relief burrow.

Remarks: Grooves appear to be surficial scraping or feeding structures. One set of long-reaching scratches is overlapped by a more proximal set to the main burrow opening. The central hole is likely part of a dwelling structure which provides protection for the producer as it grazes on the

sediment surface. The trace resembles similar fan-like grooves found in modern deep sea environments (figure 3b of Gaillard, 1991; figure 21.15 of Hollister *et al.*, 1975). It also closely resembles the burrow and surficial scratch marks of a Silurian trace fossil documented by Risk (1973). In all cases, the producer is assumed to be an echiuroid worm dwelling in the main vertical burrow and extending its proboscis out to feed on the sediment surface. It is known that some echiuroid worms produce a type of "gallery" burrow system that is mostly horizontal except for the several openings to the surface for feeding and respiration (Risk, 1973).

Location Site: Only one specimen occurs in photograph MA2-2-1.

Surficial paired openings

Figure 3.8d

Description: Two paired openings of burrows. When viewed from the sediment surface, openings are circular in cross-section. Diameter of individual openings is 6-9 mm. Total width of paired surficial openings is commonly 31-40 mm.

Remarks: These openings record connection to the sediment water interface of endichnial structures. Although the architecture of these burrows below the sediment surface is unknown, Lehigh core x-rays record several vertical simple open burrows in close proximity. Paired openings, however, are a common surface expression of U-shape burrows, which have not been identified in Lehigh core x-rays.

Location Site: Five pairs of openings were observed in the following photographs: CO2-3-3, MA2-1-4, MA2-1-5, and MA2-3-2.

Surficial single opening

Figures 3.8d

Description: Single openings of burrows. Opening cross-section in a bedding plane view is circular with a diameter of 6-11 mm. No surficial ornamentation is associated to these openings.

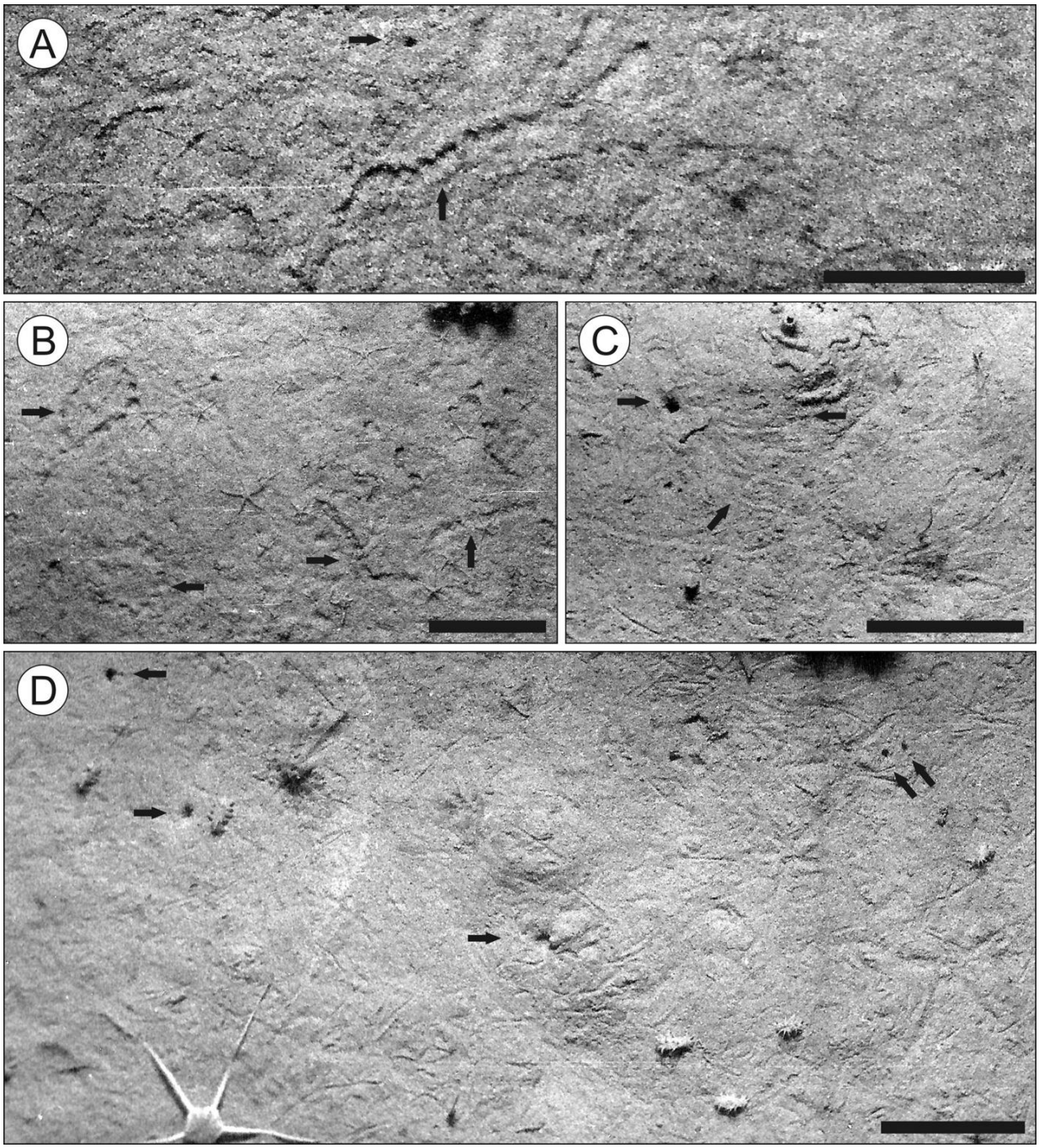

Figure 3.8. Traces from the modern seafloor. A, Photograph CO2-4-3, series of semi-circular indentations to the substrate (lower arrow) with an associated burrow opening just above (upper arrow). B, Photograph CO2-3-3, four groupings of indentations, two circular in arrangement and two straight to slightly curving. Note the numerous surficial burrow openings in the photograph. C, Photograph MA2-2-1, burrow opening (left most arrow) with surface scratchmarks extending to the right and downward from it. Also featured in this photograph, two siphon-like surface protrusions and a number of oddly arranged, elongate, positive structures. D, Photograph MA2-1-5, paired and single surficial burrow openings. Scale bars are 10 cm.

Remarks: Based on Lehigh core x-ray observations, these common single holes are presumed to represent incipient *Skolithos.* However, burrow length and morphology below the sediment surface is unknown. The buried structures most likely correspond to 3-D, full relief forms.

Location Site: Numerous specimens were observed in every photographed station within the three studied fjords.

3.4 Faunal Communities of Maktak, Coronation and North Pangnirtung Fjords

In addition to the photographic ichnologic survey, bottom photographs were used to observe and document the distribution of organisms throughout the three studied fjords (see section 3.2 Methods). Some trends in the distribution of the organisms can be seen between proximal fjord locations and more distal marine locations. Small ophiuroids are abundant in two of the most proximal fjord locations (CO2 and MA2) while rare in most others (see Table 3.2). Large ophiuroids are abundant in all locations except CO2. Tubiculous polychaetes are limited to the more distal stations and anemones only become abundant at MA5 station, being rare everywhere else.

Table 3.2. Compilation of data from visual bottom photographic survey of identifiable biota. Ophiuroid size was differentiated by the presence of two somewhat distinct groups: small ophiuroids having a disk diameter of less than 1.5cm, and large ophiuroids with disks larger than 2cm. Common (c), rare (r) and abundant (a).

Station	Large Ophiuroids	Small Ophiuroids	Gastropods	Tubiculous Polychaetes	Onuphid Polychaetes	Holothurians	Anemones	Crinoids	Pycnogonids	Paired Bivalve Siphon?	Fish	Starfish
CO-2	c	a	r	r	r							
CO-4	a	r	r	a	a	a	r	r	r	r		
MA-2	a	a	r	c	r	a	r	r	r	r	r	
MA-4	a	c	r	a	a	a	r	c	r			
MA-5	a	r	r	a	r	a	a	r	r			
NP-3	a	r	r	a	r	a	r	r	r			r

Perhaps the most curious is the distribution of onuphid polychaetes. In all three fjords, these polychaetes show a preference for intermediate fjord locations at stations CO4 and MA4. It was reported from Cambridge Fjord that onuphid polychaetes occur in high abundance near the head, while they prefer the region near the fjord-mouth sill of Itirbilung Fjord (Aitken and Fournier, 1993; figure 2). Both of these fjords are located on Baffin Island, northwest of Cumberland Peninsula (approx. 600 km northeast of Maktak Fjord). A common theme to all of these locations, including both Maktak and Coronation Fjords, is that the onuphid polychaetes occur in areas isolated from direct glacial freshwater input while also protected from directly marine conditions at fjord mouths. Cambridge Fjord contains several side-entry glaciers which supply freshwater to the fjord basin several kilometres downfjord from the head (where the highest onuphid polychaete populations are found). In Itirbilung Fjord, the onuphid polychaetes reside on the fjord side of the sill barrier some 20 km from the fjord head and several km away from the largest drainage channels on the fjord side-walls (Aitken and Fournier, 1993).

3.5 Discussion

3.5.1 Taphonomy

The boxwork burrow system contains sharp contacts with the host sediments and no compaction which signifies formation in a firm, dewatered substrate. Associated simple horizontal burrows and incipient *Skolithos* show a similar sharp contact with the host sediment but are commonly oblong in cross-section indicating that some compaction of the structure has occurred. These burrows are commonly poorly preserved and are only present in sections of the core where the bioturbation of the boxwork system is less intense. Observation of Lehigh core tops indicates that the upper few centimetres of most cores are devoid of distinct biogenic structures (Figs. 3.9, 3.10 and 3.11). Bottom photographs from the recent seafloor of all three fjords show the complete bioturbation of all surficial sediments by ophiuroids, holothurians, and onuphid polychaetes.

Following Ekdale (1985) and Savrda (1992), the shallow-tier community is associated with soupgrounds which typically make up the upper few centimetres of sediment (mixed layer). Softground substrates have undergone some dewatering and are slightly more firm than the soupgrounds. These lie below the soupground and are typically associated with intermediate-tier

structures in the transition layer (layer of tiering; Savrda, 1992). With sufficient burial, compaction and dewatering, the substrate is transformed into a firmground which lies even deeper within the transition layer, below the softground substrates, and is associated with the deep-tier community. The vertical distribution of organisms within these layers is controlled by physical (e.g. substrate consolidation) and chemical factors (e.g. oxygen and organic content; Ekdale, 1985; Savrda, 1992; Bromley, 1996).

Soupy substrates have the least preservation potential for trace fossils of all the substrate types and are typically associated with a surficial (epibenthic) to very shallow-tier community. This uppermost layer, or mixed layer is characterized by a mottled, bioturbated texture in which individual biogenic structures are not clearly discernible. Intermediate-tier structures are found in softgrounds, commonly exhibiting slight to moderate compaction. In firmgrounds, biogenic structures commonly display little to no compaction and are commonly associated with deep-tier producers. Deep-tier structures are typically the most dominant structure observed due to the simple fact that upward migration of the structure, through normal seafloor aggradation, allows it to obliterate evidence of all other tiers from the fossil record (Ekdale, 1985; Savrda, 1992; Bromley, 1996).

As the three-dimensional boxwork is the dominant structure in the cores, observations suggest that the simple horizontal burrows and incipient *Skolithos* are being overprinted by the boxwork. This also suggests that the boxwork burrow system represents the deeper tier as it commonly displays the virtual absence of compaction of the open burrows.

The simple horizontal burrows and incipient *Skolithos* likely represent the intermediate-tier while the surficial biogenic structures observed in fjord bottom photographs provide a unique look at the epibenthic and shallow-tier community. As stated previously, complete bioturbation of the surficial sediments is revealed by the bottom photographs indicating homogenization of the sediment by a mobile epibenthic fauna. Imprinted on this sediment surface, particularly in distal sites along the fjord (where sedimentation rate is particularly low), distinctive horizontal trails and trackways are commonly discernible.

The Lehigh cores record the uppermost soupy substrate and the underlying softground typically characterized by simple vertical structures penetrating from the sediment-water interface through

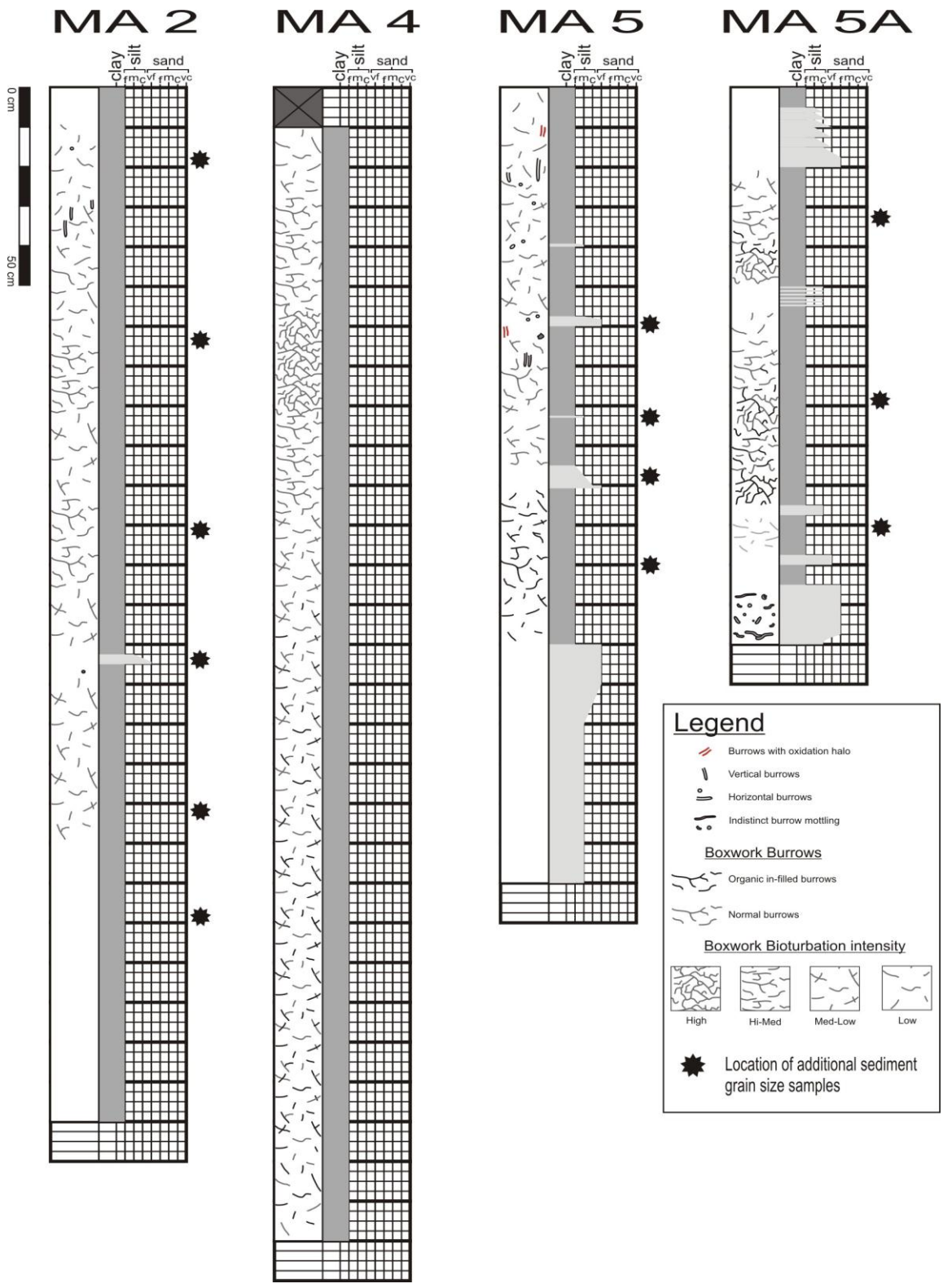

Figure 3.9. Four Lehigh core logs depicting ichnofabric and sedimentological data for Maktak Fjord.

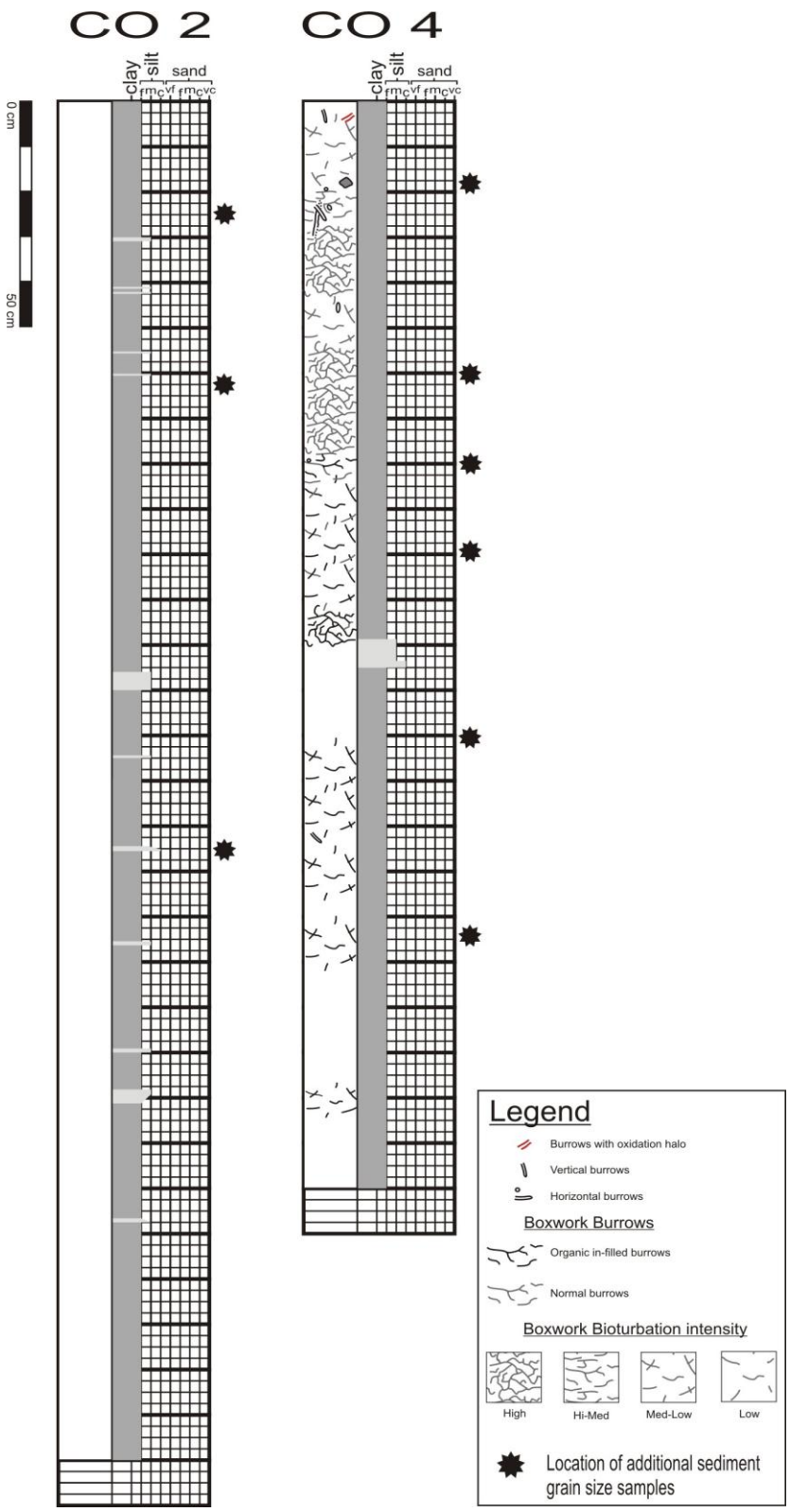

Figure 3.10. Two Lehigh cores depicting ichnofabric and sedimentology of Coronation Fjord. Notice the lack of biogenic structure shown in CO2.

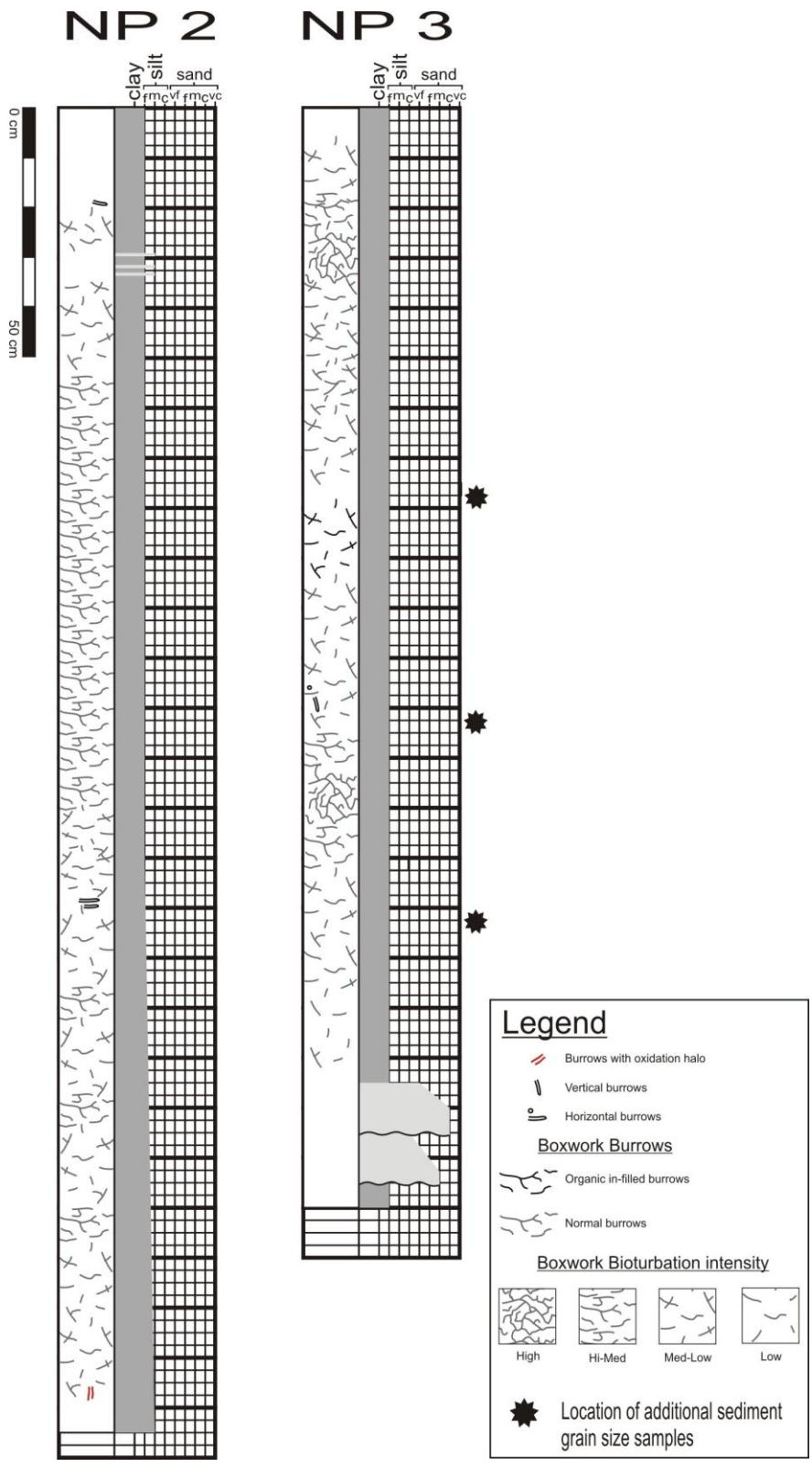

Figure 3.11. Two Lehigh cores depicting ichnofabric and sedimentological data from North Pangnirtung Fjord.

a thoroughly bioturbated sediment. Boxwork stuctures are not visible in the uppermost part of the Lehigh cores, but they can be found 4-10 cm below, suggesting relatively deep-tier structures. Essentially, the Lehigh core tops preserve a "frozen-tier" profile allowing all three tiers to be observed (Orr, 1994).

When dealing specifically with deep-tier structures, little information can be ascertained regarding the conditions at or above the substrate-water interface as these traces are so far removed from that area. However, a simple relationship between the intensity of bioturbation of the boxwork burrow system and the deposition of medium silt to fine-grained sand layers has been observed. At locations in the cores where the lithology changes abruptly from silty clay to a sandy layer, there is a distinct lowering of intensity in the boxwork burrows directly below the sand interval and there is no evidence of their existence within the sandy layer. Simple vertical or horizontal burrows are commonly seen in areas where the boxwork system is less intense (see Fig 3.9; MA2, MA5 and MA5A), suggesting that their presence is taphonomically controlled because they only exceptionally survive the destructive effect of the upward migration of the deeper tier. Boxwork burrows do not typically penetrate the fine- to medium-grained layers. The burrow system commonly re-establishes above the coarser-grained sediment and, in some cases, shows a distinctly horizontal orientation of the burrows along the interfacial surface (see Fig. 3.10; CO4 at 120 cm).

The three-dimensional burrow tracemaker would have likely maintained a connection to the sediment-water interface to allow for respiration and waste removal. This is evident in the open burrow morphology of the boxwork burrow system. Burial of the substrate surface by episodic sedimentation events (or *vice versa*; excavation by erosional events) would force the tracemaker to reposition the depth of its burrow opening(s). This may account for the abrupt change in burrow intensity above and below these sandy intervals. The fact that the boxwork tracemaker did not colonize the medium-grained sand to fine-silt layers may indicate that the organism is unable to digest sediment particles larger than clay and very fine silt that comprises the majority of the cored sediments. This may also explain the horizontal orientation of the burrows seen in CO4 core log at 120 cm depth; if confined to a thin layer of fine-grained sediment by coarser-grained layer, the most efficient use of space would be to expand feeding burrows horizontally.

The question then arises as to whether or not the changes in boxwork burrow intensity can provide any information related to sedimentation rates within these fjords. Slow sedimentation rates provide more time for the tracemaker to thoroughly bioturbate the surrounding sediment resulting in the high bioturbation intensity observed in the ichnofabric. The opposite is also true in that a high sedimentation rate causes the producer to migrate upwards repeatedly abandoning burrows that are below its maximum burrowing depth. This should result in the appearance of lower bioturbation intensity. More research must be conducted to confirm these ideas, but there appears to be some connection between bioturbation intensity of the ichnofabric and the surrounding sedimentary environment within the studied Arctic fjords.

3.5.2 Potential Tracemakers

The bottom photographs taken at each station captured the producing organisms *in fraganti* for the majority of the recent seafloor traces described previously (see section 3.3.2. Photographic Ichnologic Survey). In the case of the surficial burrow openings, no clear evidence was observed to suggest a possible producer. Based purely on visual morphology from the substrate surface, it is possible that some of these structures belong to burrowing anemones (e.g. orders Actinaria and Ceriantharia; sensu Bromley, 1996), burrowing holothurians, echiuroid worms, tubiculous polychaetes or infaunal polychaetes, the majority of which are documented to inhabit Baffin Island fjords (see Dale *et al.*, 1989). Both burrowing anemones and burrowing holothurians were noted by Farrow (1983) as being present in bottom photographs from several Baffin Island fjords studied during the S.A.F.E. cruise. However, differences in the diameter of the surficial burrow openings and the size of the proposed producing organism(s) are limiting factors in this discussion. Without knowledge of the subsurface architecture it is not possible to make any conclusions regarding the tracemaker or make it possible to understand the function of the structure and compare it to known ichnotaxa from the trace fossil record.

From the core samples, simple horizontal burrows and incipient *Skolithos* were preserved open which suggests a dwelling structure of some kind. Possible modes of life for these dwellings may include suspension feeders, detritus feeders or passive predators. The interior surface of some burrows contains a corrugated ornamentation. The body of a segmented worm would be capable of producing similar internal structure through slight compaction of the surrounding substrate

due to its peristaltic body movements (*sensu* Bromley, 1996). The corrugations would be easily preserved in deeper parts of the structure in a relatively firm substrate.

A second possibility for some of the incipient *Skolithos* burrows observed in the core samples is a U-shaped structure. Individual burrows were commonly described alongside a second burrow structure of similar size and orientation. As the burrows were commonly incomplete and passively in-filled, no connection between the two adjacent burrows was observed. Paired surficial burrow openings were detected in the bottom photographs raising the likelihood that such paired and possibly U-shaped structures would be detected in the cores. This type of paired burrow is historically described as a dwelling structure (commonly containing spreite; see section 2.2.2.2. Ethologic Classification) or as an irrigation channel of an infaunal suspension feeder.

The boxwork burrow system is one of the most impressive and confounding biogenic structures discovered in these modern Arctic fjords. Based on morphologic features (e.g. undeformed, circular cross section, open burrows) and the taphonomic analysis previously presented, the boxwork burrows are a deep-tier structure. It can be assumed from changes in sediment colour with depth that only the upper 5 cm of sediment were oxygenated in most cases (Clattenburg *et al.*, 1983; Hein and Longstaffe, 1983). These uppermost layers of the Lehigh cores are also the most highly bioturbated as observed from both bottom photographs and core samples. It is likely that the sediment below this 5-cm layer contained very little oxygen or was completely anoxic. In any case, the boxwork producer would have likely required an adequate oxygen source obtained through either the active circulation of oxygenated water through the burrow system or through the positioning of its respiratory organs proximal to the sediment-water interface (in which case the burrow system would remain anoxic at depth).

A review of the literature reveals no trace fossil or modern biogenic structure with identical morphology. There are some slightly similar structures that can serve as descriptive comparators, though none of these exactly equates to the intricate nature of the three-dimensional boxwork burrow system. Coincidentally, several of the modern structures also have known producers which have been either documented in Canadian Arctic fjords or are common inhabitants of more temperate European fjords. A comparison of the three-dimensional boxwork system to both modern and fossil examples of similar structures can be seen in Figure 3.13.

At first sight, the boxwork burrow system may display similarities with the trace fossil *Chondrites*. Both are deep-tier burrows forming branching networks and are commonly associated with limited oxygen conditions (Bromley and Ekdale, 1984). *Chondrites* is typically viewed as a chemosymbiotic structure (see Seilacher, 1990), though a recent study by Hertweck *et* al. (2007) compares the trace fossil to structures produced by the deposit feeding, conveyer belt polychaete *Heteromastus filiformis*. The branching network burrows of *H. filiformis* have been described by many authors including Schäfer (1952, 1972) and Gingras *et al*. (2008). The structures produced by this polychaete are more similar to the Holocene boxwork burrows than to the trace fossil *Chondrites*; although the burrows produced by *H. filiformis* are more vertically oriented than those of the boxwork (Fig. 3.13).

As a potential tracemaker for the boxwork burrow system, *H. filiformis* is an excellent candidate with the exception of its geographic distribution (largely inhabiting European fjords) and its primarily vertical burrow morphology. This polychaete constructs permanent, vertically oriented, branching burrow structures that are typically mucus lined and maintain a connection with the sediment-water interface for respiration (see Fig. 3.13; Cadée, 1979; Quintana *et al*., 2007). *Heteromastus filiformis* ingests fine-grained anoxic sediments, up to 30 cm depth below the sediment surface, as a head-down deposit feeder that transports sediment in the form of faecal pellets to the surface (Quintana *et al*., 2007; Gingras *et al*., 2008). It has also been found to actively irrigate its burrow system to remove harmful toxins (Quintana *et al.*, 2007).

A common inhabitant of Norwegian fjords in both shallow and deep basin localities is the bivalve genus *Thyasira*. This small bivalve utilizes chemoautotrophic bacteria living in its gill tissues to convert elemental sulphur into nutrients that the bivalve can digest (Dando and Southward, 1986; Dando and Spiro, 1993). Dando and Southward (1986) document individuals with shell sizes as small as 2-9 mm in length. *Thyasira* can burrow up to 8 cm below the sediment-water interface and then constructs a branching network of open burrows with its vermiform foot as deep as nine times the shell length of the burrowing individual (Dando and Southward, 1986; Dando and Spiro, 1993). They also construct an inhalation tube with mucus lining extending from the sediment-water interface to the individual (Fig. 3.13). Active flow of oxygenated water through the inhalation tube commonly causes oxidation of iron sulphide rich sediments 2-3 mm into the substrate from the burrow boundary (Dando and Southward, 1986).

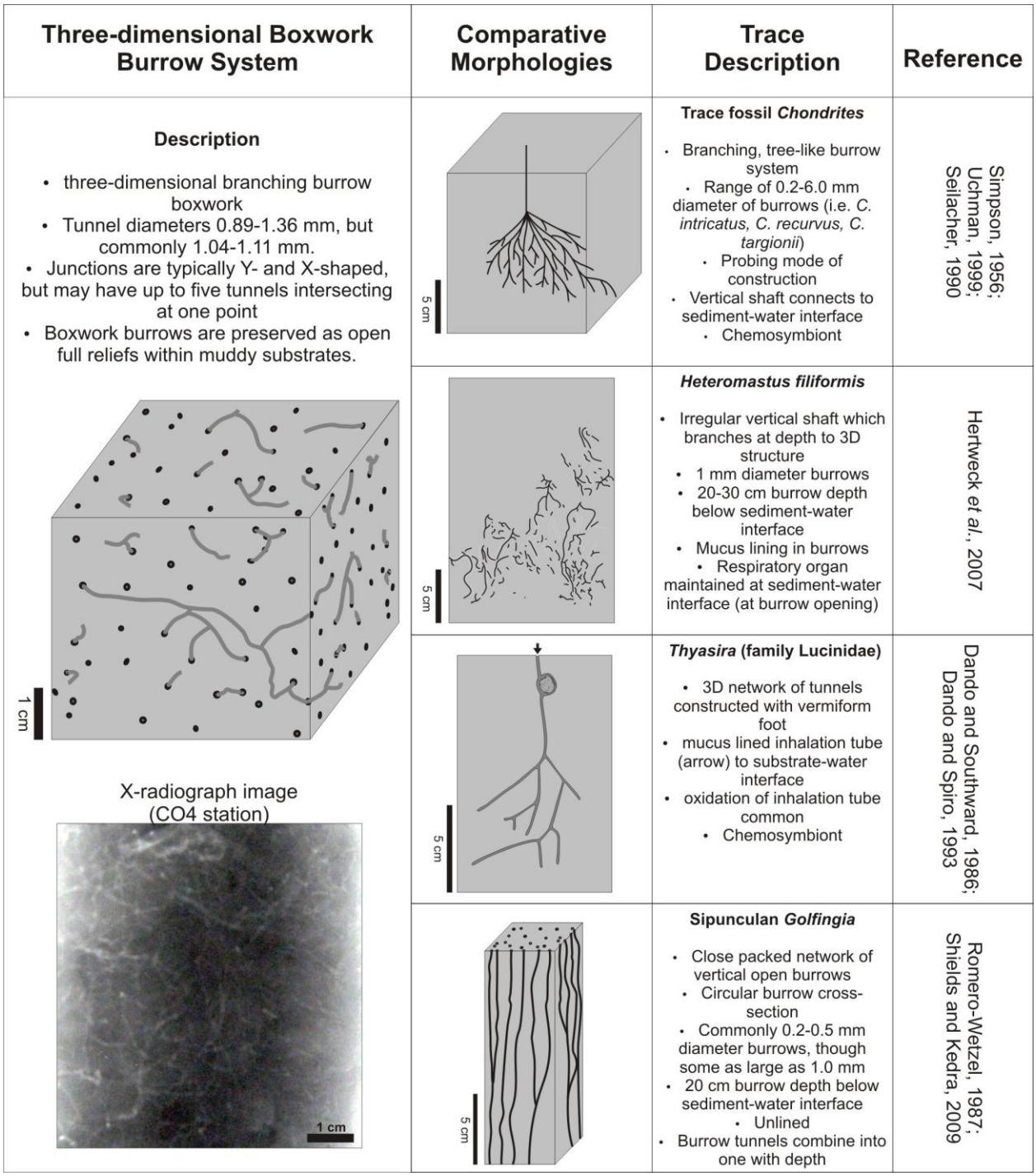

Figure 3.12. Diagram illustrating the three-dimensional boxwork burrow system in comparison with the trace fossil *Chondrites* and three modern biogenic structures. Note that the x-ray image of the boxwork burrows displays the boxwork in high abundance (from core station CO4, 70-80 cm depth).

Thyasira bivalves were observed to avoid sediment with high concentrations of hydrogen sulphide, favouring only those sediments in which the sulphide zone was within their burrowing depth (Dando and Southward, 1986; Dando and Spiro, 1993).

An example of a thyasirid bivalve burrow was discovered from the middle Miocene in Austria with a fossilized shell of the bivalve found above the burrow still in life position (Zuschin *et al*., 2001). However, the bivalve *Thyasira michelottii* inhabited much warmer water than the modern examples and its "branching network" consisted of a simple, vertical tube in the example shown by Zuschin *et al*. (2001). Seilacher (1990) also noted that in laboratory experiments, the burrows produced by modern thyasirid bivalves collapsed after the bivalve had abandoned them, suggesting that they have little preservation potential in the fossil record.

Another European example is that of the sipunculan genus *Golfingia*, subgenus *Nephasoma* (Romero-Wetzel, 1987; Shields and Kedra, 2009). It was observed to construct deep, vertical, open burrow systems within the substrate. The sipunculan is documented as a reverse conveyor-belt feeder transporting sediment from the surface to depth (Shields and Kedra, 2009). The burrow structure is commonly as deep as 30 cm into the sediment, may contain a bifurcating branching pattern, and is compared to the ichnogenus *Trichichnus* (Romero-Wetzel, 1987). Though sipunculans are primarily found in European fjords and marine settings, two species, *Golfingia* sp. and *Phascolia* sp., have been documented by Dale (1992) to inhabit Pangnirtung Fjord, Cumberland Peninsula, Baffin Island.

3.5.3 Environmental Controls

There are several controls on the production and preservation of biogenic sedimentary structures that have been observed in Maktak, Coronation and North Pangnirtung Fjords. Firstly, the absence of storm deposits and the scarcity of episodic sedimentation in general prevent rapid burial and preservation (or erosional truncation followed by burial and casting) of biogenic structures in a setting normally dominated by fallout sedimentation. Second, the scarcity of sand and coarse silt in the system results in the absence of contrasting casting media to preserve open biogenic structures in a silty clay homogenous matrix. Third, the distance from the fjord head (and the variety of processes operating along the fjord valley) can be correlated roughly to sediment shear strength; this is particularly evident in Coronation Fjord, station CO2. In turn,

substrate consolidation (as it relates to shear strength and water content; e.g. soupground vs. firmground) governs the potential of formation and preservation of surficial biogenic structures. In soupy substrates of CO2, very few structures are distinctive as animals struggle to move over the sediment surface without sinking. However, in distal MA5 station, a relatively more competent substrate promotes the formation and preservability of distinctive structures. Finally, the type of organic matter deposited in the fjords is dependent on the input source of the sediment and may either deter or promote bioturbation by different members of the fjord's biological community. These factors have implications within fjord facies models of ichnology and may explain some of the disparity seen in these modern analogs as compared to Paleozoic and Cenozoic examples.

The current ichnofacies model for fjord environments, put forth by Buatois and Mángano (2011), is primarily based on Paleozoic fjords from Gondwana as well as some Cenozoic examples (see Fig. 2.8, section 2.2.5. Fjord Models in Ichnology). The main environmental stresses associated with this fjord model are salinity, sedimentation rate, frequency of storms and substrate consolidation (Buatois and Mángano, 2011a). All of these factors have some effect on the preservation and also distribution of biogenic sedimentary structures. However, some differences exist in the manner to which these environmental factors affect modern Arctic fjords as compared to Paleozoic and Cenozoic fjords.

Input of freshwater through glacial melting or by fluvial processes creates a very stressful environment for organisms dependent on normal marine salinities, as shown specifically by studies of Paleozoic fjords (e.g. Balistieri *et al.*, 2002; Buatois *et al.*, 2006, 2010; Schatz *et al.*, 2011). Freshwater derived from tidewater glaciers, will rise to the surface of the fjord fairly quickly (depending on the sediment load it carries) encouraging more saline fjord bottom waters to flow toward the ice front to fill the gap (Syvitski, 1989). This facilitates mixing of the two water bodies at the fjord head creating a more brackish-water salinity as a result. Typically, brackish-water ichnofaunas are documented within fjord environments as their marine counterparts are unable to withstand the harsh conditions (e.g. Eyles *et al.*, 1992). The resulting trace fossils are typically small in size, less abundant and exhibit low diversity (Buatois and Mángano, 2011a).

Sediment gravity flows are a common element in Paleozoic and Cenozoic fjord environments (Eyles *et al.*, 1992; Balistieri *et al.*, 2002; Gandini *et al.*, 2007; Buatois *et al.*, 2006, 2010). High sediment and freshwater discharge at the fjord head allow for the formation of over steepened sediment deposits that result in turbidity flows due to slope failures (Syvitski, 1989). Hyperpycnal flows were common in past fjord environments, particularly during the summer months, potentially producing major changes in salinity as freshwater, laden with sediment, flowed along the fjord bottom for extended periods of time (see Buatois *et al.*, 2006, 2010). In contrast to sediment gravity flows, which involve resedimentation of previously deposited material, hyperpycnal flows are sustained currents directly fed from the river mouth (Zavala *et al.*, 2011). These deposits were briefly colonized by organisms typically associated with freshwater environments (Buatois *et al.*, 2006; Buatois and Mángano, 2011a).

Both the effects of salinity and the occurrence of turbidity flows are minor aspects in the three studied Baffin Island fjords. With the exception of the fjord head, the bottom waters within Maktak, Coronation and North Pangnirtung Fjords remain at normal marine salinity for much of the year (Gilbert, 1982b). The short summer melt period typical of Arctic fjords limits the amount of freshwater that would otherwise drastically change the composition of the basin water (Dale *et al.*, 1989; Syvitski, 1989). This also limits the formation of hyperpycnal flows, which are noted to be primarily absent from Arctic fjords (Syvitski *et al.*, 1987; Syvitski, 1989).

Sedimentation rates are noted to be high in Paleozoic fjords from western Gondwana and in Cenozoic fjords from Alaska. This is directly controlled by a steep nearby topography as these systems were emplaced in active plate tectonic boundaries. Escape structures are recorded from event beds (Eyles *et al.*, 1992; Buatois and Mángano, 2011a). In particular, Eyles *et al.* (1992) documented sediment gravity flows rich in organic matter that were deposited in deep-marine settings. The *Cruziana* ichnofacies was recognized in this deep-marine deposit which would typically have been colonized by members of the *Nereites* ichnofacies (Eyles *et al.*, 1992).

High rates of sedimentation and changes in sediment grain size contribute to excellent preservation of trace fossils. Biogenic sedimentary structures require a casting medium, typically sand or coarse silt, to be visibly preserved in contrast to the matrix material (*sensu* Seilacher, 1964). In this way, preservation of biogenic sedimentary structures in a fjord environment is dependent on the rate of episodic (e.g. storms, mass flows) and non-episodic (e.g. hyperpycnal

flows) sedimentation that can provide lithologic contrast with background sedimentation sediments.

In the case of these modern Arctic fjords, sedimentation rates are low and deposition due to storm activity is negligible due to the limited extent of wave-induced mixing as a result of a small fetch across the fjord basin. In the most distal fjord locations, MA5 and MA5A, there is a noted increase in the frequency of coarse-grained sedimentation and thick layers of sand are observed at depth (see Fig. 3.9 core log and Fig 3.1). For example, the upper 20 cm of core sample MA5A displays several fining upward sequences of fine-grained sand to medium-grained silt. Although the source of these deposits is hard to determine, their structure resembles that of turbidite deposits (Hein and Longstaffe, 1983). In the core from the MA5A station, indistinct burrow mottling is preserved within the fine-grained sand layers at the lower part of the core, 125-140 cm depth (see Fig. 3.9). These biogenic structures are best interpreted as the work of opportunistic colonizers. There is also an instance where the deep-tier boxwork burrow system is cast by an overlaying sand layer of contrasting colour to the homogeneous dark, silty clay (see Fig. 3.9, 110 cm depth). Casting the otherwise open boxwork burrows will likely increase their preservation potential. The greater diversity of traces present in MA5A core suggests that changes in lithology do play a role in trace fossil preservation and visibility.

Substrate consolidation is very important to the formation and preservation of trace fossils (Ekdale, 1985). Studies of fjords, past and present, provide a similar account of the distribution of substrates within fjord basins as was determined during research of Maktak, Coronation and North Pangnirtung Fjords (e.g. Eyles *et al.*, 1992; Dale *et al.*, 1989). Soupy substrates are found proximal to the ice front while soft substrates (softgrounds) appear farther down fjord. Firmgrounds and hardgrounds are also present in localities were water energy has removed the unconsolidated surface sediments resulting in a rocky substrate (Eyles *et al.*, 1992). Boulders and large cobbles typically serve as "faunal islands" on which organism can attach themselves (Dale *et al.*, 1989).

Hein and Longstaffe (1983) conducted numerous sediment shear strength tests on the Baffin Island core samples. Their results indicated that the core from location CO2, in Coronation Fjord, had very low shear strength and this can be confirmed by the very soupy texture of the surface sediment observed in the bottom photographs from that vicinity. They also confirmed the

observation that surficial sediments in all locations become firmer farther from the fjord head. Soupy surficial sediments typically have higher water content than the stiff, dewatered distal substrates.

Traces produced in soupgrounds commonly result in poorly defined biodeformational structures (Ekdale, 1985). However, soft substrates may allow for the formation of more distinct structures, though their appearance will likely have a smeared look if they survive the fossilization barrier (see section 2.2.3. Substrate Consolidation and Trace Fossil Morphology). In the case of the core sample CO2, no biogenic sedimentary structures are observed even though abundant surficial structures were seen in the bottom photographs; this is best explained as the difficulty in stabilizing and maintaining these shallow- to intermediate-tier burrows in such a low-shear strength surficial substrate.

Now we must consider the absence of the deep-tier boxwork structure from station CO2. Macko *et al*. (1987) compiled organic carbon and amino acid geochemical data from the sampled Baffin Island fjords of the S.A.F.E. expedition. It was found that Coronation Fjord showed considerable terrestrial carbon content in its sediments at station CO2. In contrast, station CO4 showed an increased influence of marine carbon sources with only two intervals of terrestrial carbon input (suggested to be depths 25 cm and 125 cm in CO4 by Macko *et al*., 1987). Of the three studied fjords in this paper, only station CO2 was noted to have mainly terrestrial carbon sources while all other stations were marine influenced.

This poses an interesting question as to the relationship of the boxwork burrow system and the type of carbon being deposited and likely consumed by the tracemaker. It is observed that the boxwork system is absent from the CO2 core entirely and is also absent at the 125 cm depth interval in CO4 that was indicated as a terrestrial carbon deposit. These observations suggest that, independent of its biological affinity, the producer of these deep-tier structures may in fact requires marine organic matter for consumption.

The current study of Arctic fjords further expands our understanding of ichnology in fjords and current fjord ichnofacies models (see Fig. 2.8, section 2.2.5 Fjord Models in Ichnology). Sediment source, sedimentation rate, dominant processes of deposition and organic matter input are strikingly variable in different types of modern fjord environments, outlining the complexity

of these environments (see section 2.1.3. Canadian and European Fjords). Additional research of modern fjord environments will be instrumental in acquiring a more accurate understanding of animal-sediment interactions to improve our present models of fjord ichnology.

4 Conclusions

Investigation of the recent seafloor of Maktak, Coronation and North Pangnirtung Fjords revealed a wide variety of biogenic structures. Ophiuroid producers were responsible for complex trackways, star-shaped resting structures and individual arm impressions which typically covered the majority of the fjord floor. Large buccinid gastropods produced flattened, elongate trails close in morphology to the numerous paths created by scavenging onuphid polychaetes. The majority of these structures are epigenic, shallow impressions with a known tracemaker captured *in fraganti* by the photographs. However, several types of burrow openings were more difficult to interpret from the bottom photographs without a cross-sectional view of the particular structure. The tracemakers, in these instances, were not observed.

Bottom photographs support a diverse and active epibenthic to shallow endobethic community. However, information on intermediate to deep endobenthos is derived from the analysis of preserved biogenic sedimentary structures in Lehigh core samples. Two distinct tiers representing a single community were detected: 1) a dominant deep-tier structure composed of a branching, 3-dimensional burrow system of milimetric-scale diameter; and 2) a shallow- to intermediate-tier composed of simple, open or passively in-filled horizontal and vertical burrows (incipient *Skolithos*). Though the shallow- to intermediate-tier structures could hypothetically be an extension of the surficial burrow openings observed in the bottom photographs, no evidence of the deep-tier structure or its potential tracemaker could be found in the recent seafloor.

The core samples do not accurately reflect what is seen in the bottom photographs (e.g. modern, diverse epibethic community) as the structures observed on the recent seafloor have virtually no preservation potential. The structures generated by the modern community (epibenthic and shallow-tier) were completely overprinted by the upward migration of the dominant deep-tier structure. This would explain the rare appearance of the shallow to intermediate-tier structures as well; these structures are only found in sections of the core where the boxwork system displays low bioturbation intensity. In addition, the lack of storm deposits and the rarity of sandy turbidite beds in the core samples prevent casting of shallow-tier structures (see section 3.5.3. Environmental Controls). As the boxwork burrow producer displays an obvious aversion for coarse-grained sediment layers, any structures that would have potentially been cast by such an event bed would likely have survived the fossilization barrier, in the absence of overprinting by

the deep-tier. Evidence in support of this interpretation can be seen in the bottom of core sample MA5A, which shows abundant burrow mottling on the top of a sandy turbidite deposit.

Proximal-distal trends were recognized in the distribution of the biological community within the three fjords (see Table 3.2). Locations proximal to the fjord head were dominated by small ophiuroids with disk diameters less than 1.5 cm. Central locations within all three fjords contained a large population of onuphid polychaetes which did not extend into the proximal stations or the distal, though the occasional onuphid polychaete was observed in distal photographs. In the most distal locations the biological community began to include more marine members such as anemones, pycnogonids and asteroid echinoderms.

The above trends in distribution of biota are accompanied by visible and measured changes in the consolidation of the surficial substrate. Fjord head locations (e.g. CO2) contain abundant small ophiuroids and are characterized by very soupy substrate in bottom photographs confirmed by measurements of low shear strength (Hein and Longstaffe, 1983). More distal locations within the fjords exhibit progressively firmer substrates and more distinct, prominent trace impressions are observed on the sediment surface. This change from soupy to firm substrate is at least partially explained by a decrease in sedimentation rate down fjord; sedimentation rates close the fjord head are higher and the substrates have higher water content. Other studies of modern Arctic fjord environments have concluded that distribution of the biological community is linked to substrate consolidation (e.g. Aitken *et al*., 1988; Dale *et al*., 1989).

Through observations of the core samples, no clear proximal-distal trends could be observed in the ichnofabrics, with the exception of core CO2. This core is the most proximal to Coronation Glacier and is completely devoid of biogenic sedimentary structures. The main source of the organic matter in this locality was found to be terrestrial which likely did not meet the feeding requirements of the deep-tier producer(s) (cf. Macko *et al*., 1987). The soupy texture of the substrate at this location may have also interfered with the deep-tier tracemaker's respiration and creation and maintenance of shallow-tier burrows (see section 3.5.2. Potential Tracemakers for oxygen circulation methods).

The most distal core station contains the addition of shallower-tier structures observed in its core sample (MA5A). The thick deposit of fine-grained sand at the base of this core preserves

abundant burrows seen in no other core samples (with the exception of minor structures observed in MA5). These burrows are interpreted as recording opportunistic colonization.

Finally, we have tried to frame the results of this study within current ichnofacies models of fjord environments (see section 3.5.3. Environmental Conditions). Some departures from previous ichnologic studies may be related to the absence or scarcity of storm and mass flow deposits in Baffin Island fjords. The lack of coarser-grained sediment in the system did not provide the needed casting media for of shallow- to intermediate-tier structures. Even among modern fjords, there are differences among the environmental conditions present as determined by the maturity of the fjord (glacially- vs. fluvially-dominated) and its geographical and tectonic location (see section 2.1.3. Canadian and European Fjords). Further expansion and refinements of preliminary fjord models should outline the taphonomy and diversity of environmental conditions (e.g. sedimentation rate, sediment grain-size, hydrodynamic energy).

Fjords represent a complex new frontier for ichnologic studies, and more research combining ichnology and sedimentology of Arctic fjord environments is necessary. The morphology of these three fjords, specifically, is unique; they lack sills at their mouths and have fully marine salinities in their basins. It is important that we also study those Arctic fjords which contain sills and may experience limited circulation with marine waters. These fjords may have a very different group of biogenic sedimentary structures preserved in their cores as well as captured in their bottom photographs.

Information stored in Coronation, Maktak and North Pangningtung Fjords is essential to the process of building our knowledge base of animal-substrate interactions in fjords. In this study we have been able to 1) gain an accurate understanding of fjord sedimentation rates and processes through the use of ichnofabric analysis; 2) document distribution of the epifaunal organisms present within the fjords; 3) document behaviour of the biota as recorded by burrows, trails and trackways in both core samples and fjord bottom photographs; 4) discover a deep-tier structure with a yet unidentified producer, and 5) outline the strong taphonomic overprint resulting from deep-tier upward migration. New research will further expand our knowledge of fjord ichnology and improve ichnofacies models of fjord environments.

5 References

AITKEN, A. E., RISK, M. J., AND HOWARD, J. D. 1988. Animal-sediment relationships on a subarctic intertidal flat, Pangnirtung Fjord, Baffin Island, Canada. *Journal of Sedimentary Petrology* , 58(6):969-978.

AITKEN, A.E., AND FOURNIER, J. 1993. Macrobenthos communities of Cambridge, McBeth and Itirbilung Fjords, Baffin Island, Northwest Territories, Canada. *Arctic*, 46:60-71.

AITKEN, A.E., AND GILBERT, R. 1986. The biota of intertidal flats at Pangnirtung Fiord, Baffin Island, N.W.T. *Le Naturaliste Canadien*, 113:191-200.

BALISTIERI, P.R.M.N., NETTO, R.G., AND LAVINA, E.L.C. 2002. Ichnofauna from the upper Carboniferous-lower Permian rhythmites from Mafra, Santa Catarina State, Brazil: ichnotaxonomy. *Revista Brasileira de Paleontologia*, 4:13-26.

BELL, C.M. 2004. Asteroid and ophiuroid trace fossils from the lower Cretaceous of Chile. *Paleontology*, 47:51-66.

BLOTT, S.J. AND PYE, K. 2001. GRADISTAT: a grain size distribution and statistics package for the analysis of unconsolidated sediments. *Earth Surface Processes and Landforms,* 26:1237-1248.

BOTTJER, D.J. AND DROSER, M.L. 1991. Ichnofabric and basin analysis. *Palaios*, 6:199-205.

BRIGHAM, J.K. 1983. Stratigraphy, amino acid geochronology, and correlation of Quaternary sea-level and glacial events, Broughton Island, Arctic Canada. *Canadian Journal of Earth Sciences*, 20:577-598.

BROMLEY, R.G. 1990. Trace fossils. Biology and taphonomy. Unwin Hyman, London.

BROMLEY, R.G. 1996. Trace fossils: biology, taphonomy and applications. 2nd ed. Chapman and Hall, London.

BROMLEY, R.G. AND EKDALE, A.A. 1984. *Chondrites*: a trace fossil indicator of anoxia in sediments. *Science*, 224:872-874.

BROMLEY, R.G. AND FÜRSICH, F.T. 1980. Comments on the proposed amendments to the International Code of Zoological Nomenclature regarding ichnotaxa. Z.N.(S.) 1973. *The Bulletin of Zoological Nomenclature*, 37:6-10.

BUATOIS, L.A. AND MÁNGANO, M.G. 2002. Trace fossils from Carboniferous floodplain deposits in western Argentina: implications for ichnofacies models of continental environments. *Palaeogeography, Palaeoclimatology, Palaeoecology*, 183:71-86.

BUATOIS, L.A. AND MÁNGANO, M.G. 2003. Caracterización icnológica y paleoambiental de la localidad tipo de *Orchesteropus atavus*, Huerta de Huachi, provincial de San Juán, Argentina: implicancias en el debate sobre los ambientes de sedimentación en el Carbonifero de Precordillera. *Ameghiniana*, 40:53-70.

BUATOIS, L.A. AND MÁNGANO, M.G. 2004. Animal-substrate interactions in freshwater environments: applications of ichnology in facies and sequence stratigraphic analysis of fluvio-lacustrine successions, pp. 311-333. *In* D. McIlroy (ed.), The application of ichnology to Palaeoenvironmental and stratigraphic analysis. Geological Society, London, Special Publications 228.

BUATOIS, L.A. AND MÁNGANO, M.G. 2011a. Ichnology: organism-substrate interactions in space and time. Cambridge University Press, Cambridge. 358 p.

BUATOIS, L.A. AND MÁNGANO, M.G. 2011b. The déjà vu effect: recurrent patterns in the exploitation of ecospace, the establishment of the mixed layer, and the distribution of matgrounds. *Geology*, 39:1163-1166.

BUATOIS, L.A., MÁNGANO, M.G., MAPLES, C.G., AND LANIER, W.P. 1998. Ichnology of an upper Carboniferous fluvio-estuarine paleovalley: the Tonganoxie Sandstone, Buildex Quarry, Eastern Kansas, USA. *Journal of Paleontology*, 72:152-180.

BUATOIS, L.A., NETTO, R.G., AND MÁNGANO, M.G. 2010. Ichnology of late Paleozoic post-glacial transgressive deposits in Gondwana: reconstructing salinity conditions in coastal ecosystems affected by strong meltwater discharge. *In*, O. Lopez Gamundi and L.A. Buatois (eds.), Late Paleozoic glacial events and postglacial transgressions in Gondwana. *Geological Society of America Special Paper*, 458:149-173.

BUATOIS, L.A., NETTO, R.G., MÁNGANO, M.G., AND BALISTIERI, P. 2006. Extreme freshwater release during the late Paleozoic Gondwana deglaciation and its impact on costal ecosystems. *Geology*, 34:1021-1024.

CADÉE, G.C. 1979. Sediment reworking by the polychaete *Heteromastus filiformis* on a tidal flat in the Dutch Wadden Sea. *Netherlands Journal of Sea Research*, 13:441-456.

CHURCH, M.A. 1970. Baffin Island sandar: a study of Arctic fluvial environments. Ph.D. thesis, University of British Columbia, Vancouver, Canada. 536 p.

CHURCH, M.A., STOCK, R.F., AND RYDER, J.M. 1979. Contemporary sedimentary environments on Baffin Island, N.W.T., Canada: debris slope accumulations. *Arctic and Alpine Research*, 11:371-401.

CLATTENBURG, D., COLE, F., KELLY, B., LEBLANC, W., BISHOP, P., RASHID, M., SCHAFER, G.T., AND SYVITSKI, J.P.M. 1983. SAFE: 1982 bottom grab samples, Chapter 8, pp.1-94. *In*, J.P.M. Syvitski and C.P. Blakeney, Sedimentology of Arctic Fjords Experiment: HU 82-031 Data Report, Volume 1.

DALE, J. E., AITKEN, A. E., GILBERT, R., AND RISK, M. J. 1989. Macrofauna of Canadian Arctic fjords. *Marine Geology* , 85:331-358.

DALE, J.E. 1992. The relationship between the physical environment and benthic faunal communities in Pangnirtung Fjord, Baffin Island, N.W.T. Ph.D. thesis, Queen's University, Kingston, Ontario, Canada. 425 p.

DANDO, P.R. AND SOUTHWARD, A.J. 1986. Chemoautotrophy in bivalve molluscs of the genus *Thyasira*. *Journal of the Marine Biological Association of the United Kingdom*, 66:915-929.

DANDO, P.R. AND SPIRO, B. 1993. Varying nutritional dependence of the thyasirid bivalves *Thyasira sarsi* and *T.equalis* on chemoautotrophic symbiotic bacteria, demonstrated by isotope ratios of tissue carbon and shell carbonate. *Marine Ecology Progress Series*, 92:151-158.

de GIBERT, J.M., BUATOIS, L.A., FREGENAL-MARTÍNEZ, M.A., MÁNGANO, M.G., ORTEGA, F., POYATO-ARIZA, F.J., AND WENZ, S. 1999. The fish trace fossil Undichna from the Cretaceous of Spain. *Palaeontology*, 42:409-427.

DROSER, M.L. AND BOTTJER, D.J. 1993. Trends and patterns of Phanerozoic ichnofabrics. *Annual Reviews of Earth and Planetary Sciences*, 21:205-225.

EKDALE, A.A. 1985. Paleoecology of the marine endobenthos. *Palaeogeography, Palaeoclimatology, Palaeoecology,* 50:63-81.

EKDALE, A.A. AND BROMLEY, R.G. 1991. Analysis of composite ichnofabrics: an example in uppermost Cretaceous chalk of Denmark. *Palaios*, 6:232-249.

EYLES, N., VOSSLER, S.M., AND LAGOE, M.B. 1992. Ichnology of a glacially influenced continental shelf and slope; the late Cenozoic Gulf of Alaska (Yakataga Formation). *Palaeogeography, Palaeoclimatology, Palaeoecology*, 94:193-221.

FARROW, G.E. 1983. Bottom fauna and bioturbation, Chapter 9, pp.1-26. *In* J.P.M. Syvitski and C.P. Blakeney, Sedimentology of Arctic Fjords Experiment: HU 82-031 Data Report, Volume 1.

GAILLARD, C. 1991. Recent organism traces and ichnofacies on the deep-sea floor off New Caledonia, southwestern Pacific. *SEMP Society for Sedimentary Geology*, 6:302-315.

GANDINI, R., NETTO, R.G., AND SOUZA, P.A. 2007. Paleoicnologia e a palinologia dos ritmitos do Grupo Itararé na pedreira de Águas Claras (Santa Catarina, Brasil). *Gaea*, 3:47-59.

GILBERT, R. 1982a. Contemporary sedimentary environments on Baffin Island, N.W.T., Canada: glaciomarine processes in fjords of eastern Cumberland Peninsula. *Arctic and Alpine Research*, 14(1):1-12.

GILBERT, R. 1982b. The Broughton Trough on the continental shelf of eastern Baffin Island, Northwest Territories. *Canadian Journal of Earth Sciences*, 19:1599-1607.

GILBERT, R. 1983. Sedimentary processes of Canadian Arctic fjords. *Sedimentary Geology*, 36:147-175.

GILBERT, R. 2000. Environmental assessment from the sedimentary record of high-latitude fjords. *Geomorphology*, 32:295-314.

GINGRAS, M.K., DASHTGARD, S.E., MACEACHERN, J.A., AND PEMBERTON, S.G. 2008. Biology of shallow marine ichnology: a modern perspective. *Aquatic Biology*, 2:255-268.

GOLDRING, R. 1995. Organisms and the substrate: response and effect. *Journal of the Geological Society*, London, Special Publication, 83:151-180.

HEIN, F.J. AND LONGSTAFFE, F.J. 1983. Geotechnical sedimentological and mineralogical investigation in Arctic fjords, Chapter 11, pp.1-158. *In* J.P.M. Syvitski and C.P. Blakeney, Sedimentology of Arctic Fjords Experiment: HU 82-031 Data Report, Volume 1.

HERTWECK, G., WEHRMANN, A., AND LIEBEZEIT, G. 2007. Bioturbation structures of polychaetes in modern shallow marine environments and their anologues to *Chondrites* group traces. *Palaeogeography, Palaeoclimatology, Palaeoecology*, 245:382-389.

HILTON, J. AND LISHMAN, J.P. 1985. The effect of redox changes on the magnetic susceptibility of sediments from a seasonally anoxic lake. *American Society of Limnology and Oceanography*, 30:907-909.

HIMMELMAN, J.H. AND HAMEL, J.R. 1993. Diet, behaviour and reproduction of the whelk *Buccinum undatum* in the northern Gulf of St. Lawrence, eastern Canada. *Marine Biology*, 116:423-430.

HOLLISTER, C.D., HEEZEN, B.C., AND NAFE, K.E. 1975. Animal traces on the deep-sea floor, Chapter 21, pp. 493-510. *In* R.W. Frey (ed.), The study of trace fossils: a synthesis of principles, problems, and procedures in ichnology. Springer-Verlag, New York.

HOLTE, B. AND GULLIKSEN, B. 1998. Common macrofaunal dominant species in the sediments of some north Norwegian and Svalbard glacial fjords. *Polar Biology*, 19:375-382.

HYNDMAN, R.D. 1975. Marginal basins of the Labrador Sea and the Davis Strait hot spot. *Canadian Journal of Earth Sciences*, 12:1041-1045.

JACKSON, G.D. AND TAYLOR, F.C. 1972. Correlation of major Aphebian rock units in the northeastern Canadian Shield. *Canadian Journal of Earth Sciences*, 9:1650-1669.

JENSEN, S., DROSER, M.L., AND GEHLING, J.G. 2006. A critical look at the Ediacaran trace fossil record, Chapter 5, pp. 115-157. *In*, S. Xiao and A.J. Kaufman (eds.), Neoproterozoic geobiology and paleobiology. Springer.

KEIM, R.D., SANBORN-BARRIE, M., ANSDELL, K, AND YOUNG, M. 2011. Totnes Road metavolcanic rocks: a fragmental, Ti-enriched komatiitic volcanic suite on Cumberland Peninsula, Baffin Island, Nunavut. *Geological Survey of Canada*, Current Research:13-18.

LARSEN, L. 1997. Soft-bottom macro invertebrate fauna of north Norwegian coastal waters with particular reference to sill-basins. Part one: bottom topography and species diversity. *Hydrobiologia*, 355:101-113.

LEWIS, E.L. AND PERKIN, R.G. 1982. Seasonal mixing processes in an Arctic fjord system. *Journal of Physical Oceanography*, 12:74-83.

MACKO, S.A., PULCHAN, K. AND IVANY, D.E. 1987. Organic geochemistry of Baffin Island Fjords, Chapter 13, pp. 1-27. *In*, J.P.M. Syvitski and D.B. Praeg, Sedimentology of Arctic fjords experiment: data report, volume 3. Canadian Data Report of Hydrography and Ocean Sciences, 54.

MÁNGANO, M.G. AND BUATOIS, L.A. 1999. Feeding adaptations: invertebrates, pp. 458-465. *In*, R. Singer (ed.), Encyclopedia of Paleontology, Volume 1. Fitzroy Dearborn Publishers, Chicago.

MÁNGANO, M.G., BUATOIS, L.A., WEST, R.R., AND MAPLES, C.G. 1998. Contrasting behavioural and feeding strategies recorded by tidal-flat bivalve trace fossils from the upper Carboniferous of eastern Kansas. *Palaios*, 13:335-351.

MÁNGANO, M.G., BUATOIS, L.A., WEST, R.R., AND MAPLES, C.G. 1999. The origin and paleoecologic significance of the trace fossil *Asteriacites* in the Pennsylvanian of Kansas and Missouri. *Lethaia*, 32:17-30.

MARTINSSON, A. 1965. Aspects of middle Cambrian thanatotope on Öland. *Geologiskaa Förening is Stockholm Förhandlingar*, 87:181-230.

MCKENNA NEUMAN, C. 1989. Kinetic energy transfer through impact and its role in entrainment by wind of particles from frozen surfaces. *Sedimentology*, 36:1007-1015.

MCKENNA-NEUMAN, C. AND GILBERT, R. 1986. Aeolian processes and landforms in glaciofluvial environments of southeastern Baffin Island, N.W.T., Canada, pp. 213-235. *In*, W. Nickling (ed.), Aeolian Geomorphology, Proceedings of the 17th annual Binghamton Geomorphology Symposium, September 1986. Allen and Unwin, Boston.

MIRZA, F.B. AND GRAY, J.S. 1981. The fauna of benthic sediments from the organically enriched Oslofjord, Norway. *Journal of Experimental Marine Biology and Ecology*, 54:181-207.

NOFFKE, N. 2010. Geobiology: microbial mats in sandy deposits from the Archaean Era to today. Berlin, Heidelberg, Springer-Verlag. 194 p.

ORR, P.J. 1994. Trace fossil tiering within event beds and preservation of frozen profiles: an example from the lower Carboniferous of Menorca. *Palaios*, 9:202-210.

OUG, E. 2001. Polychaetes in intertidal rocky and sedimentary habitats in the region of Tromsø, northern Norway. *Sarsia*, 86:75-83.

QUINTANA, C.O., TANG, M., AND KRISTENSEN, E. 2007. Simultaneous study of particle reworking, irrigation transport and reaction rates in sediment bioturbated by the polychaetes *Heteromastus* and *Marenzelleria*. *Journal of Experimental Marine Biology and Ecology*, 352:392-406.

RISK, M.J. 1973. Silurian Echiuroids: possible feeding traces in the Thorold Sandstone. *American Association for the Advancement of Science*, 180:1285-1287.

ROMERO-WETZEL, M.B. 1987. Sipunculans as inhabitants of very deep, narrow burrows in deep-sea sediments. *Marine Biology*, 96:87-91.

SAVRDA, C.E. 1992. Trace fossils and benthic oxygenation. *Short Courses in Paleontology*, 5:172-196.

SCHAFER, C.T. 1983. Introduction, Chapter 1, pp. 1-4. *In*, J.P.M. Syvitski and C.P Blakeney, Sedimentology of Arctic Fjords Experiment: HU 82-031 Data Report, Volume 1.

SCHAFER, C.T., COLE, F.E., AND SYVITSKI, J.P.M. 1989. Bio- and lithofacies of modern sediments in Knight and Bute Inlets, British Columbia. *Palaios*, 4:107-126.

SCHÄFER, W. 1952. Biogene sedimentation im gefolge von bioturbation. *Senckenbergiana*, 33:1-12.

SCHÄFER, W. 1972. Traces of life habits preserved in the sediment: I. Locomotion, pp. 193-407. *In* G.Y. Craig (ed.), Ecology and palaeoecology of marine environments. The University of Chicago Press, Chicago.

SCHATZ, E.R., MÁNGANO, M.G., BUATOIS, L.A., AND LIMARINO, C.O. 2011. Life in the late Paleozoic ice age: trace fossils from glacially influenced deposits in a late Carboniferous fjord of western Argentina. *Journal of Paleontology*, 85:502-518.

SEILACHER, A. 1953. Studien zur palichnologie. II. Die fossilen ruhespuren (Cubichnia). *Neues Jahrbuch für Geologie und Paläontologie*, 98:87-124.

SEILACHER, A. 1964. Biogenic sedimentary structures, pp. 296-316. *In* J. Imbrie and N. Newell (eds.), Approaches to paleoecology. Wiley, New York.

SEILACHER, A. 1990. Aberrations in bivalve evolution related to photo- and chemosymbiosis. *Historical Biology*, 3:289-311.

SEILACHER, A. 2007. Trace fossil analysis. Springer, Berlin. 226 p.

SEILACHER, A. 2008. Biomats, biofilms, and bioglue as preservational agents for arthropod trackways. *Palaeogeography, Palaeoclimatology, Palaeoecology*, 270:252-257.

SHIELDS, M.A. AND KEDRA, M. 2009. A deep burrowing sipunculan of ecological and geochemical importance. *Deep Sea Research I,* 56:2057-2064.

SIMPSON, S. 1956. On the trace-fossil *Chondrites*. *Quarterly Journal of the Geological Society of London*, 112:475-499.

SUTCLIFFE, O.E. 1997. An ophiuroid trackway from the lower Devonian Hunsrück Slate, Germany. *Lethia*, 30:33-39.

SYVITSKI, J. P.M., AND SHAW, J. 1995. Sedimentology and Geomorphology of Fjords. *In* G.M.E.Perillo, Chapter 5, Geomorphology and Sedimentology of Estuaries: Developments in Sedimentology 53. Elsevier Science.

SYVITSKI, J.P.M. 1989. On the deposition of sediment within glacier-influenced fjords: oceanographic controls. *Marine Geology*, 85:301-329.

SYVITSKI, J.P.M., AND BLAKENEY, C.P.1983. Sedimentology of Arctic Fjords Experiment: HU 82-031 Data Report, Volume 1.

SYVITSKI, J.P.M., BURRELL, D.C., AND SKEI, J.M. 1987. Fjords; processes and products. Springer-Verlag, New York, United States. 379 p.

SYVITSKI, J.P.M., FARROW, G.E., ATKINSON, R.J.A., MOORE, P.G., AND ANDREWS, J.T. 1989. Baffin Island Fjord Macrobenthos: Bottom Communities and Environmental Significance. *Arctic*, 42(3):232-247.

TAYLOR, A.M., GOLDRING, R., AND GOWLAND, S. 2003. Analysis and application of ichnofabrics. *Earth-Science Reviews*, 60:227-259.

THAYER, C.W. 1979. Biological bulldozers and the evolution of marine benthic communities. *American Association for the Advancement of Science*, 203:458-461.

TREWIN, N.H. 1994. A draft system for the identification and description of arthropod trackways. *Palaeontology,* 37:811-823.

UCHMAN, A. 1999. Ichnology of the Rhenodanubian Flysch (lower Cretaceous-Eocene) in Austria and Germany. *Beringeria*, 25:67-173.

VALDERHAUG, V.A. AND GRAY, J.S. 1984. Stable macrofauna community structure despite fluctuating food supply in subtidal soft sediments of Oslofjord, Norway. *Marine Biology*, 82:307-322.

WALKER, K.R. AND BAMBACH, R.K. 1974. Feeding by benthic invertebrates: classification and terminology for paleoecological analysis. *Lethaia*, 7:67-78.

ZAVALA, C. ARCURI, M., DI MEGLIO, M., GAMERO DIAZ, H., AND CONTRERAS, C. 2011. A genetic facies tract for the analysis of sustained hyperpycnal flow deposits, pp. 31-51. *In*, R.M. Slatt and C. Zavala (eds.), Sediment transfer from shelf to deep water: revisiting the delivery system. AAPG Studies in Geology 61.

ZORN, M.E., LALONDE, S.V., GINGRAS, M.K., PEMBERTON, S.G., AND KONHAUSER, K.O. 2006. Microscale oxygen distribution in various invertebrate burrow walls. *Geobiology*, 4:137-145.

ZUSCHIN, M., MANDIC, O., HARZHAUSER, M, AND PERVESLER, P. 2001. Fossil evidence for chemoautotrophic bacterial symbiosis in the thyasirid bivalve *Thyasira michelottii* from the middle Miocene (Badenium) of Austria. *Historical Biology*, 15:223-234.

APPENDIX I:

Grain Size Analysis of Cores MA2, MA5, MA5A, CO2, CO4, and NP3

SAMPLE STATISTICS

		CO2	CO2	CO2	CO2	CO2	CO2	CO2	CO2
	DEPTH OF SAMPLE:	24.5,	25.5,	61.5,	62.5,	63,	164.5,	165.5,	166.5,
	SIEVING ERROR:								
	SAMPLE TYPE:	Polymodal, Poorly Sorted	Polymodal, Poorly Sorted	Bimodal, Poorly Sorted	Trimodal, Poorly Sorted	Trimodal, Very Poorly Sorted	Trimodal, Poorly Sorted	Polymodal, Very Poorly Sorted	Bimodal, Poorly Sorted
	TEXTURAL GROUP:	Mud	Mud	Mud	Mud	Mud	Mud	Mud	Mud
	SEDIMENT NAME:	Medium Silt	Medium Silt	Medium Silt	Fine Silt	Fine Silt	Medium Silt	Coarse Silt	Fine Silt
METHOD OF MOMENTS Arithmetic (μm)	MEAN	10.70	12.28	12.25	11.67	14.71	12.44	13.65	12.40
	SORTING	11.88	16.21	15.87	17.29	21.79	14.05	18.42	16.78
	SKEWNESS	1.714	3.138	3.051	3.489	3.378	1.609	2.834	2.900
	KURTOSIS	5.836	17.74	17.37	19.74	18.06	5.147	14.32	15.07
METHOD OF MOMENTS Geometric (μm)	MEAN	5.562	5.862	5.935	5.247	6.374	6.175	6.059	5.693
	SORTING	3.423	3.622	3.585	3.653	3.862	3.602	3.875	3.701
	SKEWNESS	-0.133	-0.050	-0.066	0.117	0.028	-0.131	-0.015	0.024
	KURTOSIS	2.030	2.095	2.111	2.191	2.162	1.997	2.013	2.086
METHOD OF MOMENTS Logarithmic (ϕ)	MEAN	7.490	7.414	7.397	7.574	7.294	7.339	7.367	7.456
	SORTING	1.775	1.857	1.842	1.869	1.949	1.849	1.954	1.888
	SKEWNESS	0.133	0.050	0.066	-0.117	-0.028	0.131	0.015	-0.024
	KURTOSIS	2.030	2.095	2.111	2.191	2.162	1.997	2.013	2.086
FOLK AND WARD METHOD (μm)	MEAN	5.546	5.790	5.877	5.162	6.254	6.178	5.961	5.629
	SORTING	3.635	3.798	3.774	3.839	4.038	3.842	4.075	3.913
	SKEWNESS	-0.074	-0.057	-0.061	0.018	-0.026	-0.064	-0.036	-0.010
	KURTOSIS	0.807	0.797	0.812	0.828	0.813	0.799	0.773	0.808
FOLK AND WARD METHOD (ϕ)	MEAN	7.494	7.432	7.411	7.598	7.321	7.339	7.390	7.473
	SORTING	1.862	1.925	1.916	1.941	2.014	1.942	2.027	1.968
	SKEWNESS	0.074	0.057	0.061	-0.018	0.026	0.064	0.036	0.010
	KURTOSIS	0.807	0.797	0.812	0.828	0.813	0.799	0.773	0.808
FOLK AND WARD METHOD (Description)	MEAN:	Fine Silt	Fine Silt	Fine Silt	Fine Silt	Fine Silt	Fine Silt	Fine Silt	Fine Silt
	SORTING:	Poorly Sorted	Poorly Sorted	Poorly Sorted	Poorly Sorted	Very Poorly Sorted	Poorly Sorted	Very Poorly Sorted	Poorly Sorted
	SKEWNESS:	Symmetrical	Symmetrical	Symmetrical	Symmetrical	Symmetrical	Symmetrical	Symmetrical	Symmetrical
	KURTOSIS:	Platykurtic	Platykurtic	Platykurtic	Platykurtic	Platykurtic	Platykurtic	Platykurtic	Platykurtic
	MODE 1 (μm):	19.78	19.78	19.78	5.361	5.885	19.78	19.78	5.885
	MODE 2 (μm):	16.41	7.091	7.091	19.78	19.78	7.091	5.885	19.78
	MODE 3 (μm):	7.091	5.885		16.41	127.8	11.31	11.31	
	MODE 1 (ϕ):	5.661	5.661	5.661	7.545	7.410	5.661	5.661	7.410
	MODE 2 (ϕ):	5.931	7.141	7.141	5.661	5.661	7.141	7.410	5.661
	MODE 3 (ϕ):	7.141	7.410		5.931	2.970	6.468	6.468	
	D_{10} (μm):	0.974	0.975	0.993	0.919	0.993	1.013	0.937	0.949
	D_{50} (μm):	5.938	6.126	6.232	5.128	6.434	6.540	6.207	5.704
	D_{90} (μm):	27.63	31.00	31.20	30.01	37.51	33.72	35.87	33.02
	(D_{90} / D_{10}) (μm):	28.37	31.80	31.43	32.65	37.75	33.30	38.30	34.79
	(D_{90} - D_{10}) (μm):	26.66	30.03	30.21	29.09	36.51	32.71	34.94	32.07
	(D_{75} / D_{25}) (μm):	7.377	8.082	7.767	7.755	8.600	8.145	9.465	8.260
	(D_{75} - D_{25}) (μm):	13.25	14.70	14.52	12.51	16.52	15.76	16.67	14.37
	D_{10} (ϕ):	5.178	5.011	5.002	5.058	4.737	4.890	4.801	4.921
	D_{50} (ϕ):	7.396	7.351	7.326	7.608	7.280	7.257	7.332	7.454
	D_{90} (ϕ):	10.00	10.00	9.976	10.09	9.975	9.947	10.06	10.04
	(D_{90} / D_{10}) (ϕ):	1.932	1.996	1.994	1.994	2.106	2.034	2.095	2.041
	(D_{90} - D_{10}) (ϕ):	4.826	4.991	4.974	5.029	5.238	5.057	5.259	5.120
	(D_{75} / D_{25}) (ϕ):	1.478	1.511	1.501	1.483	1.541	1.522	1.564	1.513
	(D_{75} - D_{25}) (ϕ):	2.883	3.015	2.957	2.955	3.104	3.026	3.243	3.046
	% GRAVEL:	0.0%	0.0%	0.0%	0.0%	0.0%	0.0%	0.0%	0.0%
	% SAND:	0.2%	1.5%	1.3%	1.9%	3.2%	0.6%	2.4%	1.8%
	% MUD:	99.8%	98.5%	98.7%	98.1%	96.8%	99.4%	97.6%	98.2%
	% V COARSE GRAVEL:	0.0%	0.0%	0.0%	0.0%	0.0%	0.0%	0.0%	0.0%
	% COARSE GRAVEL:	0.0%	0.0%	0.0%	0.0%	0.0%	0.0%	0.0%	0.0%
	% MEDIUM GRAVEL:	0.0%	0.0%	0.0%	0.0%	0.0%	0.0%	0.0%	0.0%
	% FINE GRAVEL:	0.0%	0.0%	0.0%	0.0%	0.0%	0.0%	0.0%	0.0%
	% V FINE GRAVEL:	0.0%	0.0%	0.0%	0.0%	0.0%	0.0%	0.0%	0.0%
	% V COARSE SAND:	0.0%	0.0%	0.0%	0.0%	0.0%	0.0%	0.0%	0.0%
	% COARSE SAND:	0.0%	0.0%	0.0%	0.0%	0.0%	0.0%	0.0%	0.0%
	% MEDIUM SAND:	0.0%	0.0%	0.0%	0.0%	0.0%	0.0%	0.0%	0.0%
	% FINE SAND:	0.0%	0.2%	0.2%	0.3%	0.9%	0.0%	0.3%	0.2%
	% V FINE SAND:	0.2%	1.3%	1.2%	1.6%	2.3%	0.6%	2.1%	1.6%
	% V COARSE SILT:	7.5%	8.4%	8.6%	7.4%	10.2%	11.0%	10.3%	9.2%
	% COARSE SILT:	16.9%	17.0%	16.7%	13.8%	15.7%	16.9%	16.6%	15.0%
	% MEDIUM SILT:	18.3%	17.1%	17.6%	15.9%	16.1%	17.1%	15.5%	16.1%
	% FINE SILT:	18.0%	17.0%	17.5%	18.0%	16.9%	16.9%	15.7%	17.3%
	% V FINE SILT:	15.6%	15.3%	15.3%	16.7%	15.0%	15.0%	14.7%	15.8%
	% CLAY:	23.7%	23.7%	23.1%	26.2%	22.8%	22.5%	24.8%	24.7%

SAMPLE STATISTICS

		CO4	CO4	CO4	CO4	CO4	CO4	CO4	CO4	CO4
	DEPTH OF SAMPLE:	17.5,	18.5,	19.5,	59.5,	60.5,	61.5,	79.5,	80.5,	81.5,
	SIEVING ERROR:									
	SAMPLE TYPE:	Unimodal, Poorly Sorted	Unimodal, Poorly Sorted	Unimodal, Poorly Sorted	Bimodal, Poorly Sorted	Unimodal, Poorly Sorted	Unimodal, Poorly Sorted	Unimodal, Poorly Sorted	Unimodal, Poorly Sorted	Unimodal, Poorly Sorted
	TEXTURAL GROUP:	Mud	Mud	Mud	Mud	Mud	Mud	Mud	Mud	Mud
	SEDIMENT NAME:	Fine Silt	Fine Silt	Fine Silt	Fine Silt	Fine Silt	Fine Silt	Fine Silt	Fine Silt	Fine Silt
METHOD OF MOMENTS Arithmetic (μm)	MEAN	13.33	10.61	10.42	9.208	9.671	9.760	10.75	11.42	11.76
	SORTING	28.94	19.86	18.66	16.30	16.90	17.16	17.64	18.50	19.72
	SKEWNESS	5.334	4.864	4.917	4.751	4.657	4.276	3.918	3.921	3.946
	KURTOSIS	38.82	32.50	33.98	31.70	30.39	25.93	22.35	22.36	22.41
METHOD OF MOMENTS Geometric (μm)	MEAN	4.989	4.523	4.632	4.267	4.482	4.337	4.850	5.209	5.140
	SORTING	3.754	3.524	3.465	3.288	3.317	3.395	3.473	3.469	3.570
	SKEWNESS	0.406	0.330	0.263	0.329	0.289	0.368	0.240	0.197	0.228
	KURTOSIS	2.816	2.617	2.563	2.733	2.692	2.676	2.501	2.500	2.493
METHOD OF MOMENTS Logarithmic (ϕ)	MEAN	7.647	7.789	7.754	7.873	7.802	7.849	7.688	7.585	7.604
	SORTING	1.908	1.817	1.793	1.717	1.730	1.764	1.796	1.795	1.836
	SKEWNESS	-0.406	-0.330	-0.263	-0.329	-0.289	-0.368	-0.240	-0.197	-0.228
	KURTOSIS	2.816	2.617	2.563	2.733	2.692	2.676	2.501	2.500	2.493
FOLK AND WARD METHOD (μm)	MEAN	4.741	4.382	4.501	4.105	4.325	4.186	4.716	5.077	4.980
	SORTING	3.810	3.619	3.569	3.373	3.412	3.509	3.622	3.608	3.718
	SKEWNESS	0.053	0.053	0.026	0.038	0.027	0.073	0.036	0.022	0.027
	KURTOSIS	0.931	0.901	0.894	0.967	0.958	0.975	0.936	0.934	0.930
FOLK AND WARD METHOD (ϕ)	MEAN	7.721	7.834	7.796	7.928	7.853	7.900	7.728	7.622	7.650
	SORTING	1.930	1.856	1.836	1.754	1.771	1.811	1.857	1.851	1.895
	SKEWNESS	-0.053	-0.053	-0.026	-0.038	-0.027	-0.073	-0.036	-0.022	-0.027
	KURTOSIS	0.931	0.901	0.894	0.967	0.958	0.975	0.936	0.934	0.930
FOLK AND WARD METHOD (Description)	MEAN:	Fine Silt	Fine Silt	Fine Silt	Fine Silt	Fine Silt	Fine Silt	Fine Silt	Fine Silt	Fine Silt
	SORTING:	Poorly Sorted	Poorly Sorted	Poorly Sorted	Poorly Sorted	Poorly Sorted	Poorly Sorted	Poorly Sorted	Poorly Sorted	Poorly Sorted
	SKEWNESS:	Symmetrical	Symmetrical	Symmetrical	Symmetrical	Symmetrical	Symmetrical	Symmetrical	Symmetrical	Symmetrical
	KURTOSIS:	Mesokurtic	Mesokurtic	Platykurtic	Mesokurtic	Mesokurtic	Mesokurtic	Mesokurtic	Mesokurtic	Mesokurtic
	MODE 1 (μm):	5.361	4.884	4.884	4.884	4.884	4.449	5.361	5.885	5.885
	MODE 2 (μm):				38.01					
	MODE 3 (μm):									
	MODE 1 (ϕ):	7.545	7.679	7.679	7.679	7.679	7.814	7.545	7.410	7.410
	MODE 2 (ϕ):				4.719					
	MODE 3 (ϕ):									
	D_{10} (μm):	0.904	0.879	0.896	0.897	0.918	0.895	0.929	0.985	0.942
	D_{50} (μm):	4.715	4.298	4.504	4.128	4.373	4.082	4.699	5.092	5.003
	D_{90} (μm):	27.09	24.12	23.82	20.83	21.78	23.30	25.93	27.22	28.36
	(D_{90} / D_{10}) (μm):	29.97	27.44	26.59	23.23	23.72	26.03	27.92	27.64	30.12
	(D_{90} - D_{10}) (μm):	26.19	23.24	22.92	19.94	20.86	22.40	25.00	26.24	27.42
	(D_{75} / D_{25}) (μm):	6.640	6.349	6.274	5.320	5.443	5.528	6.047	6.036	6.329
	(D_{75} - D_{25}) (μm):	10.15	9.045	9.285	7.504	8.077	7.766	9.461	10.29	10.37
	D_{10} (ϕ):	5.206	5.374	5.392	5.585	5.521	5.424	5.269	5.199	5.140
	D_{50} (ϕ):	7.728	7.862	7.795	7.920	7.837	7.936	7.733	7.617	7.643
	D_{90} (ϕ):	10.11	10.15	10.12	10.12	10.09	10.13	10.07	9.988	10.05
	(D_{90} / D_{10}) (ϕ):	1.942	1.889	1.878	1.813	1.827	1.867	1.912	1.921	1.956
	(D_{90} - D_{10}) (ϕ):	4.905	4.778	4.733	4.538	4.568	4.702	4.803	4.789	4.913
	(D_{75} / D_{25}) (ϕ):	1.428	1.408	1.408	1.357	1.367	1.367	1.402	1.409	1.420
	(D_{75} - D_{25}) (ϕ):	2.731	2.666	2.649	2.411	2.445	2.467	2.596	2.593	2.662
	% GRAVEL:	0.0%	0.0%	0.0%	0.0%	0.0%	0.0%	0.0%	0.0%	0.0%
	% SAND:	4.1%	2.4%	2.1%	1.8%	1.9%	2.1%	2.4%	2.5%	2.9%
	% MUD:	95.9%	97.6%	97.9%	98.2%	98.1%	97.9%	97.6%	97.5%	97.1%
	% V COARSE GRAVEL:	0.0%	0.0%	0.0%	0.0%	0.0%	0.0%	0.0%	0.0%	0.0%
	% COARSE GRAVEL:	0.0%	0.0%	0.0%	0.0%	0.0%	0.0%	0.0%	0.0%	0.0%
	% MEDIUM GRAVEL:	0.0%	0.0%	0.0%	0.0%	0.0%	0.0%	0.0%	0.0%	0.0%
	% FINE GRAVEL:	0.0%	0.0%	0.0%	0.0%	0.0%	0.0%	0.0%	0.0%	0.0%
	% V FINE GRAVEL:	0.0%	0.0%	0.0%	0.0%	0.0%	0.0%	0.0%	0.0%	0.0%
	% V COARSE SAND:	0.0%	0.0%	0.0%	0.0%	0.0%	0.0%	0.0%	0.0%	0.0%
	% COARSE SAND:	0.0%	0.0%	0.0%	0.0%	0.0%	0.0%	0.0%	0.0%	0.0%
	% MEDIUM SAND:	0.2%	0.0%	0.0%	0.0%	0.0%	0.0%	0.0%	0.0%	0.0%
	% FINE SAND:	1.6%	0.9%	0.7%	0.4%	0.5%	0.4%	0.4%	0.5%	0.7%
	% V FINE SAND:	2.2%	1.5%	1.3%	1.4%	1.5%	1.8%	2.0%	2.0%	2.2%
	% V COARSE SILT:	4.4%	4.5%	4.5%	4.0%	4.2%	4.8%	5.5%	5.6%	6.0%
	% COARSE SILT:	11.0%	10.6%	11.1%	8.5%	9.3%	8.6%	10.6%	11.6%	11.1%
	% MEDIUM SILT:	16.1%	15.4%	16.2%	15.3%	16.2%	14.4%	16.2%	17.1%	16.7%
	% FINE SILT:	19.8%	20.0%	20.3%	22.2%	22.1%	21.5%	21.0%	21.0%	20.6%
	% V FINE SILT:	17.7%	18.7%	18.3%	20.2%	19.6%	20.2%	18.4%	18.0%	17.6%
	% CLAY:	26.9%	28.6%	27.5%	28.0%	26.8%	28.4%	26.0%	24.0%	25.1%

SAMPLE STATISTICS

		CO4	CO4	CO4	CO4	CO4	CO4	CO4	NP3	NP3
	DEPTH OF SAMPLE:	98.5,	99.5,	100.5,	141.5,	183.5,	184.5,	185.5,	77.5,	78.5,
	SIEVING ERROR:									
	SAMPLE TYPE:	Unimodal, Poorly Sorted	Unimodal, Poorly Sorted	Unimodal, Poorly Sorted	Polymodal, Very Poorly Sorted	Unimodal, Poorly Sorted	Bimodal, Poorly Sorted	Bimodal, Poorly Sorted	Trimodal, Very Poorly Sorted	Polymodal, Poorly Sorted
	TEXTURAL GROUP:	Mud	Mud	Mud	Sandy Mud	Mud	Mud	Mud	Mud	Mud
	SEDIMENT NAME:	Fine Silt	Fine Silt	Fine Silt	Fine Sandy Fine Silt	Fine Silt	Fine Silt	Fine Silt	Fine Silt	Fine Silt
METHOD OF MOMENTS Arithmetic (μm)	MEAN	10.12	9.924	10.01	42.44	11.17	12.69	13.45	13.65	12.36
	SORTING	15.80	16.92	16.54	98.15	19.79	23.77	24.25	22.13	20.44
	SKEWNESS	4.284	4.416	4.479	3.627	3.984	3.916	3.582	2.918	3.324
	KURTOSIS	27.51	28.20	28.95	17.86	21.97	20.85	17.45	12.60	16.00
METHOD OF MOMENTS Geometric (μm)	MEAN	4.891	4.550	4.767	8.001	4.773	4.941	5.271	5.319	5.111
	SORTING	3.347	3.367	3.309	5.732	3.516	3.734	3.770	3.934	3.712
	SKEWNESS	0.130	0.290	0.212	0.639	0.348	0.401	0.359	0.303	0.295
	KURTOSIS	2.462	2.614	2.602	2.640	2.663	2.656	2.598	2.302	2.438
METHOD OF MOMENTS Logarithmic (ϕ)	MEAN	7.676	7.780	7.713	6.966	7.711	7.661	7.568	7.555	7.612
	SORTING	1.743	1.751	1.726	2.519	1.814	1.901	1.914	1.976	1.892
	SKEWNESS	-0.130	-0.290	-0.212	-0.639	-0.348	-0.401	-0.359	-0.303	-0.295
	KURTOSIS	2.462	2.614	2.602	2.640	2.663	2.656	2.598	2.302	2.438
FOLK AND WARD METHOD (μm)	MEAN	4.773	4.413	4.634	7.970	4.610	4.755	5.074	5.243	4.991
	SORTING	3.474	3.486	3.416	6.194	3.646	3.875	3.933	4.201	3.915
	SKEWNESS	-0.017	0.045	0.009	0.266	0.067	0.092	0.084	0.117	0.081
	KURTOSIS	0.902	0.954	0.944	1.054	0.987	0.977	0.984	0.906	0.948
FOLK AND WARD METHOD (ϕ)	MEAN	7.711	7.824	7.754	6.971	7.761	7.716	7.623	7.575	7.646
	SORTING	1.796	1.802	1.772	2.631	1.866	1.954	1.976	2.071	1.969
	SKEWNESS	0.017	-0.045	-0.009	-0.266	-0.067	-0.092	-0.084	-0.117	-0.081
	KURTOSIS	0.902	0.954	0.944	1.054	0.987	0.977	0.984	0.906	0.948
FOLK AND WARD METHOD (Description)	MEAN:	Fine Silt	Fine Silt	Fine Silt	Medium Silt	Fine Silt	Fine Silt	Fine Silt	Fine Silt	Fine Silt
	SORTING:	Poorly Sorted	Poorly Sorted	Poorly Sorted	Very Poorly Sorted	Poorly Sorted	Poorly Sorted	Poorly Sorted	Very Poorly Sorted	Poorly Sorted
	SKEWNESS:	Symmetrical	Symmetrical	Symmetrical	Coarse Skewed	Symmetrical	Symmetrical	Symmetrical	Coarse Skewed	Symmetrical
	KURTOSIS:	Mesokurtic	Mesokurtic	Mesokurtic	Mesokurtic	Mesokurtic	Mesokurtic	Mesokurtic	Mesokurtic	Mesokurtic
	MODE 1 (μm):	5.885	4.884	5.361	4.884	4.884	4.884	4.884	4.884	4.884
	MODE 2 (μm):				169.0		116.4	116.4	19.78	19.78
	MODE 3 (μm):				41.72				41.72	38.01
	MODE 1 (ϕ):	7.410	7.679	7.545	7.679	7.679	7.679	7.679	7.679	7.679
	MODE 2 (ϕ):				2.566		3.104	3.104	5.661	5.661
	MODE 3 (ϕ):				4.585				4.585	4.719
	D_{10} (μm):	0.942	0.923	0.958	1.010	0.930	0.912	0.946	0.909	0.921
	D_{50} (μm):	4.936	4.379	4.712	5.838	4.504	4.540	4.875	4.753	4.747
	D_{90} (μm):	23.35	23.33	22.76	137.9	26.63	30.82	33.72	39.46	33.25
	(D_{90} / D_{10}) (μm):	24.79	25.27	23.75	136.6	28.62	33.79	35.63	43.39	36.08
	(D_{90} - D_{10}) (μm):	22.41	22.40	21.80	136.9	25.70	29.91	32.77	38.55	32.32
	(D_{75} / D_{25}) (μm):	5.966	5.621	5.535	9.576	5.707	6.268	6.339	7.638	6.531
	(D_{75} - D_{25}) (μm):	9.670	8.381	8.831	18.98	8.754	9.568	10.36	12.13	10.38
	D_{10} (ϕ):	5.420	5.422	5.458	2.858	5.231	5.020	4.890	4.663	4.911
	D_{50} (ϕ):	7.662	7.835	7.729	7.420	7.795	7.783	7.680	7.717	7.719
	D_{90} (ϕ):	10.05	10.08	10.03	9.952	10.07	10.10	10.05	10.10	10.08
	(D_{90} / D_{10}) (ϕ):	1.855	1.859	1.837	3.482	1.925	2.012	2.054	2.166	2.053
	(D_{90} - D_{10}) (ϕ):	4.632	4.660	4.570	7.094	4.839	5.079	5.155	5.439	5.173
	(D_{75} / D_{25}) (ϕ):	1.401	1.376	1.378	1.586	1.383	1.410	1.420	1.476	1.426
	(D_{75} - D_{25}) (ϕ):	2.577	2.491	2.469	3.259	2.513	2.648	2.664	2.933	2.707
	% GRAVEL:	0.0%	0.0%	0.0%	0.0%	0.0%	0.0%	0.0%	0.0%	0.0%
	% SAND:	1.7%	2.0%	1.9%	15.9%	3.1%	4.2%	4.7%	4.8%	3.7%
	% MUD:	98.3%	98.0%	98.1%	84.1%	96.9%	95.8%	95.3%	95.2%	96.3%
	% V COARSE GRAVEL:	0.0%	0.0%	0.0%	0.0%	0.0%	0.0%	0.0%	0.0%	0.0%
	% COARSE GRAVEL:	0.0%	0.0%	0.0%	0.0%	0.0%	0.0%	0.0%	0.0%	0.0%
	% MEDIUM GRAVEL:	0.0%	0.0%	0.0%	0.0%	0.0%	0.0%	0.0%	0.0%	0.0%
	% FINE GRAVEL:	0.0%	0.0%	0.0%	0.0%	0.0%	0.0%	0.0%	0.0%	0.0%
	% V FINE GRAVEL:	0.0%	0.0%	0.0%	0.0%	0.0%	0.0%	0.0%	0.0%	0.0%
	% V COARSE SAND:	0.0%	0.0%	0.0%	0.0%	0.0%	0.0%	0.0%	0.0%	0.0%
	% COARSE SAND:	0.0%	0.0%	0.0%	1.0%	0.0%	0.0%	0.0%	0.0%	0.0%
	% MEDIUM SAND:	0.0%	0.0%	0.0%	3.8%	0.0%	0.0%	0.0%	0.0%	0.0%
	% FINE SAND:	0.3%	0.4%	0.4%	6.1%	0.6%	1.3%	1.3%	0.5%	0.5%
	% V FINE SAND:	1.4%	1.5%	1.5%	5.0%	2.4%	2.9%	3.4%	4.3%	3.2%
	% V COARSE SILT:	4.5%	4.8%	4.4%	5.3%	5.3%	5.7%	6.1%	6.1%	7.1%
	% COARSE SILT:	11.9%	9.6%	10.5%	7.8%	9.4%	9.5%	9.9%	10.3%	10.0%
	% MEDIUM SILT:	17.8%	15.7%	17.2%	13.3%	15.2%	14.6%	15.3%	13.3%	14.7%
	% FINE SILT:	21.1%	21.6%	22.0%	18.9%	21.6%	20.6%	20.7%	19.0%	20.4%
	% V FINE SILT:	17.9%	19.6%	19.0%	16.5%	19.3%	18.7%	18.2%	17.9%	18.2%
	% CLAY:	25.1%	26.9%	25.1%	22.4%	26.2%	26.7%	25.1%	26.6%	25.9%

SAMPLE STATISTICS

		NP3	NP3	NP3	NP3	NP3	NP3	NP3	MA2	MA2
	DEPTH OF SAMPLE:	79.5,	123.5,	124.5,	125.5,	161.5,	162.5,	163.5,	17.5,	18.5,
	SIEVING ERROR:									
	SAMPLE TYPE:	Polymodal, Very Poorly Sorted	Bimodal, Poorly Sorted	Polymodal, Very Poorly Sorted	Polymodal, Very Poorly Sorted	Trimodal, Poorly Sorted	Unimodal, Poorly Sorted	Trimodal, Poorly Sorted	Trimodal, Poorly Sorted	Trimodal, Poorly Sorted
	TEXTURAL GROUP:	Mud	Mud	Mud	Mud	Mud	Mud	Mud	Mud	Mud
	SEDIMENT NAME:	Fine Silt	Fine Silt	Fine Silt	Fine Silt	Fine Silt	Fine Silt	Fine Silt	Fine Silt	Mud
METHOD OF MOMENTS Arithmetic (μm)	MEAN	13.01	11.91	11.92	11.71	11.62	10.86	11.70	9.707	9.927
	SORTING	21.32	20.49	20.41	20.02	20.35	18.41	20.24	18.79	21.02
	SKEWNESS	3.092	3.536	3.457	3.445	3.616	3.780	3.525	4.124	4.709
	KURTOSIS	14.03	17.94	17.43	17.35	18.76	20.40	17.77	22.23	29.34
METHOD OF MOMENTS Geometric (μm)	MEAN	5.185	4.778	4.687	4.612	4.616	4.759	4.726	3.946	3.828
	SORTING	3.838	3.760	3.824	3.811	3.747	3.484	3.710	3.497	3.532
	SKEWNESS	0.311	0.341	0.355	0.366	0.383	0.323	0.367	0.516	0.600
	KURTOSIS	2.359	2.441	2.390	2.392	2.479	2.601	2.500	2.868	3.049
METHOD OF MOMENTS Logarithmic (ϕ)	MEAN	7.591	7.709	7.737	7.760	7.759	7.715	7.725	7.985	8.029
	SORTING	1.940	1.911	1.935	1.930	1.906	1.801	1.891	1.806	1.821
	SKEWNESS	-0.311	-0.341	-0.355	-0.366	-0.383	-0.323	-0.367	-0.516	-0.600
	KURTOSIS	2.359	2.441	2.390	2.392	2.479	2.601	2.500	2.868	3.049
FOLK AND WARD METHOD (μm)	MEAN	5.098	4.654	4.582	4.517	4.495	4.607	4.600	3.724	3.566
	SORTING	4.073	3.956	4.035	4.022	3.934	3.633	3.901	3.570	3.571
	SKEWNESS	0.108	0.096	0.114	0.121	0.115	0.068	0.105	0.104	0.116
	KURTOSIS	0.922	0.924	0.905	0.906	0.931	0.987	0.953	0.995	1.025
FOLK AND WARD METHOD (ϕ)	MEAN	7.616	7.747	7.770	7.790	7.798	7.762	7.764	8.069	8.131
	SORTING	2.026	1.984	2.012	2.008	1.976	1.861	1.964	1.836	1.836
	SKEWNESS	-0.108	-0.096	-0.114	-0.121	-0.115	-0.068	-0.105	-0.104	-0.116
	KURTOSIS	0.922	0.924	0.905	0.906	0.931	0.987	0.953	0.995	1.025
FOLK AND WARD METHOD (Description)	MEAN:	Fine Silt	Fine Silt	Fine Silt	Fine Silt	Fine Silt	Fine Silt	Fine Silt	Very Fine Silt	Very Fine Silt
	SORTING:	Very Poorly Sorted	Poorly Sorted	Very Poorly Sorted	Very Poorly Sorted	Poorly Sorted	Poorly Sorted	Poorly Sorted	Poorly Sorted	Poorly Sorted
	SKEWNESS:	Coarse Skewed	Symmetrical	Coarse Skewed	Coarse Skewed	Coarse Skewed	Symmetrical	Coarse Skewed	Coarse Skewed	Coarse Skewed
	KURTOSIS:	Mesokurtic	Mesokurtic	Mesokurtic	Mesokurtic	Mesokurtic	Mesokurtic	Mesokurtic	Mesokurtic	Mesokurtic
	MODE 1 (μm):	4.884	4.884	4.449	4.449	4.449	4.884	4.884	4.449	4.449
	MODE 2 (μm):	19.78	19.78	1.453	1.453	19.78		19.78	45.80	1.453
	MODE 3 (μm):	41.72		19.78	19.78	38.01		38.01	106.1	45.80
	MODE 1 (ϕ):	7.679	7.679	7.814	7.814	7.814	7.679	7.679	7.814	7.814
	MODE 2 (ϕ):	5.661	5.661	9.429	9.429	5.661		5.661	4.450	9.429
	MODE 3 (ϕ):	4.585		5.661	5.661	4.719		4.719	3.239	4.450
	D_{10} (μm):	0.913	0.869	0.846	0.842	0.860	0.934	0.880	0.823	0.807
	D_{50} (μm):	4.682	4.386	4.224	4.136	4.167	4.498	4.314	3.623	3.474
	D_{90} (μm):	36.81	31.32	32.41	31.96	30.54	26.71	30.86	21.46	21.39
	(D_{90} / D_{10}) (μm):	40.33	36.05	38.33	37.97	35.50	28.60	35.06	26.07	26.50
	(D_{90} - D_{10}) (μm):	35.90	30.46	31.57	31.12	29.68	25.78	29.98	20.64	20.58
	(D_{75} / D_{25}) (μm):	7.129	6.890	7.263	7.211	6.771	5.679	6.474	5.654	5.506
	(D_{75} - D_{25}) (μm):	11.22	9.947	10.10	9.873	9.456	8.727	9.383	6.973	6.539
	D_{10} (ϕ):	4.764	4.997	4.947	4.968	5.033	5.226	5.018	5.542	5.547
	D_{50} (ϕ):	7.739	7.833	7.887	7.917	7.907	7.797	7.857	8.109	8.169
	D_{90} (ϕ):	10.10	10.17	10.21	10.21	10.18	10.06	10.15	10.25	10.27
	(D_{90} / D_{10}) (ϕ):	2.120	2.035	2.063	2.056	2.023	1.926	2.023	1.849	1.852
	(D_{90} - D_{10}) (ϕ):	5.334	5.172	5.261	5.247	5.150	4.838	5.132	4.704	4.728
	(D_{75} / D_{25}) (ϕ):	1.453	1.433	1.446	1.442	1.425	1.382	1.415	1.363	1.353
	(D_{75} - D_{25}) (ϕ):	2.834	2.784	2.861	2.850	2.759	2.506	2.695	2.499	2.461
	% GRAVEL:	0.0%	0.0%	0.0%	0.0%	0.0%	0.0%	0.0%	0.0%	0.0%
	% SAND:	4.2%	3.5%	3.5%	3.4%	3.5%	2.8%	3.5%	2.9%	3.1%
	% MUD:	95.8%	96.5%	96.5%	96.6%	96.5%	97.2%	96.5%	97.1%	96.9%
	% V COARSE GRAVEL:	0.0%	0.0%	0.0%	0.0%	0.0%	0.0%	0.0%	0.0%	0.0%
	% COARSE GRAVEL:	0.0%	0.0%	0.0%	0.0%	0.0%	0.0%	0.0%	0.0%	0.0%
	% MEDIUM GRAVEL:	0.0%	0.0%	0.0%	0.0%	0.0%	0.0%	0.0%	0.0%	0.0%
	% FINE GRAVEL:	0.0%	0.0%	0.0%	0.0%	0.0%	0.0%	0.0%	0.0%	0.0%
	% V FINE GRAVEL:	0.0%	0.0%	0.0%	0.0%	0.0%	0.0%	0.0%	0.0%	0.0%
	% V COARSE SAND:	0.0%	0.0%	0.0%	0.0%	0.0%	0.0%	0.0%	0.0%	0.0%
	% COARSE SAND:	0.0%	0.0%	0.0%	0.0%	0.0%	0.0%	0.0%	0.0%	0.0%
	% MEDIUM SAND:	0.0%	0.0%	0.0%	0.0%	0.0%	0.0%	0.0%	0.0%	0.0%
	% FINE SAND:	0.5%	0.6%	0.5%	0.5%	0.6%	0.4%	0.5%	0.4%	1.0%
	% V FINE SAND:	3.7%	2.9%	2.9%	2.9%	2.9%	2.4%	3.0%	2.5%	2.2%
	% V COARSE SILT:	7.8%	6.5%	6.9%	6.9%	6.3%	5.6%	6.3%	4.0%	3.9%
	% COARSE SILT:	10.1%	9.9%	9.9%	9.8%	9.5%	9.2%	9.4%	7.0%	6.2%
	% MEDIUM SILT:	13.7%	14.0%	13.1%	13.0%	13.3%	15.2%	13.7%	13.1%	12.2%
	% FINE SILT:	19.5%	19.4%	18.7%	18.6%	19.3%	21.6%	20.0%	20.6%	20.7%
	% V FINE SILT:	18.2%	18.2%	18.2%	18.3%	18.8%	19.4%	18.8%	20.2%	20.6%
	% CLAY:	26.5%	28.5%	29.6%	30.1%	29.4%	26.1%	28.2%	32.1%	33.1%

SAMPLE STATISTICS

		MA2	MA2	MA2	MA2	MA2	MA2	MA2	MA2	MA2
	DEPTH OF SAMPLE:	19.5,	63.5,	64.5,	65.5,	110.5,	111.5,	112.5,	142.5,	143.5,
	SIEVING ERROR:									
	SAMPLE TYPE:	Bimodal, Poorly Sorted	Bimodal, Poorly Sorted	Bimodal, Poorly Sorted	Bimodal, Poorly Sorted	Trimodal, Poorly Sorted	Bimodal, Poorly Sorted	Bimodal, Poorly Sorted	Trimodal, Poorly Sorted	Bimodal, Poorly Sorted
	TEXTURAL GROUP:	Mud	Mud	Mud	Mud	Mud	Mud	Mud	Mud	Mud
	SEDIMENT NAME:	Fine Silt	Fine Silt	Fine Silt	Fine Silt	Mud	Fine Silt	Fine Silt	Medium Silt	Coarse Silt
METHOD OF MOMENTS Arithmetic (μm)	MEAN	10.67	10.26	10.90	10.17	9.336	11.42	11.74	11.07	14.56
	SORTING	21.78	18.74	18.89	19.12	17.49	20.87	21.52	13.87	18.11
	SKEWNESS	4.387	3.927	3.770	4.433	4.227	3.613	3.452	3.307	2.540
	KURTOSIS	25.43	21.70	20.49	27.15	25.31	18.10	16.18	21.11	12.15
METHOD OF MOMENTS Geometric (μm)	MEAN	4.163	4.168	4.600	4.286	3.842	4.442	4.570	5.714	6.908
	SORTING	3.553	3.587	3.559	3.471	3.494	3.709	3.677	3.381	3.749
	SKEWNESS	0.547	0.458	0.371	0.426	0.519	0.463	0.485	-0.107	-0.143
	KURTOSIS	2.980	2.663	2.589	2.783	2.763	2.645	2.731	2.183	2.072
METHOD OF MOMENTS Logarithmic (ϕ)	MEAN	7.908	7.906	7.764	7.866	8.024	7.815	7.773	7.451	7.178
	SORTING	1.829	1.843	1.831	1.795	1.805	1.891	1.879	1.758	1.906
	SKEWNESS	-0.547	-0.458	-0.371	-0.426	-0.519	-0.463	-0.485	0.107	0.143
	KURTOSIS	2.980	2.663	2.589	2.783	2.763	2.645	2.731	2.183	2.072
FOLK AND WARD METHOD (μm)	MEAN	3.904	4.001	4.449	4.078	3.672	4.264	4.349	5.673	6.836
	SORTING	3.617	3.725	3.718	3.568	3.598	3.870	3.831	3.548	3.936
	SKEWNESS	0.105	0.115	0.091	0.075	0.134	0.124	0.125	-0.082	-0.097
	KURTOSIS	1.031	0.981	0.982	0.995	0.993	0.998	1.049	0.834	0.799
FOLK AND WARD METHOD (ϕ)	MEAN	8.001	7.965	7.812	7.938	8.089	7.874	7.845	7.462	7.193
	SORTING	1.855	1.897	1.895	1.835	1.847	1.952	1.938	1.827	1.977
	SKEWNESS	-0.105	-0.115	-0.091	-0.075	-0.134	-0.124	-0.125	0.082	0.097
	KURTOSIS	1.031	0.981	0.982	0.995	0.993	0.998	1.049	0.834	0.799
FOLK AND WARD METHOD (Description)	MEAN:	Very Fine Silt	Fine Silt	Fine Silt	Fine Silt	Very Fine Silt	Fine Silt	Fine Silt	Fine Silt	Fine Silt
	SORTING:	Poorly Sorted	Poorly Sorted	Poorly Sorted	Poorly Sorted	Poorly Sorted	Poorly Sorted	Poorly Sorted	Poorly Sorted	Poorly Sorted
	SKEWNESS:	Coarse Skewed	Coarse Skewed	Symmetrical	Symmetrical	Coarse Skewed	Coarse Skewed	Coarse Skewed	Symmetrical	Symmetrical
	KURTOSIS:	Mesokurtic	Mesokurtic	Mesokurtic	Mesokurtic	Mesokurtic	Mesokurtic	Mesokurtic	Platykurtic	Platykurtic
	MODE 1 (μm):	4.449	4.449	4.884	4.884	3.691	4.449	4.449	7.091	21.72
	MODE 2 (μm):	45.80	41.72	41.72	41.72	19.78	45.80	45.80	16.41	7.091
	MODE 3 (μm):					41.72			19.78	
	MODE 1 (ϕ):	7.814	7.814	7.679	7.679	8.084	7.814	7.814	7.141	5.527
	MODE 2 (ϕ):	4.450	4.585	4.585	4.585	5.661	4.450	4.450	5.931	7.141
	MODE 3 (ϕ):					4.585			5.661	
	D_{10} (μm):	0.854	0.835	0.900	0.870	0.815	0.855	0.891	1.018	1.055
	D_{50} (μm):	3.814	3.793	4.269	4.031	3.441	4.003	4.120	6.093	7.488
	D_{90} (μm):	22.88	25.50	27.51	23.27	22.97	29.52	29.99	27.14	37.00
	(D_{90} / D_{10}) (μm):	26.80	30.54	30.57	26.74	28.18	34.52	33.66	26.67	35.08
	(D_{90} - D_{10}) (μm):	22.03	24.66	26.61	22.40	22.15	28.66	29.10	26.12	35.94
	(D_{75} / D_{25}) (μm):	5.521	5.961	5.901	5.582	5.629	6.109	5.713	6.797	8.501
	(D_{75} - D_{25}) (μm):	7.195	7.655	8.555	7.610	6.743	8.253	8.078	12.89	18.11
	D_{10} (ϕ):	5.450	5.293	5.184	5.426	5.444	5.082	5.059	5.203	4.756
	D_{50} (ϕ):	8.035	8.042	7.872	7.955	8.183	7.965	7.923	7.359	7.061
	D_{90} (ϕ):	10.19	10.23	10.12	10.17	10.26	10.19	10.13	9.940	9.889
	(D_{90} / D_{10}) (ϕ):	1.871	1.932	1.952	1.874	1.885	2.005	2.003	1.910	2.079
	(D_{90} - D_{10}) (ϕ):	4.744	4.932	4.934	4.741	4.817	5.109	5.073	4.737	5.133
	(D_{75} / D_{25}) (ϕ):	1.361	1.381	1.388	1.367	1.360	1.392	1.377	1.457	1.551
	(D_{75} - D_{25}) (ϕ):	2.465	2.576	2.561	2.481	2.493	2.611	2.514	2.765	3.088
	% GRAVEL:	0.0%	0.0%	0.0%	0.0%	0.0%	0.0%	0.0%	0.0%	0.0%
	% SAND:	3.7%	2.9%	3.0%	2.7%	2.4%	3.9%	4.5%	0.8%	2.4%
	% MUD:	96.3%	97.1%	97.0%	97.3%	97.6%	96.1%	95.5%	99.2%	97.6%
	% V COARSE GRAVEL:	0.0%	0.0%	0.0%	0.0%	0.0%	0.0%	0.0%	0.0%	0.0%
	% COARSE GRAVEL:	0.0%	0.0%	0.0%	0.0%	0.0%	0.0%	0.0%	0.0%	0.0%
	% MEDIUM GRAVEL:	0.0%	0.0%	0.0%	0.0%	0.0%	0.0%	0.0%	0.0%	0.0%
	% FINE GRAVEL:	0.0%	0.0%	0.0%	0.0%	0.0%	0.0%	0.0%	0.0%	0.0%
	% V FINE GRAVEL:	0.0%	0.0%	0.0%	0.0%	0.0%	0.0%	0.0%	0.0%	0.0%
	% V COARSE SAND:	0.0%	0.0%	0.0%	0.0%	0.0%	0.0%	0.0%	0.0%	0.0%
	% COARSE SAND:	0.0%	0.0%	0.0%	0.0%	0.0%	0.0%	0.0%	0.0%	0.0%
	% MEDIUM SAND:	0.0%	0.0%	0.0%	0.0%	0.0%	0.0%	0.0%	0.0%	0.0%
	% FINE SAND:	1.0%	0.5%	0.4%	0.7%	0.4%	0.6%	0.6%	0.1%	0.2%
	% V FINE SAND:	2.7%	2.4%	2.5%	2.1%	2.0%	3.3%	3.9%	0.7%	2.2%
	% V COARSE SILT:	3.9%	5.3%	5.8%	4.6%	4.8%	5.6%	5.2%	6.5%	11.4%
	% COARSE SILT:	7.0%	7.8%	8.7%	7.8%	7.3%	7.9%	7.4%	16.8%	18.5%
	% MEDIUM SILT:	13.5%	12.9%	14.3%	14.3%	11.6%	13.1%	13.5%	18.9%	16.7%
	% FINE SILT:	21.2%	20.2%	20.9%	21.5%	19.9%	20.3%	21.2%	18.9%	16.1%
	% V FINE SILT:	20.4%	19.7%	19.4%	19.9%	20.7%	19.4%	20.0%	15.7%	14.0%
	% CLAY:	30.4%	31.2%	27.8%	29.1%	33.2%	29.8%	28.3%	22.3%	20.9%

SAMPLE STATISTICS

		MA2	MA2	MA2	MA2	MA2	MA2	MA2	MA5	MA5
	DEPTH OF SAMPLE:	144.5,	181.5,	182.5,	183.5,	207.5,	208.5,	209.5,	58.5,	59.5,
	SIEVING ERROR:									
	SAMPLE TYPE:	Bimodal, Very Poorly Sorted	Polymodal, Poorly Sorted	Polymodal, Poorly Sorted	Polymodal, Poorly Sorted	Bimodal, Poorly Sorted	Trimodal, Poorly Sorted	Trimodal, Poorly Sorted	Polymodal, Very Poorly Sorted	Unimodal, Very Poorly Sorted
	TEXTURAL GROUP:	Mud	Mud	Mud	Mud	Mud	Mud	Mud	Sandy Mud	Sandy Mud
	SEDIMENT NAME:	Very Coarse Silt	Mud	Mud	Mud	Fine Silt	Mud	Fine Silt	Very Fine Sandy Very Coarse Silt	Very Fine Sandy Very Coarse Silt
METHOD OF MOMENTS Arithmetic (μm)	MEAN	23.43	8.948	8.935	8.823	9.340	9.359	9.929	40.20	50.98
	SORTING	25.44	17.16	16.98	17.17	16.72	16.89	17.82	38.31	44.16
	SKEWNESS	1.619	4.589	4.389	4.499	4.356	4.181	4.172	1.361	1.181
	KURTOSIS	6.005	29.05	26.65	27.80	27.18	24.96	24.80	4.906	4.182
METHOD OF MOMENTS Geometric (μm)	MEAN	10.78	3.764	3.702	3.625	4.029	3.937	4.157	19.77	27.72
	SORTING	4.238	3.427	3.469	3.456	3.462	3.510	3.554	4.388	4.072
	SKEWNESS	-0.415	0.501	0.516	0.548	0.405	0.440	0.404	-0.833	-1.132
	KURTOSIS	2.064	2.822	2.777	2.847	2.619	2.623	2.580	2.653	3.492
METHOD OF MOMENTS Logarithmic (ϕ)	MEAN	6.536	8.053	8.077	8.108	7.955	7.989	7.910	5.661	5.173
	SORTING	2.083	1.777	1.795	1.789	1.792	1.812	1.829	2.134	2.026
	SKEWNESS	0.415	-0.501	-0.516	-0.548	-0.405	-0.440	-0.404	0.833	1.132
	KURTOSIS	2.064	2.822	2.777	2.847	2.619	2.623	2.580	2.653	3.492
FOLK AND WARD METHOD (μm)	MEAN	10.80	3.574	3.529	3.436	3.900	3.806	4.036	19.54	28.19
	SORTING	4.431	3.499	3.557	3.525	3.586	3.642	3.699	4.538	4.098
	SKEWNESS	-0.277	0.103	0.123	0.128	0.096	0.113	0.102	-0.478	-0.461
	KURTOSIS	0.783	0.979	0.970	0.980	0.940	0.947	0.935	0.967	1.357
FOLK AND WARD METHOD (ϕ)	MEAN	6.533	8.128	8.147	8.185	8.002	8.037	7.953	5.678	5.149
	SORTING	2.148	1.807	1.831	1.817	1.843	1.865	1.887	2.182	2.035
	SKEWNESS	0.277	-0.103	-0.123	-0.128	-0.096	-0.113	-0.102	0.478	0.461
	KURTOSIS	0.783	0.979	0.970	0.980	0.940	0.947	0.935	0.967	1.357
FOLK AND WARD METHOD (Description)	MEAN:	Medium Silt	Very Fine Silt	Very Fine Silt	Very Fine Silt	Very Fine Silt	Very Fine Silt	Fine Silt	Coarse Silt	Coarse Silt
	SORTING:	Very Poorly Sorted	Poorly Sorted	Poorly Sorted	Poorly Sorted	Poorly Sorted	Poorly Sorted	Poorly Sorted	Very Poorly Sorted	Very Poorly Sorted
	SKEWNESS:	Fine Skewed	Coarse Skewed	Coarse Skewed	Coarse Skewed	Symmetrical	Coarse Skewed	Coarse Skewed	Very Fine Skewed	Very Fine Skewed
	KURTOSIS:	Platykurtic	Mesokurtic	Mesokurtic	Mesokurtic	Mesokurtic	Mesokurtic	Mesokurtic	Mesokurtic	Leptokurtic
	MODE 1 (μm):	38.01	4.449	3.691	3.691	4.449	4.449	4.449	45.80	50.26
	MODE 2 (μm):	1.921	1.453	1.453	1.921	19.78	1.453	1.453	5.885	
	MODE 3 (μm):		19.78	1.205	1.453		19.78	19.78	7.091	
	MODE 1 (ϕ):	4.719	7.814	8.084	8.084	7.814	7.814	7.814	4.450	4.315
	MODE 2 (ϕ):	9.025	9.429	9.429	9.025	5.661	9.429	9.429	7.410	
	MODE 3 (ϕ):		5.661	9.698	9.429		5.661	5.661	7.141	
	D_{10} (μm):	1.211	0.805	0.790	0.785	0.829	0.809	0.829	1.702	2.516
	D_{50} (μm):	14.52	3.461	3.349	3.263	3.726	3.594	3.819	32.98	42.19
	D_{90} (μm):	57.12	20.88	21.30	20.68	22.75	23.17	24.53	91.36	115.9
	(D_{90} / D_{10}) (μm):	47.15	25.96	26.96	26.35	27.45	28.65	29.61	53.68	46.06
	(D_{90} - D_{10}) (μm):	55.91	20.08	20.51	19.90	21.92	22.37	23.70	89.66	113.4
	(D_{75} / D_{25}) (μm):	10.56	5.566	5.728	5.627	5.934	6.013	6.210	7.675	4.224
	(D_{75} - D_{25}) (μm):	32.63	6.584	6.591	6.353	7.508	7.331	7.980	49.64	53.61
	D_{10} (ϕ):	4.130	5.581	5.553	5.595	5.458	5.431	5.349	3.452	3.109
	D_{50} (ϕ):	6.106	8.175	8.222	8.260	8.068	8.120	8.033	4.922	4.567
	D_{90} (ϕ):	9.689	10.28	10.31	10.32	10.24	10.27	10.24	9.199	8.635
	(D_{90} / D_{10}) (ϕ):	2.346	1.842	1.856	1.843	1.875	1.891	1.914	2.664	2.777
	(D_{90} - D_{10}) (ϕ):	5.559	4.698	4.753	4.720	4.778	4.840	4.888	5.746	5.525
	(D_{75} / D_{25}) (ϕ):	1.709	1.356	1.361	1.355	1.378	1.379	1.392	1.712	1.543
	(D_{75} - D_{25}) (ϕ):	3.401	2.477	2.518	2.492	2.569	2.588	2.635	2.940	2.079
	% GRAVEL:	0.0%	0.0%	0.0%	0.0%	0.0%	0.0%	0.0%	0.0%	0.0%
	% SAND:	7.9%	2.1%	2.2%	2.2%	2.0%	2.1%	2.3%	21.1%	30.2%
	% MUD:	92.1%	97.9%	97.8%	97.8%	98.0%	97.9%	97.7%	78.9%	69.8%
	% V COARSE GRAVEL:	0.0%	0.0%	0.0%	0.0%	0.0%	0.0%	0.0%	0.0%	0.0%
	% COARSE GRAVEL:	0.0%	0.0%	0.0%	0.0%	0.0%	0.0%	0.0%	0.0%	0.0%
	% MEDIUM GRAVEL:	0.0%	0.0%	0.0%	0.0%	0.0%	0.0%	0.0%	0.0%	0.0%
	% FINE GRAVEL:	0.0%	0.0%	0.0%	0.0%	0.0%	0.0%	0.0%	0.0%	0.0%
	% V FINE GRAVEL:	0.0%	0.0%	0.0%	0.0%	0.0%	0.0%	0.0%	0.0%	0.0%
	% V COARSE SAND:	0.0%	0.0%	0.0%	0.0%	0.0%	0.0%	0.0%	0.0%	0.0%
	% COARSE SAND:	0.0%	0.0%	0.0%	0.0%	0.0%	0.0%	0.0%	0.0%	0.0%
	% MEDIUM SAND:	0.0%	0.0%	0.0%	0.0%	0.0%	0.0%	0.0%	0.0%	0.0%
	% FINE SAND:	0.5%	0.4%	0.4%	0.4%	0.4%	0.3%	0.4%	4.7%	8.2%
	% V FINE SAND:	7.4%	1.7%	1.8%	1.8%	1.6%	1.8%	1.9%	16.4%	21.9%
	% V COARSE SILT:	21.9%	4.1%	4.3%	4.1%	4.6%	4.8%	5.1%	30.7%	32.0%
	% COARSE SILT:	18.7%	7.2%	7.3%	6.9%	8.7%	8.3%	9.0%	14.9%	13.6%
	% MEDIUM SILT:	12.7%	12.2%	11.8%	11.5%	13.1%	12.5%	13.1%	7.7%	6.0%
	% FINE SILT:	11.6%	20.5%	19.8%	19.7%	20.1%	19.8%	19.8%	7.3%	5.1%
	% V FINE SILT:	10.4%	20.5%	20.4%	20.6%	19.9%	19.8%	19.4%	6.9%	4.9%
	% CLAY:	16.7%	33.3%	34.4%	35.0%	31.6%	32.7%	31.3%	11.3%	8.2%

SAMPLE STATISTICS

		MA5	MA5	MA5	MA5	MA5	MA5	MA5	MA5	MA5
	DEPTH OF SAMPLE:	60.5,	82.5,	83.5,	84.5,	96,	97,	98,	119.5,	120.5,
	SIEVING ERROR:									
	SAMPLE TYPE:	Unimodal, Poorly Sorted	Bimodal, Poorly Sorted	Unimodal, Poorly Sorted	Unimodal, Poorly Sorted	Bimodal, Poorly Sorted	Unimodal, Poorly Sorted	Bimodal, Poorly Sorted	Unimodal, Poorly Sorted	Unimodal, Poorly Sorted
	TEXTURAL GROUP:	Mud	Mud	Mud	Mud	Mud	Mud	Mud	Mud	Mud
	SEDIMENT NAME:	Fine Silt	Fine Silt	Fine Silt	Fine Silt	Fine Silt	Fine Silt	Fine Silt	Fine Silt	Fine Silt
METHOD OF MOMENTS Arithmetic (μm)	MEAN	11.43	12.47	12.28	13.19	13.74	10.63	13.95	10.51	10.54
	SORTING	17.50	18.21	17.54	22.80	21.99	12.53	20.46	14.85	14.65
	SKEWNESS	4.295	3.610	3.561	4.202	3.906	2.088	3.100	3.987	4.011
	KURTOSIS	27.45	20.81	20.39	24.22	22.54	7.617	14.46	25.24	25.84
METHOD OF MOMENTS Geometric (μm)	MEAN	5.592	5.736	5.851	5.728	6.132	5.593	6.353	5.435	5.548
	SORTING	3.365	3.642	3.530	3.621	3.626	3.302	3.633	3.229	3.190
	SKEWNESS	0.044	0.023	0.004	0.153	0.092	-0.078	0.048	0.007	-0.020
	KURTOSIS	2.466	2.221	2.281	2.527	2.429	2.212	2.344	2.464	2.487
METHOD OF MOMENTS Logarithmic (ϕ)	MEAN	7.482	7.446	7.417	7.448	7.349	7.482	7.298	7.524	7.494
	SORTING	1.751	1.865	1.820	1.856	1.858	1.724	1.861	1.691	1.674
	SKEWNESS	-0.044	-0.023	-0.004	-0.153	-0.092	0.078	-0.048	-0.007	0.020
	KURTOSIS	2.466	2.221	2.281	2.527	2.429	2.212	2.344	2.464	2.487
FOLK AND WARD METHOD (μm)	MEAN	5.470	5.608	5.735	5.495	5.947	5.559	6.190	5.345	5.470
	SORTING	3.466	3.806	3.689	3.714	3.766	3.506	3.788	3.346	3.299
	SKEWNESS	-0.054	-0.046	-0.050	-0.031	-0.024	-0.051	-0.027	-0.056	-0.065
	KURTOSIS	0.895	0.835	0.867	0.907	0.914	0.898	0.907	0.924	0.932
FOLK AND WARD METHOD (ϕ)	MEAN	7.514	7.478	7.446	7.508	7.394	7.491	7.336	7.548	7.514
	SORTING	1.793	1.928	1.883	1.893	1.913	1.810	1.922	1.742	1.722
	SKEWNESS	0.054	0.046	0.050	0.031	0.024	0.051	0.027	0.056	0.065
	KURTOSIS	0.895	0.835	0.867	0.907	0.914	0.898	0.907	0.924	0.932
FOLK AND WARD METHOD (Description)	MEAN:	Fine Silt	Fine Silt	Fine Silt	Fine Silt	Fine Silt	Fine Silt	Fine Silt	Fine Silt	Fine Silt
	SORTING:	Poorly Sorted	Poorly Sorted	Poorly Sorted	Poorly Sorted	Poorly Sorted	Poorly Sorted	Poorly Sorted	Poorly Sorted	Poorly Sorted
	SKEWNESS:	Symmetrical	Symmetrical	Symmetrical	Symmetrical	Symmetrical	Symmetrical	Symmetrical	Symmetrical	Symmetrical
	KURTOSIS:	Platykurtic	Platykurtic	Platykurtic	Mesokurtic	Mesokurtic	Platykurtic	Mesokurtic	Mesokurtic	Mesokurtic
	MODE 1 (μm):	7.091	7.091	7.091	7.091	7.091	7.091	7.091	7.091	7.091
	MODE 2 (μm):		16.41			5.885		96.60		
	MODE 3 (μm):									
	MODE 1 (ϕ):	7.141	7.141	7.141	7.141	7.141	7.141	7.141	7.141	7.141
	MODE 2 (ϕ):		5.931			7.410		3.373		
	MODE 3 (ϕ):									
	D_{10} (μm):	1.044	0.958	1.013	0.993	1.048	1.043	1.072	1.064	1.096
	D_{50} (μm):	5.793	5.941	6.083	5.833	6.205	5.858	6.442	5.656	5.809
	D_{90} (μm):	25.71	30.72	29.99	28.91	32.62	27.14	35.05	24.11	24.10
	(D_{90} / D_{10}) (μm):	24.63	32.07	29.61	29.11	31.13	26.02	32.70	22.67	21.99
	(D_{90} - D_{10}) (μm):	24.66	29.76	28.97	27.92	31.57	26.10	33.98	23.05	23.00
	(D_{75} / D_{25}) (μm):	6.046	7.584	6.879	6.636	6.650	6.071	6.750	5.515	5.347
	(D_{75} - D_{25}) (μm):	11.39	13.52	13.00	12.11	13.20	11.52	13.92	10.39	10.43
	D_{10} (ϕ):	5.282	5.025	5.060	5.112	4.938	5.203	4.834	5.374	5.375
	D_{50} (ϕ):	7.432	7.395	7.361	7.422	7.332	7.415	7.278	7.466	7.428
	D_{90} (ϕ):	9.904	10.03	9.948	9.976	9.898	9.905	9.865	9.877	9.834
	(D_{90} / D_{10}) (ϕ):	1.875	1.996	1.966	1.951	2.005	1.904	2.041	1.838	1.830
	(D_{90} - D_{10}) (ϕ):	4.623	5.003	4.888	4.863	4.960	4.702	5.031	4.503	4.459
	(D_{75} / D_{25}) (ϕ):	1.419	1.487	1.461	1.445	1.455	1.421	1.464	1.391	1.385
	(D_{75} - D_{25}) (ϕ):	2.596	2.923	2.782	2.730	2.733	2.602	2.755	2.463	2.419
	% GRAVEL:	0.0%	0.0%	0.0%	0.0%	0.0%	0.0%	0.0%	0.0%	0.0%
	% SAND:	2.0%	2.2%	2.0%	3.4%	3.6%	0.6%	3.7%	1.4%	1.4%
	% MUD:	98.0%	97.8%	98.0%	96.6%	96.4%	99.4%	96.3%	98.6%	98.6%
	% V COARSE GRAVEL:	0.0%	0.0%	0.0%	0.0%	0.0%	0.0%	0.0%	0.0%	0.0%
	% COARSE GRAVEL:	0.0%	0.0%	0.0%	0.0%	0.0%	0.0%	0.0%	0.0%	0.0%
	% MEDIUM GRAVEL:	0.0%	0.0%	0.0%	0.0%	0.0%	0.0%	0.0%	0.0%	0.0%
	% FINE GRAVEL:	0.0%	0.0%	0.0%	0.0%	0.0%	0.0%	0.0%	0.0%	0.0%
	% V FINE GRAVEL:	0.0%	0.0%	0.0%	0.0%	0.0%	0.0%	0.0%	0.0%	0.0%
	% V COARSE SAND:	0.0%	0.0%	0.0%	0.0%	0.0%	0.0%	0.0%	0.0%	0.0%
	% COARSE SAND:	0.0%	0.0%	0.0%	0.0%	0.0%	0.0%	0.0%	0.0%	0.0%
	% MEDIUM SAND:	0.0%	0.0%	0.0%	0.0%	0.0%	0.0%	0.0%	0.0%	0.0%
	% FINE SAND:	0.5%	0.4%	0.4%	1.3%	1.0%	0.0%	0.4%	0.2%	0.2%
	% V FINE SAND:	1.5%	1.8%	1.7%	2.1%	2.6%	0.6%	3.3%	1.2%	1.2%
	% V COARSE SILT:	5.1%	7.5%	7.3%	5.6%	7.0%	7.2%	7.9%	4.9%	4.9%
	% COARSE SILT:	14.3%	15.2%	15.0%	13.7%	14.2%	14.1%	14.5%	13.2%	13.5%
	% MEDIUM SILT:	19.5%	17.8%	18.7%	18.9%	18.5%	19.4%	18.4%	20.1%	20.6%
	% FINE SILT:	20.4%	18.0%	18.9%	19.4%	19.5%	20.5%	19.4%	21.7%	22.0%
	% V FINE SILT:	16.7%	15.3%	15.7%	16.0%	15.8%	16.5%	15.5%	17.3%	17.1%
	% CLAY:	21.9%	24.0%	22.4%	23.0%	21.3%	21.8%	20.7%	21.4%	20.5%

SAMPLE STATISTICS

		MA5	MA5A	MA5A	MA5A	MA5A	MA5A	MA5A	MA5A	MA5A	MA5A
	DEPTH OF SAMPLE:	121.5,	32,	33,	34,	77.5,	78.5,	79.5,	110.5,	111.5,	112.5,
	SIEVING ERROR:										
	SAMPLE TYPE:	Unimodal, Poorly Sorted	Unimodal, Very Poorly Sorted	Unimodal, Poorly Sorted	Trimodal, Very Poorly Sorted	Unimodal, Poorly Sorted	Unimodal, Poorly Sorted	Bimodal, Poorly Sorted	Trimodal, Poorly Sorted	Trimodal, Poorly Sorted	Unimodal, Poorly Sorted
	TEXTURAL GROUP:	Mud	Mud	Mud	Mud	Mud	Mud	Mud	Mud	Mud	Mud
	SEDIMENT NAME:	Fine Silt	Fine Silt	Fine Silt	Fine Silt	Fine Silt	Fine Silt	Fine Silt	Fine Silt	Fine Silt	Fine Silt
METHOD OF MOMENTS Arithmetic (μm)	MEAN	10.98	16.05	14.86	16.01	12.46	11.39	14.33	11.17	11.48	11.63
	SORTING	14.99	22.10	20.85	22.11	19.28	18.16	23.42	18.78	19.26	19.50
	SKEWNESS	3.942	2.570	3.003	2.448	3.505	3.617	3.246	3.645	3.585	3.627
	KURTOSIS	25.12	10.80	14.49	10.01	18.15	19.28	15.18	19.27	18.63	18.77
METHOD OF MOMENTS Geometric (μm)	MEAN	5.824	7.108	6.837	6.786	5.705	5.159	5.921	4.784	4.878	5.016
	SORTING	3.189	3.832	3.684	3.994	3.522	3.488	3.767	3.563	3.592	3.554
	SKEWNESS	-0.054	-0.011	-0.027	0.018	0.131	0.211	0.228	0.327	0.325	0.303
	KURTOSIS	2.492	2.200	2.280	2.089	2.454	2.496	2.438	2.530	2.511	2.546
METHOD OF MOMENTS Logarithmic (ϕ)	MEAN	7.424	7.136	7.193	7.203	7.453	7.599	7.400	7.708	7.680	7.639
	SORTING	1.673	1.938	1.881	1.998	1.816	1.802	1.913	1.833	1.845	1.829
	SKEWNESS	0.054	0.011	0.027	-0.018	-0.131	-0.211	-0.228	-0.327	-0.325	-0.303
	KURTOSIS	2.492	2.200	2.280	2.089	2.454	2.496	2.438	2.530	2.511	2.546
FOLK AND WARD METHOD (μm)	MEAN	5.766	7.063	6.728	6.723	5.553	5.022	5.770	4.668	4.765	4.876
	SORTING	3.292	4.086	3.876	4.277	3.677	3.653	3.967	3.740	3.770	3.710
	SKEWNESS	-0.073	-0.016	-0.047	0.001	0.000	0.031	0.056	0.085	0.089	0.070
	KURTOSIS	0.933	0.879	0.893	0.831	0.947	0.964	0.959	0.968	0.961	0.969
FOLK AND WARD METHOD (ϕ)	MEAN	7.438	7.145	7.216	7.217	7.492	7.637	7.437	7.743	7.713	7.680
	SORTING	1.719	2.031	1.954	2.097	1.879	1.869	1.988	1.903	1.914	1.891
	SKEWNESS	0.073	0.016	0.047	-0.001	0.000	-0.031	-0.056	-0.085	-0.089	-0.070
	KURTOSIS	0.933	0.879	0.893	0.831	0.947	0.964	0.959	0.968	0.961	0.969
FOLK AND WARD METHOD (Description)	MEAN:	Fine Silt	Fine Silt	Fine Silt	Fine Silt	Fine Silt	Fine Silt	Fine Silt	Fine Silt	Fine Silt	Fine Silt
	SORTING:	Poorly Sorted	Very Poorly Sorted	Poorly Sorted	Very Poorly Sorted	Poorly Sorted	Poorly Sorted	Poorly Sorted	Poorly Sorted	Poorly Sorted	Poorly Sorted
	SKEWNESS:	Symmetrical	Symmetrical	Symmetrical	Symmetrical	Symmetrical	Symmetrical	Symmetrical	Symmetrical	Symmetrical	Symmetrical
	KURTOSIS:	Mesokurtic	Platykurtic	Platykurtic	Platykurtic	Mesokurtic	Mesokurtic	Mesokurtic	Mesokurtic	Mesokurtic	Mesokurtic
	MODE 1 (μm):	7.091	7.091	7.784	5.885	5.885	5.885	5.885	4.884	4.884	4.884
	MODE 2 (μm):				19.78			106.1	19.78	19.78	
	MODE 3 (μm):				38.01				38.01	38.01	
	MODE 1 (ϕ):	7.141	7.141	7.007	7.410	7.410	7.410	7.410	7.679	7.679	7.679
	MODE 2 (ϕ):				5.661			3.239	5.661	5.661	
	MODE 3 (ϕ):				4.719				4.719	4.719	
	D_{10} (μm):	1.144	1.098	1.101	1.008	1.029	0.969	1.018	0.919	0.930	0.958
	D_{50} (μm):	6.129	7.165	7.082	6.716	5.679	5.022	5.601	4.448	4.512	4.713
	D_{90} (μm):	25.11	43.45	38.08	44.65	30.54	28.29	38.17	28.58	29.66	29.16
	(D_{90} / D_{10}) (μm):	21.95	39.59	34.60	44.28	29.68	29.21	37.48	31.10	31.88	30.43
	(D_{90} - D_{10}) (μm):	23.97	42.35	36.98	43.64	29.51	27.32	37.15	27.66	28.73	28.20
	(D_{75} / D_{25}) (μm):	5.330	7.709	7.056	8.975	6.103	5.871	6.606	5.988	6.112	5.967
	(D_{75} - D_{25}) (μm):	11.02	17.32	15.61	18.14	11.46	9.887	12.36	9.116	9.456	9.600
	D_{10} (ϕ):	5.315	4.525	4.715	4.485	5.033	5.144	4.711	5.129	5.076	5.100
	D_{50} (ϕ):	7.350	7.125	7.142	7.218	7.460	7.638	7.480	7.813	7.792	7.729
	D_{90} (ϕ):	9.772	9.832	9.827	9.954	9.925	10.01	9.940	10.09	10.07	10.03
	(D_{90} / D_{10}) (ϕ):	1.838	2.173	2.084	2.219	1.972	1.946	2.110	1.967	1.984	1.966
	(D_{90} - D_{10}) (ϕ):	4.456	5.307	5.113	5.469	4.891	4.868	5.228	4.959	4.995	4.928
	(D_{75} / D_{25}) (ϕ):	1.389	1.521	1.488	1.564	1.422	1.400	1.446	1.396	1.404	1.400
	(D_{75} - D_{25}) (ϕ):	2.414	2.947	2.819	3.166	2.609	2.554	2.724	2.582	2.612	2.577
	% GRAVEL:	0.0%	0.0%	0.0%	0.0%	0.0%	0.0%	0.0%	0.0%	0.0%	0.0%
	% SAND:	1.4%	4.8%	3.7%	5.0%	3.1%	2.7%	4.8%	2.9%	3.1%	3.2%
	% MUD:	98.6%	95.2%	96.3%	95.0%	96.9%	97.3%	95.2%	97.1%	96.9%	96.8%
	% V COARSE GRAVEL:	0.0%	0.0%	0.0%	0.0%	0.0%	0.0%	0.0%	0.0%	0.0%	0.0%
	% COARSE GRAVEL:	0.0%	0.0%	0.0%	0.0%	0.0%	0.0%	0.0%	0.0%	0.0%	0.0%
	% MEDIUM GRAVEL:	0.0%	0.0%	0.0%	0.0%	0.0%	0.0%	0.0%	0.0%	0.0%	0.0%
	% FINE GRAVEL:	0.0%	0.0%	0.0%	0.0%	0.0%	0.0%	0.0%	0.0%	0.0%	0.0%
	% V FINE GRAVEL:	0.0%	0.0%	0.0%	0.0%	0.0%	0.0%	0.0%	0.0%	0.0%	0.0%
	% V COARSE SAND:	0.0%	0.0%	0.0%	0.0%	0.0%	0.0%	0.0%	0.0%	0.0%	0.0%
	% COARSE SAND:	0.0%	0.0%	0.0%	0.0%	0.0%	0.0%	0.0%	0.0%	0.0%	0.0%
	% MEDIUM SAND:	0.0%	0.0%	0.0%	0.0%	0.0%	0.0%	0.0%	0.0%	0.0%	0.0%
	% FINE SAND:	0.2%	0.4%	0.5%	0.4%	0.4%	0.3%	1.0%	0.4%	0.4%	0.5%
	% V FINE SAND:	1.2%	4.4%	3.2%	4.6%	2.6%	2.4%	3.8%	2.5%	2.7%	2.7%
	% V COARSE SILT:	5.2%	11.1%	9.6%	11.5%	6.6%	6.1%	7.6%	6.1%	6.4%	6.1%
	% COARSE SILT:	14.5%	14.5%	15.4%	14.2%	12.3%	10.6%	11.2%	9.7%	9.8%	10.0%
	% MEDIUM SILT:	20.9%	17.3%	18.5%	15.6%	18.2%	16.7%	16.5%	14.3%	14.4%	15.5%
	% FINE SILT:	21.9%	18.2%	18.5%	17.1%	20.9%	21.6%	20.4%	21.0%	20.8%	21.1%
	% V FINE SILT:	16.7%	14.4%	14.5%	14.6%	16.8%	18.1%	17.0%	19.3%	19.2%	18.9%
	% CLAY:	19.4%	19.7%	19.7%	22.0%	22.0%	24.1%	22.4%	26.6%	26.3%	25.2%